FUZZY-NEURO CONTROL OF MAXIMUM POWER POINT TRACKING FOR PHOTOVOLTAIC PANEL

BY

FADI MOHAMMAD FAREED ABU SAMRA

A Thesis Presented to the
DEANSHIP OF GRADUATE STUDIES

KING FAHD UNIVERSITY OF PETROLEUM & MINERALS
DHAHRAN, SAUDI ARABIA

In Partial Fulfillment of the
Requirements for the Degree of

MASTER OF SCIENCE

In

ELECTRICAL ENGINEERING

DECEMBER 2015

KING FAHD UNIVERSITY OF PETROLEUM & MINERALS

DHAHRAN- 31261, SAUDI ARABIA

DEANSHIP OF GRADUATE STUDIES

This thesis, written by **FADI MOHAMMAD FAREED ABU SAMRA** under the direction of his thesis advisor and approved by his thesis committee, has been presented and accepted by the Dean of Graduate Studies, in partial fulfillment of the requirements for the degree of **MASTER OF SCIENCE IN ELECTRICAL ENGINEERING**.

Dr. Belhaj Ahmed Chokri
(Advisor)

Dr. Ali Ahmad Al-Shaikhi
Department Chairman

Dr. Mahmoud Kassas
(Member)

Dr. Salam A. Zummo
Dean of Graduate Studies

Dr. Alaa El-Din Hussein
(Member)

25/5/16
Date

عمادة الدراسات العليا
DEANSHIP OF GRADUATE STUDIES

Dedicated to

My Beloved Parents

My Beloved Brothers and Sisters

And

Muath, Mustafa, Mohammad, Omar and My Home ***PALESTINE***

ACKNOWLEDGMENTS

In the Name of Allah, the Most Beneficent, the Most Merciful.

> Praise belongs to Allah, the Lord of all the worlds (2) The All Merciful, the Very-Merciful. (3) The Master of the Day of Requital. (4) You alone do we worship, and from You alone do we seek help. (5) Take us on the straight path (6) The path of those on whom You have bestowed Your Grace, Not of those who have incurred Your wrath, nor of those who have gone astray. (7)
>
> Al-Fatiha

In the name of Allah, the most Merciful, the most Gracious. All praise is due to Allah; we praise Him, seek His help, and ask for forgiveness. Peace be upon the Prophet Mohammad, his family, his companions, and all those who followed him until the Day of Judgment.

I then would like to show my deepest gratitude and respect to my family, especially my parents, the ones to whom I owe all the success in my life. No words can express my gratitude to them, but I pray God to bless them and reward them. Any success in my life so far is mostly charged to them and consequently any success in the future will have their signature as well.

Acknowledgements are due to King Fahd University of Petroleum and Minerals which gave me the opportunity to pursue a graduate degree and also for all the support I received in carrying out this research.

I would like to thank my research and academic supervisor Dr. Chokri Belhaj for his continuous supervision, advice, and guidance from the very beginning of this research.

He taught me how to think, analyze, and solve problems independently in a professional and friendly manner. My appreciations are also extended to my committee members: Dr. Mahmoud Kassas and Dr. A. Hussein for their useful discussions. Also, many thanks to my colleagues in the Electrical Engineering department for their help and support.

I would also like to thank all my colleagues, friends and seniors at KFUPM for providing the moral support and a pleasant atmosphere.

For everyone who had helped and supported me:

Thank you very much..!!

TABLE OF CONTENTS

LIST OF TABLES

LIST OF FIGURES

LIST OF ABBREVIATIONS

P_{mp}	:	Power at maximum power point (W)
P_{PV}	:	Power of Photo Voltaic panel (W)
$\mu_{I,SC}$	:	Temperature coefficient of short circuit current
$\mu_{V,OC}$	:	Temperature coefficient of open circuit voltage
a	:	Modified ideality factor
Eg	:	Band-gap energy
I_D	:	Diode current (A)
I_L	:	Light current (A)
$I_{L,ref}$	:	Light current at STC condition (A)
I_{mp}	:	Current at maximum power point (A)
$I_{mp,ref}$	:	Maximum power point current at STC condition (A)
I_o	:	Diode saturation current (A)
$I_{o,ref}$	:	Diode saturation current at STC condition (A)
I_{PV}	:	Photo Voltaic current (A)
I_{SC}	:	Short circuit current (A)
$I_{SC,ref}$	:	Short circuit current at STC condition (A)

I_{SH}	:	Current in shunt branch (A)
K	:	Boltzmann's constant (1.38e-23 J/K)
n	:	Ideality factor
I_{Max}	:	Number of training data points
N_{PP}	:	Number of PV panel connected in parallel
N_{S}	:	Number of cells in PV panel
N_{SS}	:	Number of PV panel connected in series
q	:	Electronic charge (1.6021e-19 coulombs)
R_{S}	:	Series resistance (Ω)
R_{SH}	:	Shunt resistance (Ω)
G	:	Irradiation Value (W/m2)
G_{max}	:	Maximum range of irradiation for ANFIS (W/m2)
G_{min}	:	Minimum range of irradiation for ANFIS (W/m2)
G_{ref}	:	Irradiation value at STC (1000 W/m2)
T	:	Temperature value (degree C)
T_{max}	:	Maximum range of temperature for ANFIS (degree C)
T_{min}	:	Minimum range of temperature for ANFIS (degree C)

T_{ref}	:	Temperature value at STC (25 ^{o}C)
V_{mp}	:	Voltage at maximum power point (V)
V_{OC}	:	Open circuit voltage (V)
V_{PV}	:	Voltage of Photo Voltaic panel (V)
AIT	:	Artificial Intelligence Techniques
ANFIS	:	Adaptive Neuro-Fuzzy Inference System
ANN	:	Artificial Neural Network
DS1103	:	dSPACE controller
ECU	:	Electronic Control Unit
EPIA	:	European Photovoltaic Industry Association
FIS	:	Fuzzy Inference System
GTAI	:	Gigabit Transceiver Analogue Input
GTAO	:	Gigabit Transceiver Analogue Output
HC	:	Hill Climbing
InCond	:	Incremental Conductance
LSE	:	Least Square Error
MAE	:	Mean Absolute Error

MPP	:	Maximum Power Point
MPPT	:	Maximum Power Point Tracking
OC	:	Open Circuit
P & O	:	Perturb and Observe
PCI	:	Peripheral Component Interconnect
RMSE	:	Root Means Square Error
STC	:	Standard Test Condition

ABSTRACT

Full Name : Fadi Mohammad Fareed Abu Samra

Thesis Title : Fuzzy-Neuro Control of Maximum Power Point Tracking for Photovoltaic Panel

Major Field : Electrical Engineering

Date of Degree : December, 2015

In this thesis, a generalized Photovoltaic (PV) array simulator is developed in MATLAB/Simulink based on the five parameters equivalent electric circuit model. The values of the five unknown parameters are estimated. Then, an efficient Adaptive Neuro-Fuzzy Inference System (ANFIS) based MPPT controller is proposed. Maximum Power Point Tracking (MPPT) is very important to improve the efficiency of PV panel. It can help PV panel to generate the maximum power possible at any weather conditions. When the resistance seen from the source is equal to the source resistance, the maximum power can be taken from the source in this time. For a variable load, we can change the value of the resistance until reaches the PV resistance then the maximum power is achieved. For a fixed load, we must use a power converter like a DC-DC converter to change the resistance seen by the PV panel by controlling the Duty Cycle for the switch device in DC-DC converter.

The proposed ANFIS-based MPPT controller is tested under rapidly changing irradiation conditions compared to the conventional MPPT methods. ANFIS-based MPPT simulation results are compared with the performance of conventional Incremental Conductance (InCond) method. The obtained results demonstrate that the proposed ANFIS-based MPPT controller has better dynamic and steady state performance than the

conventional method. Finally, its performance is investigated experimentally. A dSPACE DS1103 is used to run the proposed ANFIS and tested it with a real data. The experimental results are compared with those obtained from MATLAB simulation.

ملخص الرسالة

الاسم الكامل : فادي محمد فريد أبو سمرة

عنوان الرسالة : وحدة التحكم العصبي المنطقي لتتبع النقطة العظمي للطاقة الكهربائيه المولده عن طريق استخدام الخلايا الشمسية.

التخصص : **الهندسة الكهربائية**

تاريخ الدرجة العلمية : كانون أول 2015

في هذه الأطروحة يتم محاكاة مجموعة من الخلايا الكهروضوئية ويتم تطويرها ومعالجتها بالماتلاب على أساس خمسة عوامل تعادل نموذج الدائرة الكهربائية. بعد ذلك يتم بناء وتصميم نظام التحكم الذكي الخاص بهذه الخلايا الكهروضوئية ويسمى هذا المتحكم بنظام كفاءة الاستدلال العصبي الضبابي والمستند على وحدة التحكم والذي يعمل على استخراج أقصى قدرة ممكنة من الخلايا الكهروضوئية تحت جميع ظروف التشغيل. وحدة التحكم هذه لديها القدرة على تتبع النقطة المثلى في ظل ظروف الاشعاع المتغير.

النتائج التي تم الحصول عليها من المتحكم المستدل العصبي الضبابي والمسند الى وحدة التحكم لديه أداء أفضل من الناحية الديناميكية ومستقر أكثر من الطرق التقليدية.

يتم التحقق من أداء هذا المتحكم والمستدل العصبي من خلال تجربة عملية يتم من خلالها توصيل الخلايا الشمسية مع المحول ومن ثم الى الحمل الكهربائي ويتم التحكم بالمحول عن طريق المفتاح الموجود بداخله (الترانزستور) عن طريق المستدل العصبي. عملية التحكم هذه تعمل على تغيير نقطة العمل التي تعمل عندها الخلية الكهروضوئية بحيث تكون نقطة العمل الجديدة هي النقطة التي بامكانها أن تعطيك أكبر قدر ممكن من القدرة عند هذه الظروف الجوية.

وفي النهاية يتم عمل مقارنة بين النتائج العملية التي حصلناها والنتائج النظرية.

CHAPTER 1

INTRODUCTION

Sunlight is a natural resources, which uses as a source of energy. It is free and always available especially here in the Gulf area. Solar panel electricity systems, also known as solar photovoltaics (PV), catch the sun's ray and generate an energy. This process can be done by photovoltaic cells. The cells convert the sunlight into electricity, which can be used to run household appliances and lighting.

1.1 Background

There is a growing demand for energy, this growing demand forcing the electric utilities to increment the production. Recent researches say the net electricity generation in 2005 is 17.3 trillion kWh and this value will be increased to 24.4 trillion kWh (nearly 41%) in 2015 and in 2030 the percentage increase from 41% to 92.5% (about 33.3 trillion kWh)[1, 2]. Nowadays, the biggest quantity of electricity is produced by fossils fuels because the price of generation is low. But the use of fossils fuels lead to environmental pollution and greenhouse gas emissions which causes global warming. Some statistics say, in 2020 the increase in the emissions of carbon dioxide is 35% more than the expected increase in electricity generation[3]. From here search began for alternative sources of energy.

There is a search became increasingly specialized in renewable energy sources. An electrical energy generates by using solar energy. The PV is characterized by long life, low maintenance cost, environment friendly and it is abundant because it depends on the sun as a source. On the other hand, the governments encouraged the investment in renewable energy resources and give him a lot of facilities in this field.

In 20th century, the loads fed by electricity through using the photovoltaic (PV) systems. In 2009, the PV in the world was generated 23GW. In 2011, more than 69GW of PV power is installed worldwide that can generate 85TWh of electricity per year. The European Photovoltaic Industry Association (EPIA) expects that the global cumulative PV capacity will reach 200 GW by the year 2020 and 800 GW by the year 2030 [4]. For this reasons, the researchers try to develop and modify the PV panel in different ways for example, PV cells material, modeling of the PV panel, maximum power point tracking algorithms, power electronics converter used to integrate PV array with grid and its impact on power system etc.

1.2 Motivation and Problem Description

PV panels are used as a standalone which is the only source of feeding for the loads, or it connected to the grid with the distributed generator to help feed the loads. We know that the PV is affected by the weather conditions like irradiation and ambient temperature. From here, we need to study and analyze the energy provided from the PV generation system. The energy from the PV system can be increased in two ways; one is to build a larger Photovoltaic (PV) array generation system and the other is to achieve higher

efficiency in converting solar energy into electrical energy. Power generates from PV is depending on the weather conditions such as irradiation and temperature. These natural conditions changing continuously. This is a big issue and the PV needs an external controller to get the maximum power from it.

Figure (1) shows the I-V and P-V curves for PV panel. These two curves represent the behavior of PV panel. The red curve shows the array's output current as a function of its output voltage (I−V curve). The blue one shows the output power as a function of the output voltage (P−V curve).

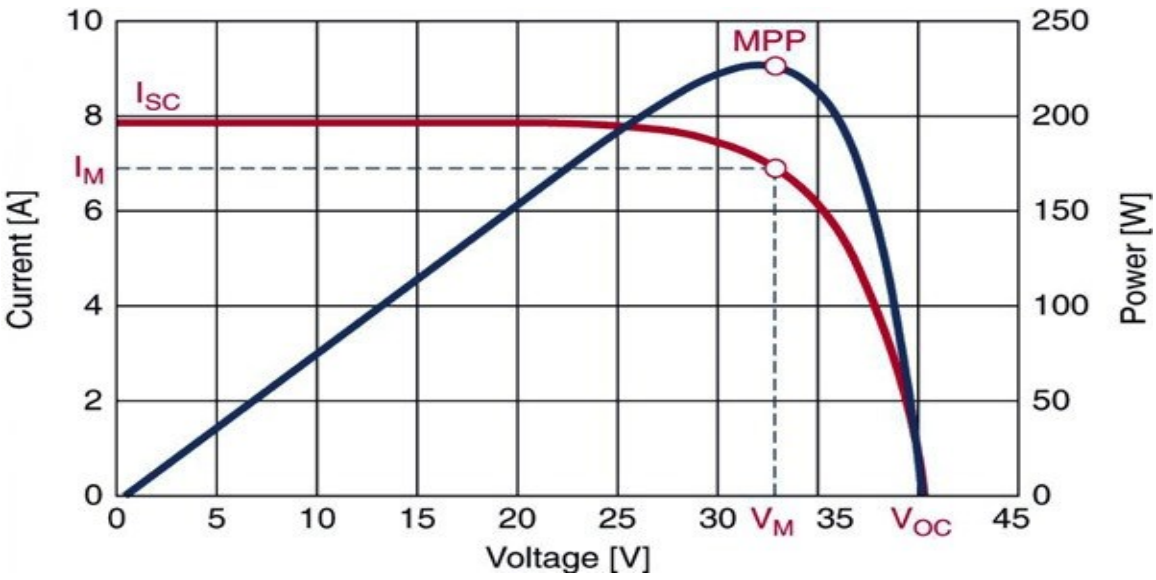

Figure 1: I-V Curve and P-V Curve for a typical solar cell.

The small white circle on both curves called maximum power point (MMP), which occurs when the array current is maximum and the voltage is maximum too. In this point the efficiency of PV panel is the most one i.e. the maximum power converted from solar energy to electrical energy has been happen at this point. The MPP is not fixed; it can

vary along the day depending on the weather conditions (irradiations and temperature). So, through a day, they are many MPP that depends on the weather conditions (operating conditions).

It is a necessary to use an intelligent control that can be integrated to the PV system to get the MPP. This MPPT controller forced the PV system to operate at specific point from the P-V curve. At this specific point, PV panel works to give the maximum efficiency. PV system efficiency is depending on the efficiency of each device use in it. These devices are PV panels, converters and MPP algorithm. PV panels have efficiency around 8-20% only, converters have 95-98% and MPPT algorithm has more than 98%. The efficiencies of electronic converters and PV arrays depend on technology but MPPT efficiency can be increased by improving its tracking methods.

1.3 Thesis Objective

The main objective of this project is to build and test a real time intelligent controller to extract the MPPT from an actual PV system under any environmental conditions (irradiation and temperature). This intelligent control based on Fuzzy-Neuro controllers.

Following are the major objectives that are considered in this work:

- LabVIEW software based PV generator and its converter circuit MPPT model.
- Develop a LabVIEW software based Fuzzy-Neuro controller for MPPT tracking simulation.

- Integrating of the developed intelligent controller with PV and MPPT system for testing of the functionality, stability and accuracy.

1.4 Thesis Approach

The approach that is used to fulfill the objectives is comprised two major phases:

1.4.1 Modeling of PV system

- The non-linear model of the PV panel using five parameter equivalent circuit is developed.
- Behavior of the PV panel output characteristics with respect to these parameters is investigated.
- MATLAB/SIMULINK model of the PV model is developed that is flexible enough to simulate any number of series and parallel connected panels.
- LabVIEW model of the PV model is developed that is flexible enough to simulate any number of series and parallel connected panels.
- Robustness of the developed model is verified using simulation study at different operating condition.
- Develop a program for measure and analyzing the performance using I-V and P-V curves under different conditions and saving the data in Excel file for further investigations.

1.4.2 Design and Implementation of MPPT Controller

- The complete non-linear model of the PV panel, DC-DC Converter, Maximum Power Tracking Point (MPPT) controller and load is developed.
- An Adaptive Neuro-Fuzzy Inference System (ANFIS) based on Maximum Power Tracking Point (MPPT) is developed.
- The dynamic performance of the complete system is investigated under different operating point.
- Practical validation of the proposed controller is verified by using the LabVIEW software and dSPACE DS1103.

1.5 Outline of the Thesis

The thesis is structured as follows.

Chapter 2 presents brief description details on previous work and literature survey on PV modeling and maximum power tracking point (MPPT) techniques.

Chapter 3 describes the modeling for the PV panel and the proposed Adaptive Neuro-Fuzzy Inference System (ANFIS) based MPPT controller.

Chapter 4 describes the experimental set-up used to verify the proposed ANFIS-based MPPT controller practically.

Chapter 5 investigates the performance, comparison between the experimental and simulation results and discussions the results.

Chapter 6 concludes the thesis work and gives directions for the possible future work.

CHAPTER 2

LITERATURE REVIEW

The energy produced from the photovoltaic (PV) is too expensive comparing to the energy generated by the fuel fossil. So, many research and work are still done to model and develop the PV systems. This Chapter presents a literature survey on the PV array modeling and MPPT techniques.

2.1 PV Electrical Model

There is a growing demand for energy, which led to a search for alternative sources of energy, so there is a search became increasingly specialized in renewable energy sources[5]. Solar energy can be converted into electrical energy. There are two methods to generate electrical power from the solar energy, through photovoltaic (PV) and solar thermal systems.

Solar energy is one of the most important sources of renewable energy, there are several features, low cost of maintenance, there is no pollution to the environment, a long life and zero input cost because solar cell are used the sun as a source and the sun is abundant source. Solar arrays convert directly the sunlight to electrical power. The output of solar arrays depends on the irradiation intensity and the ambient temperature[6].

The relationship between the current and the voltage of photovoltaic cell is nonlinear. It is a P-N semiconductor junction. So when a sunlight falls on the solar cell, it generates a DC current depends on the amount of radiation and temperature in the atmosphere[7]. Through this relationship, we can note that there is only one point where the output of power is the maximum, this point can be achieved when the change of power for the voltage equals zero, this point is called the Maximum Power Point (MPP)[8].

They are many models can be represented the PV characteristics, models depended on experimental correlation, models need analytical data depending on structure of PV cell and finally models that made a combined between the two methods before. Some of these models are using and the other didn't because the complexity of these models in power system studies. The simplest one can be expected the performance of PV at specific point depending on the irradiation coefficient and ambient temperature[9]. In[10], convert the I-V curve from one environmental parameter to another by using a translation method. A four point decide the I-V curve, two points for irradiation, each point represent a value different from the other and two at different temperatures this method called bilinear interpolation method [11].

These models are complex to use it and need a huge data that can't provide from the producer. The simple and practical model for PV arrays is explained in [12]. It needs thirty constants to simulate the PV panel behavior and these constant can be provided by the manufacturing.

The electrical circuit that has been adopted to represent the PV panel is classified in four categories. First one is the ideal diode model which has a three parameters only. Second

one is the RS model which has a four parameters. Third one is R_{SH} model that has a five parameters. Last one is the double diode model which has a seven parameters. Figure.2 is illustrated each one of them.

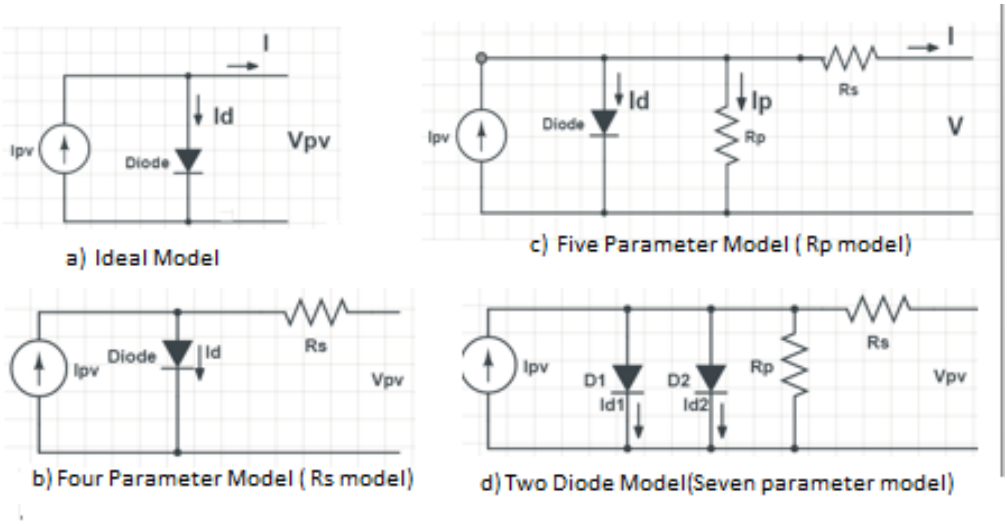

Figure 2: Equivalent electric circuit model of PV panel.

Ideal model in Figure.2.a is the simplest between these models; it needs to find three parameters, IL light current, Io saturation current of diode and "a" ideality factor of diode to generate the complete output characteristics of a PV device. In Figure.2.b, a resistance added in series to the ideal model so it is called a four parameters model [13, 14]. This model is easy to implement and gives reasonable results, but it breaks down at high temperatures and low radiation which led to improve it by adding a shunt resistance. This new model called RSH model (five parameters model) as shown in Figure.2.c. This model is able to find the current and the power at different weather conditions. A two diode model Figure.2.d was found to improve the efficiency of the circuit for PV panel. In this model we calculate seven parameters to run the simulation [15]. Some researcher

says the RS model is the perfect model because it is simple and the results are relatively accurate. When a cloud came over the solar cell, it covered in the shadow of this cloud and this makes the cell behave differently. This partial shaded condition may be happen through dust or snow covering the PV panel, shadows of trees or birds litters [16].

It's important to take into account the value of the parameters during the implementation of electric circuit for PV panel. These parameters should be taken into account because it is an important part in determining the efficiency and the performance for these models. There are two ways to find these values; the first is predicted using certain points such as the short circuit point (SC), open circuit point (OC) and maximum power point (MPP) [17], while the second way apply the curve fitting principle[18]. There are advantages and disadvantages to both, but the second relies on experimental data and this information can't be provided by manufacturers. So in our study we are going to adopt the first method. In order to find the value of these parameters, researchers followed some algorithms. In general most of these algorithms are imposing a certain value to one parameter and calculated the other by using analytical equations and iterative methods[19]. In Ref. [20], the author used the highly complex diode current equation but after simplified it to solve the nonlinear I-V equation but this approach reduced the efficiency of this method. Some methods calculated the parameters by using nonlinear solver software but still some limitation to using it [21, 22]. Some algorithms have gone to depend on optimization process to give an accurate value for the parameters.

Recently, some intelligent control techniques like fuzzy logic [23] and artificial neural network have been used to find these parameters [24]. Results obtained were good but there was a problem when integrated to PV system.

2.2 Maximum Power Point Tracking

Maximum Power Point Tracking (MPPT) is very important to improve the efficiency of PV panel. It can help PV panel to generate the maximum power possible at any weather conditions. Figure.3 shows the difference between the power generates with using MPPT and without using it.

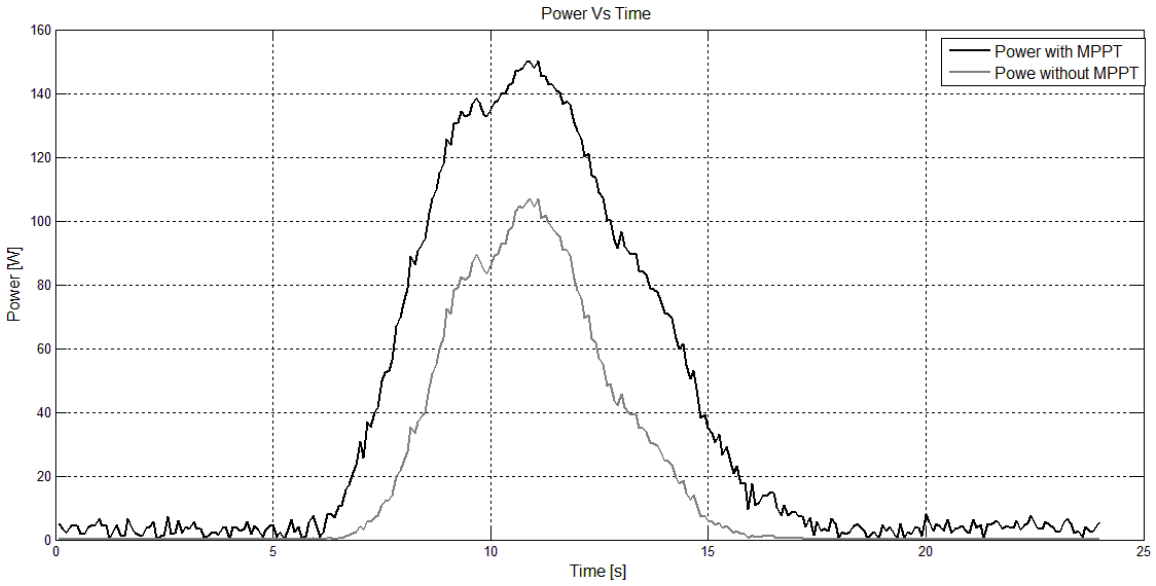

Figure 3: Power curve for PV module with MPPT and without MPPT.

We can suck a maximum power from the source which is connected to a load when the input resistance seen by the source equals to the source resistance. So, to transfer the maximum power from the PV panel to the load; the internal resistance for the PV panel must equal to the resistance seen by the PV panel. For a variable load, we can change the value of the resistance until reaches the PV resistance then the maximum power is achieved. For a fixed load, we must use a power converter like a DC-DC converter to

control the equivalent resistance seen by the PV panel by changing the Duty Cycle as shown in Figure.4 [25-27].

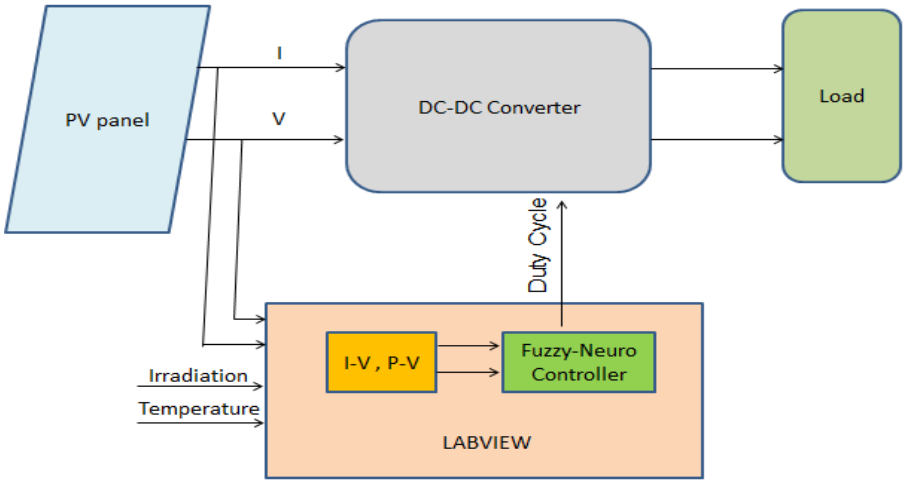

Figure 4: Photovoltaic System.

They are many MPPT techniques which are suggested by researchers. These methods differ in cost, control variables, sensor required, complexity, reliability, convergence speed, efficiency and hardware implementation [6, 28, 29]. We can classify the MPPT techniques in two categories: basic MPPT techniques and artificial intelligent techniques.

The Hill Climbing / Perturb and Observe are commonly used as a MPPT techniques and available practically because of its simplicity and its results convincing [30-35]. In the HC, the power value is calculated by measuring the Vpv and Ipv at fixed intervals. After that the power increment is calculated as this equation ($\Delta P = P(K) - P(k-1)$) every sampling time. Then, according to its sign, the duty cycle can be incremented or decremented with a fixed steps depending on the Vpv and the Ppv calculated values until reached the MPP.

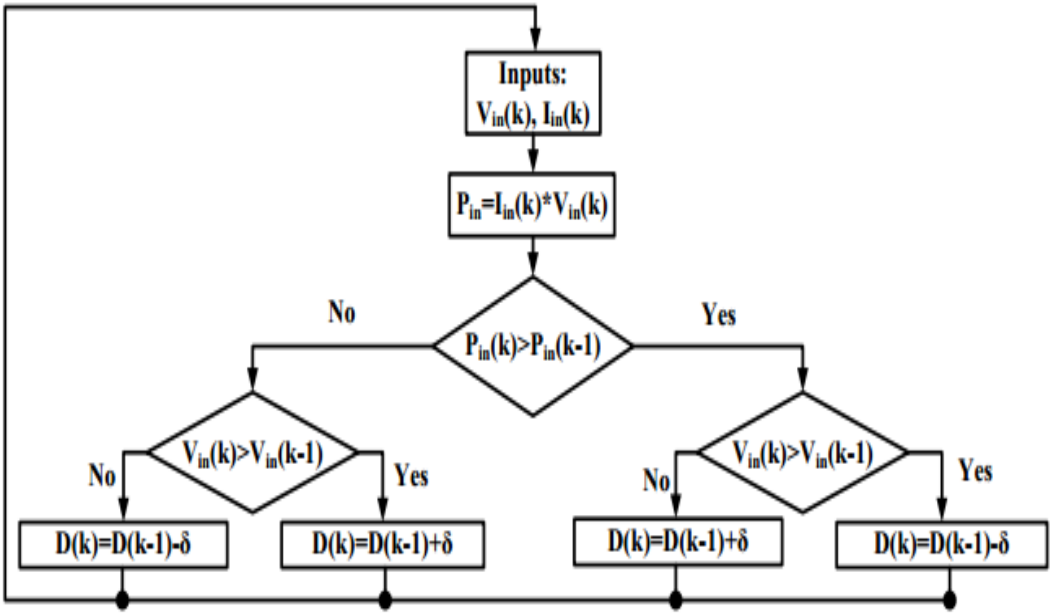

Figure 5: HC method Flow Chart

Same principle in P&O method, but after calculated the panel power through the measured voltage and current from the panel, the increment and the decrement are happened in the reference voltage. Which is later converted to a duty cycle value to achieve the maximum power point.

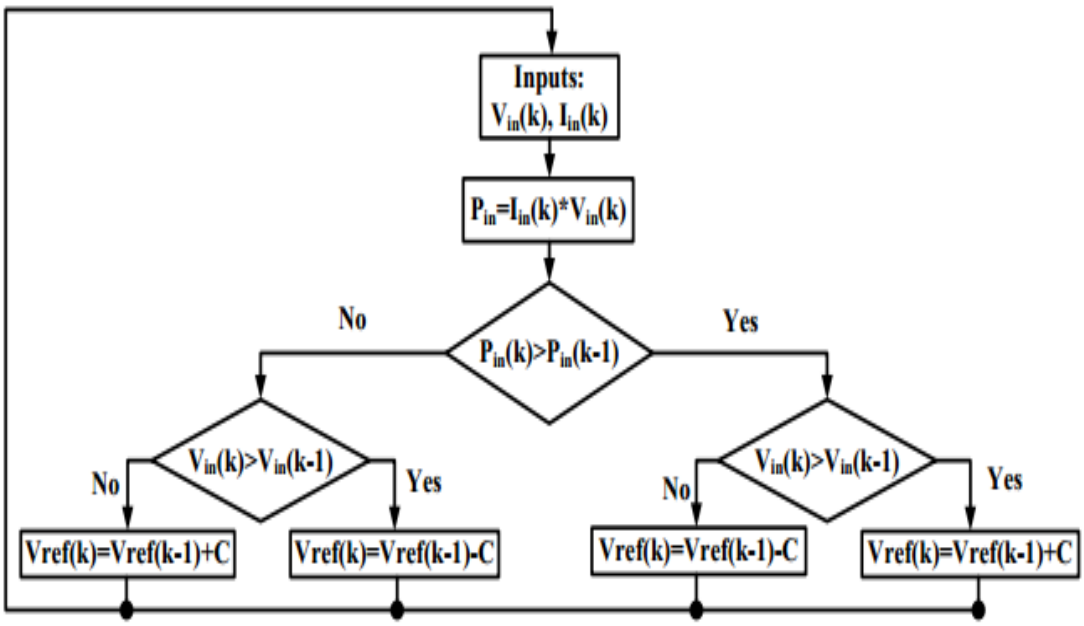

Figure 6: P&O method Flow Chart

In Figure.7, if the initial operation point was at point 1, then it is moved to point 2. Therefore, the power in point 2 is greater than the power at point 1 but the voltage at point 2 is less than the voltage at point 1, so the MPPT controller action decrease the reference voltage with a fixed step (increase the duty cycle).

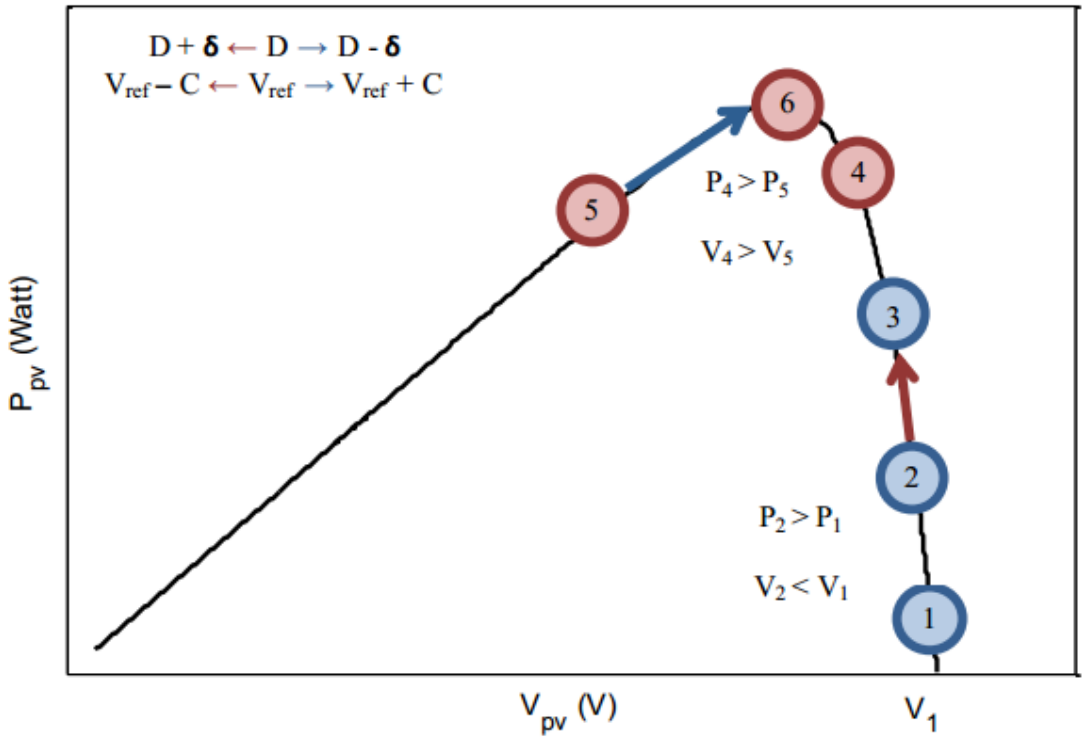

Figure 7: HC and P&O methods Operation

This step will take the operation point to the left side of the maximum point. Now it reached at point 4 and still decreasing in the reference voltage. If the step size is large, the operation point may exceed the maximum point until reached the point 5. In point 5, the value of power is less than the power at point 4 and the voltage in point 5 is also less than the voltage in point 4 so, the reference voltage is increased (the duty cycle decreased). This action moved the operation point to the right side of MPP. Then the process is repeating and the operation point oscillate around the MPP.

The disadvantages of these methods are that the voltage oscillation around the MPP which considered as power losses and under fast changing in weather, the response is very slow.

In [36] an Incremental Conductance (InCond) method was presented. This method eliminated the oscillation around the maximum power point (MPP) through the changing in environmental conditions in P&O method by comparing the instantaneous panel conductance (current divided by the voltage) with the incremental panel conductance (the derivative of current divided by the derivative of voltage). This method is better than other because it is easy to implement, effectiveness good and high tracking speed. Existing improvements in literature of this method focuses on modifying the step size of the algorithm. However, the high complexity of the method requires high sampling accuracy and fast control speed, which may result in a high cost system.

There is a method called open circuit voltage and short circuit current [37]. This method is the simplest one on MPPT techniques. It depends on the ratio between the maximum power value and the open circuit voltage or short circuit current is approximately a linear dependence for change in solar radiation and temperature. So to implement the open circuit voltage you must keep in mind that the ratio of the maximum power voltage (Vmp) and the open circuit voltage (Voc) are approximately linearly proportional under varying weather conditions.

Same principle for short circuit current the ratio of the maximum power current (Imp) and the short circuit current (Isc) are linearly proportional. Because of this method uses the approximation, the power produced from PV is less than the real power and another disadvantage in open circuit voltage when measured the open circuit voltage, we must disconnect the load and this causes the power dissipation.

In recent years some Evolutionary Algorithm (EA) [38] and Artificial Intelligence Techniques (AIT) like Artificial Neural Network (ANN) [39] and Fuzzy Logic [40] have been exposed to treat these problems as they have the ability to deal with non-linear objective functions. Some examples on Evolutionary Algorithm, Tabu search, differential evolution, evolutionary programming particle swam optimization and genetic algorithm have been explained in [41-45]. The results of these techniques show that they can improve the response of MMPT when they used with the traditional methods.

In [44, 46] is proposed the Artificial Neural Network (ANN) technique. This method has the ability to deal with the nonlinear equations and parameters controlled by different weather conditions. ANN can map the input output nonlinear functions as multilevel neural networks, so it is good in the nonlinear system. The Figure.8 is explained the NN technique. The PV panel voltage, current and another parameter (like irradiation and temperature) are measured. These values are the input of the NN controller. The output from the NN controller is a voltage reference which is converted to a duty cycle. Then, using this duty cycle to control the DC-DC converter to change the power transfer and get the maximum power point from the PV panel at these measured values. NN is more stable than other methods but it works as a black box that limiting their use in MPPT. Because the PV array characteristic is changed with time an Adaptive Neuro-Fuzzy Inference System (ANFIS) is proposed. ANFIS is an adaptive technique, so it can deal with any change in the parameters. It is a combination of the Sugeno fuzzy model and NN [47].

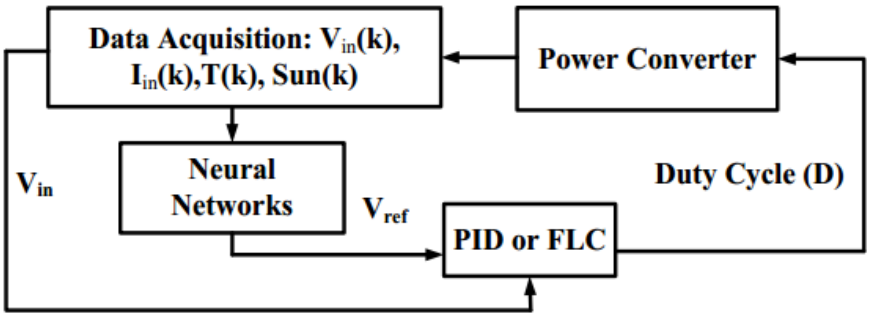

Figure 8: NN method Block Diagram

Now most of the researches talk about the Fuzzy Inference System (FIS) [40, 46]. The output for this method is adjusted the duty cycle (dD) and controlled it. FIS is an algorithm that correlated the input for a specific output. In this method, the input represented to other formula to handle it. So it has an input variable, membership function and linguistic rules to get the output. FIS controllers have error and change in error as input variables. These represent the slope and change in slope of the P-V curve.

For our MPPT system, the panel voltage and current are measured, and then the power is calculated. After that we can calculate the error (E) and the change in error (CE) to become an input for our fuzzy system and the output from the fuzzy system is the duty cycle (dD). The problem is that the duty cycle is not considered as input, which means that the operating point can go away from the original MPP in the varying atmospheric conditions [48].

From Ref [49], MMPT based on Fuzzy logic controllers have been presented. Fuzzy logic used to modify the P&O and Hill climbing methods. The fuzzy method has an advantage because it doesn't need a mathematical model and used inaccurate inputs.

In [50, 51], the Fuzzy modified and the input to fuzzy control became the variation in voltage and current array (power array) and the duty cycle (dD). Here, the dynamic behavior is improved in changing ambient conditions but this method added the steady state oscillation in the PV output which causes the power loss. In Ref [52], a modified method has been proposed; it was composed of the integration of last two methods in[49, 50]. The inputs are now three; the derivative of power over array current derivative, change of this derivative and variation of duty cycle. A fuzzy cognitive network was presented in Ref [53]. In this method the time which required reaching the MMP is reduced. But the disadvantage, it needed to connect an extra switch in parallel with PV system and a current sensor to calculate the short circuit current. This makes the implementation difficult.

CHAPTER 3

PROPSED SYSTEM DESIGN & SIMULATION

In this chapter a brief description for the electrical model of the PV panel. This model build using the five parameters equivalent circuit and how the values of these parameters are be determining. Then, building the PV circuit in SIMULINK/MATLAB. After that, talking about the Adaptive Neuro Fuzzy Inference System (ANFIS) based on the Maximum Power Point Tracking (MPPT).

3.1 PV Electric Circuit Model

A photovoltaic is a compound of a two semiconductor layers (p-n semiconductor). So it has the capability to convert the light directly to electricity. PV cell temperature and weather radiation are determining the behavior of the PV cell. Therefore, the relationship between the current and the voltage (I-V) or the power and the voltage (P-V) is nonlinear.

In ideal case Figure.9, the PV cell represents as a photo-generated current source and a diode. But mathematically, the semiconductor principle is used to describe the ideal photovoltaic cell as in equation (1):

$$I = I_{PV} - I_d = I_{PV} - I_0 \left(e^{\left(\frac{qv}{aKT}\right)} - 1\right) \qquad (1)$$

Where I_{PV} is the incident light generated current, I_d is Shockley diode current, I_0 is diode dark saturation current, T is cell temperature of p-n semiconductor junction, k is

Boltzmann's constant (k= $1.3806503*10^{-23}$J/K), q is charge of an electron (q= $1.60217646*10^{-19}$C) and a is the ideal factor of cell type that depends on PV technology.

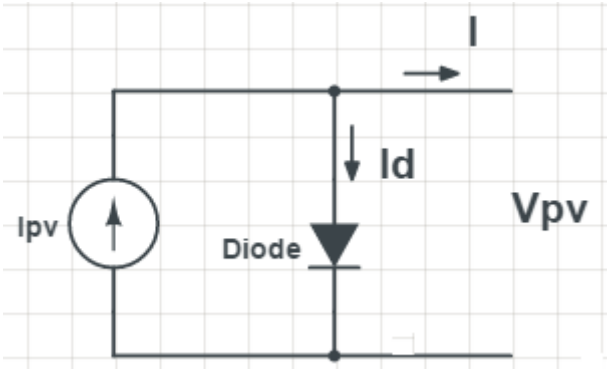

Figure 9: Ideal equivalent electric circuit model of PV device.

3.1.1 Modeling of PV Panel

Ideal model has not enough information to represent the behavior of the PV panel. Many of the PV cells are connected in series or parallel to perform the practical PV arrays. So, a good characteristics observation for the PV panel needs additional parameters to include in the ideal equation.

This model is designed based on the five parameters equivalent electric circuit shown in Figure.10 [54, 55]. This model can represent the I-V characteristics of the PV panel. But, there is a problem in what the value of these parameters and how can determine these values. These parameters can be always changed and they are depending on the weather conditions. These parameters is required to determine the I-V characteristics.

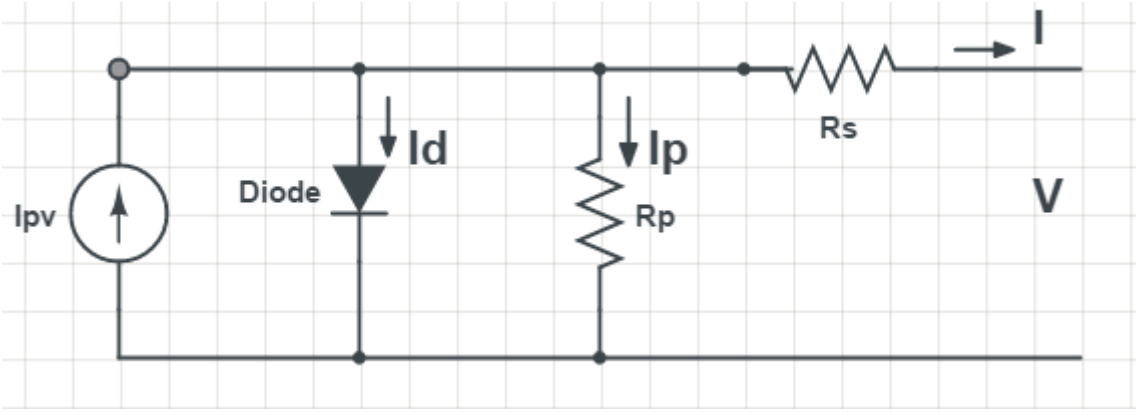

Figure 10: Five parameter equivalent electric circuit model of PV device.

Using Kirchhoff's current law on the five parameters electric circuit model, the following relationship can be found describe by equation (2)

$$I = I_{PV} - I_d - I_{sh} = I_{PV} - I_0 \left(e^{\left(\frac{q(V+IR_s)}{aKTN_s} \right)} - 1 \right) - \frac{(V + IR_s)}{R_p} \quad (2)$$

Where I_{pv}, I_o, I_d and I_{sh} are depicts the photovoltaic current, saturated current, diode current and shunt branch current respectively. I and V represents the current and voltage generated from the PV panel. R_p and R_s are the parallel and series resistance. 'a' is the ideality factor for diode and its value between 1 to 2. Ns is the number of cells in the PV panel and V_t = KTNs/q is the PV array's thermal voltage. The above equation shows the I-V characteristics of a PV panel depends on the five parameters (I_{pv}, I_o, R_s, R_p and 'a').

The transcendental non-linear characteristics for the PV panel are added the complexity in the modeling of the PV panels. The nameplate on the PV devices or the data supplied by the manufacture haven't given enough information, it is provided some experimental data for the thermal and electrical characteristics. The datasheet provides the open circuit

voltage, the short circuit current, maximum power point and maximum power conditions at nominal condition Standard Test Condition (STC) (1000 W/m^2 and 25^0 C). These parameters (I_{pv}, I_o, R_s, R_p and 'a') are depending on the operation conditions (irradiation and temperature) and this added more difficulty in the modeling. These parameters are required for adjusting the PV panel models.

The photovoltaic devices I-V characteristics depend on external influences like cell temperature and radiation intensity and on internal characteristics such as R_s and R_p of device. The photo-generated current (I_{pv}) of photovoltaic (PV) cell directly depends on amount of charge carriers generated and influenced by the cell temperature and also linearly depend on the radiation intensity as describe by [56-58] as equation (3):

$$I_{PV} = (I_{PVn} + K_i \Delta T)\frac{G}{G_n} \qquad (3)$$

$$\Delta T = T - T_n \qquad (4)$$

Where, I_{pvn} is photo-generated current at STC, T & T_n is actual and reference cell temperatures respectively, G is solar radiation intensity on surface of panel and G_n is reference solar irradiation. K_i is the cell short circuit current temperature coefficient.

In contrast, saturation current of diode Io varies with the cell temperature and may be expressed either of equation (5) and equation (6)

$$I_o = I_{on}\left(\frac{T}{T_n}\right)^3 . \; e^{\frac{qE_g}{aK}\left(\frac{1}{T_n}-\frac{1}{T}\right)} \qquad (5)$$

Where I_{on} is saturated current found by evaluating equation (3) at STC, V = V_{ocn}, I = 0, $I_{pv} = I_{scn}$:

$$I_{on} = \left[\frac{I_{scn}}{e^{\left(\frac{V_{ocn}}{aV_{tn}}\right)} - 1} \right] \qquad (6)$$

With V_{tn} is thermal voltage at reference temperature, E_g is semiconductor band gap energy used in cell (approximately 1.12eV). The value of a (diode ideality factor) may be randomly chosen, typically, $1 \leq a \leq 1.5$ and other parameters also depend on this choice of PV model.

$$I_o = \left[\frac{I_{scn} + K_i \Delta T}{e^{\left(\frac{V_{ocn} + K_v \Delta T}{aV_t}\right)} - 1} \right] \qquad (7)$$

This equation (7) is obtained and differs by including the voltage and current coefficients Kv and Ki in equation (7). Thus, equation (5) express different approach that shows Io dependence on cell temperature. This results the linear variation effect on open-circuit voltage of cell temperature with respect to practical voltage temperature coefficient.

Two parameters R_s and R_p remain unknown and the photo-generated current (I_{pv}) is difficult to determine without the influence of parallel and series resistance. The assumption $I_{pv} \approx I_{sc}$ is usually used in photovoltaic modeling because of high parallel resistance and low series resistance practically.

A method defined in [19] is used for adjusting R_p and R_s based on the pair (R_s, R_p) that warranties the experimental maximum power at MPP (V_{mp}, I_{mp}) from datasheet ($P_{max,e}$) is

equal to I-V model calculated maximum power ($P_{max,m}$) i.e. $P_{max,e} = P_{max,m} = V_{mp} * I_{mp}$ of I-V curve at the (V_{mp}, I_{mp}) point. By making $P_{max,e} = P_{max,m}$, the relation between R_s and R_p is establish as shown by the following equations

$$P_{max,m} = V_{mp}\left\{I_{pv} - I_o\left[e^{\left(\frac{V_{mp}+R_s I_{mp}}{aV_t}\right)} - 1\right] - \left[\frac{V_{mp} + R_s I_{mp}}{R_p}\right]\right\} = P_{max,e} \qquad (8)$$

$$R_p = \frac{V_{mp}\left(V_{mp} + I_{mp} R_s\right)}{\left[V_{mp} I_{pv} - V_{mp} I_o e^{\left(\frac{V_{mp}+I_{mp}R_s}{aV_t}\right)} + V_{mp} I_o - P_{max,e}\right]} \qquad (9)$$

These equations makes the I-V curve of model mathematically cross the experimental maximum power points (V_{mp}, I_{mp}) which means for value of R_s there will be a unique value of R_p. The aim is to get the value of R_s and thus R_p that makes P-V curve peak of mathematical model coincide with peak experimental power at the (V_{mp}, I_{mp}) point.

To calculate the maximum power, equation (2) was solved for current for the entire range of voltages from 0 to the open circuit voltage V_{oc} and the maximum power was found by multiplying currents and voltages and searching for the maximum value. If the error of the predicted power from the experimental value were within the specified tolerance, the solution terminated otherwise the value of R_s was incremented and the process was repeated. This requires numerous iteration until $P_{max,e} = P_{max,m}$. Every iteration updates R_p and R_s towards the optimal model solution. The values of R_s and R_p are primarily unknown but after several iterations as solution refined the values of Rs and Rp tend to finest model solution. Thus I_{pv} photo-generated current is determined effectively by consideration the influence of parallel and series resistance of PV panel. It represented by the following equation:

$$I_{pvn} = \left(R_p + R_s\right) \frac{I_{scn}}{R_p} \qquad (10)$$

Initial guesses for Rs and Rp are required before the beginning of iterative process. The Rs initial value is zero and Rp initial value is given by

$$R_{p\,min} = \frac{V_{mp}}{(I_{scn} - I_{mp})} - \frac{\left(V_{ocn} - V_{mp}\right)}{I_{mp}} \qquad (11)$$

This is actually a line segment (slope) between MPP and short circuit that determines the R_p minimum value. The series resistance controls the I-V characteristics curve slope at open circuit condition and impact the shape near MPP. Although $R_{p,min}$ is surely smaller than actual R_p thus this is better initial guess.

In iterative scheme, series resistance R_s should be increase slowly that adjusting the model curve of P-V towards experimental MPP data which requires a number of values of R_s and R_p for finding the best curve. Plotting the curves for I-V & P-V requires solving the basic equation (1) for voltage, Vϵ [0, V_{ocn}], and current, I ϵ [0, I_{scn}]. Direct solution is not possible from equation (1) because V=f (I, V) and I=f (V, I). Numerical method is used to solve this transcendental equation. By solving numerically g (V, I) = I – f (V, I) = 0, I-V points are obtained by obtaining the corresponding current I points for set voltage values. P-V points are obtained by multiplying corresponding I and V points.

Once all the five parameters are available the P-V and I-V characteristics curves could be drawn. With the aim of including cell temperature and solar irradiation dependence on V_{oc}, equation (2) is also solved using Newton-Raphson algorithm at I=0 and the result is found after few iteration.

3.1.2 Matlab/Simulink Model of PV Panel

The environmental parameters such as ambient temperature, irradiation, humidity, dust, wind speed have major impact on PV performance. I-V curve of the PV panel reflects its performance for all loading level at specific panel temperature and solar irradiation. The method applied to reach the I-V at any environments condition consists of fast variation of the load resistance from a very high value (open circuit) to a zero resistance (short circuit) passes by the maximum power point.

Rp and Rs are respectively the parallel and series resistance. Figure 11 shows the corresponding slopes relevant to each resistance. Equation 12 and equation 13 describes the slope of resistances.

$$R_p = \frac{\Delta V_P}{\Delta I_P} \qquad (12)$$

$$R_s = \frac{\Delta V_S}{\Delta I_S} \qquad (13)$$

In this work, only the environmental parameters temperature and irradiation are taken. The five parameters electric circuit model is determined at STC. Table 1 shows the value of PV parameters which used in our research.

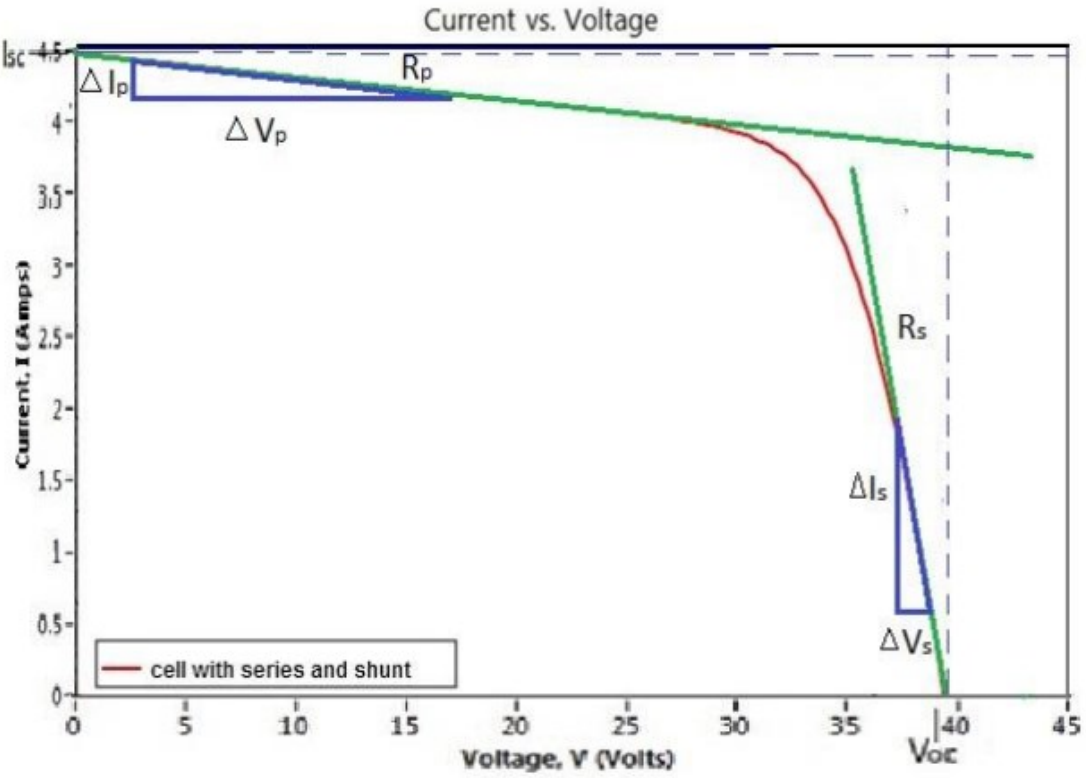

Figure 11: Slopes of Rp and Rs

Table 1: Specification of PV panel at STC.

Panel parameters from data sheet	**Value**	**Estimated model parameter**	**Value**
V_{OC} (V)	43.2	**R_S (Ω)**	0.13080
I_{SC} (A)	5	**R_P (Ω)**	693.271
V_{MP} (V)	36	**a**	1.3
I_{MP} (A)	4.5	**Ns**	72

PV panel with the estimated five parameters are developed in Matlab/Simulink. Figure 12 shows the non-linear equations for PV panel. From the datasheet and the solution of these equations, we can get the values of the five parameters for our model. Figure 13 describes the behavior of the PV panel when connected to a variable load. When the load is changed, I-V and P-V characteristic curve are plotted. Figure 14 and Figure 15 are showing how the I-V and P-V characteristic curves are changed when the Temperature value is constant (25^0C) and the Irradiation changed (200, 400, 600, 800 and 1000 W/m^2). Figure 16 and Figure 17 are showing how the I-V and P-V characteristic curves are changed when the Irradiation value is constant (1000 W/m^2) and the Temperature changed (25, 35, 45, 55, 65 and 75 ^{0}C).

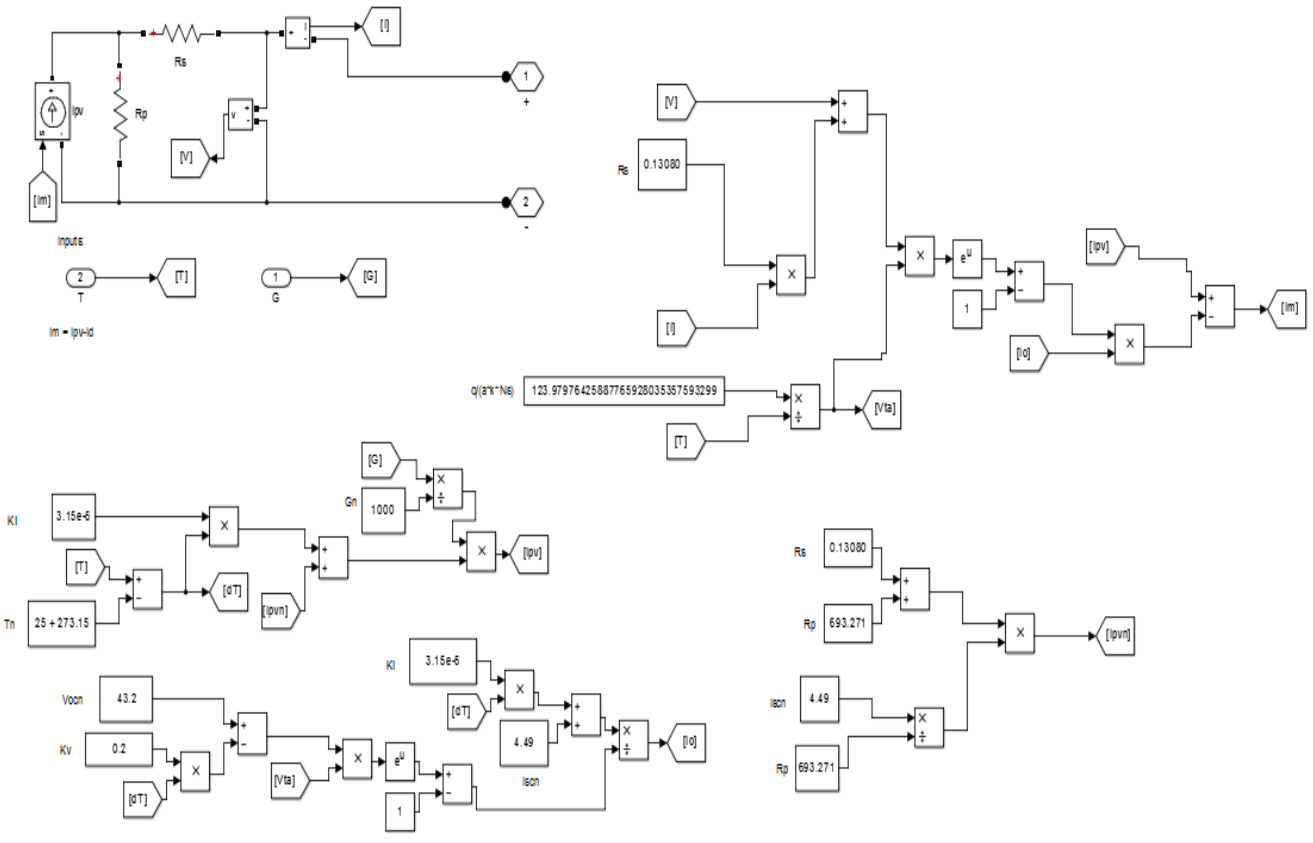

Figure 12: Five parameters electric circuit model build in Matlab/Simulink

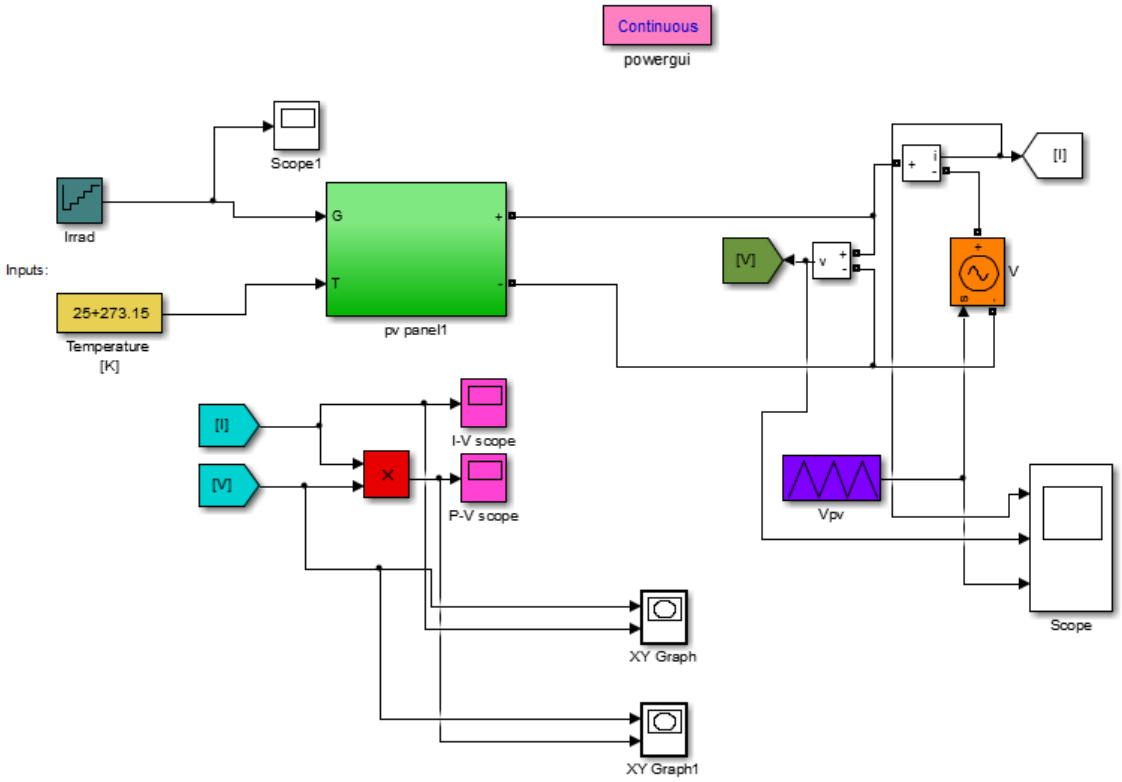

Figure 13: PV Matlab/Simulink model to draw I-V and P-V curves

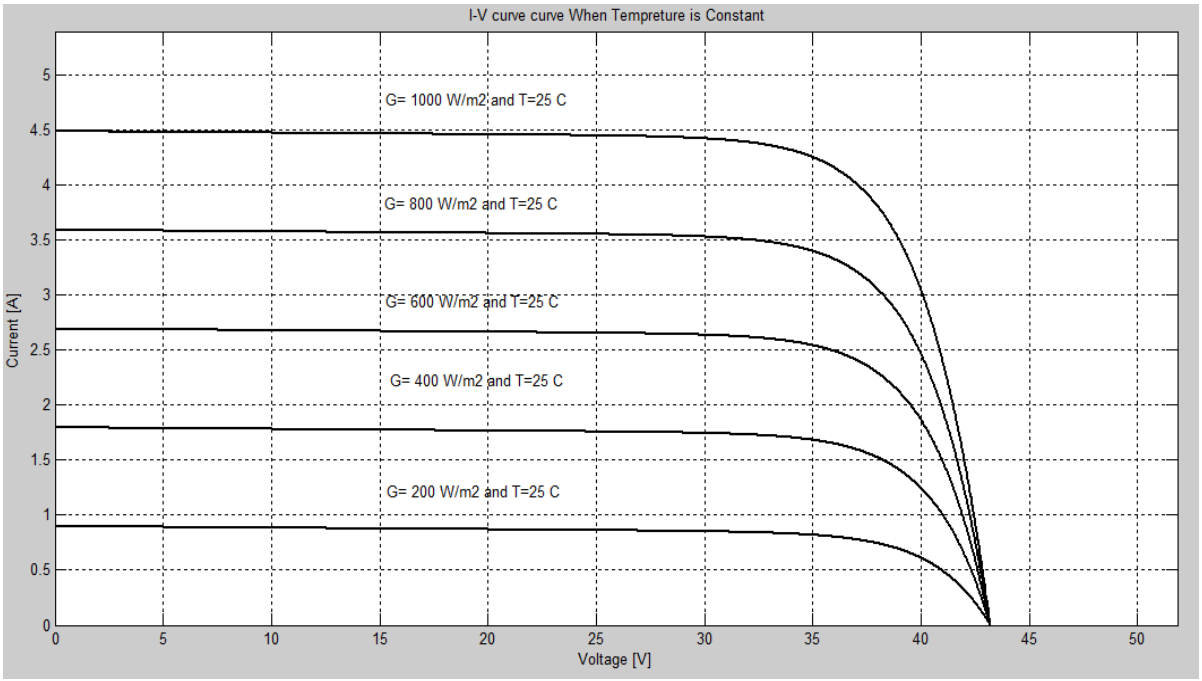

Figure 14: I-V curve when Irradiation is varying and Temperature is constant

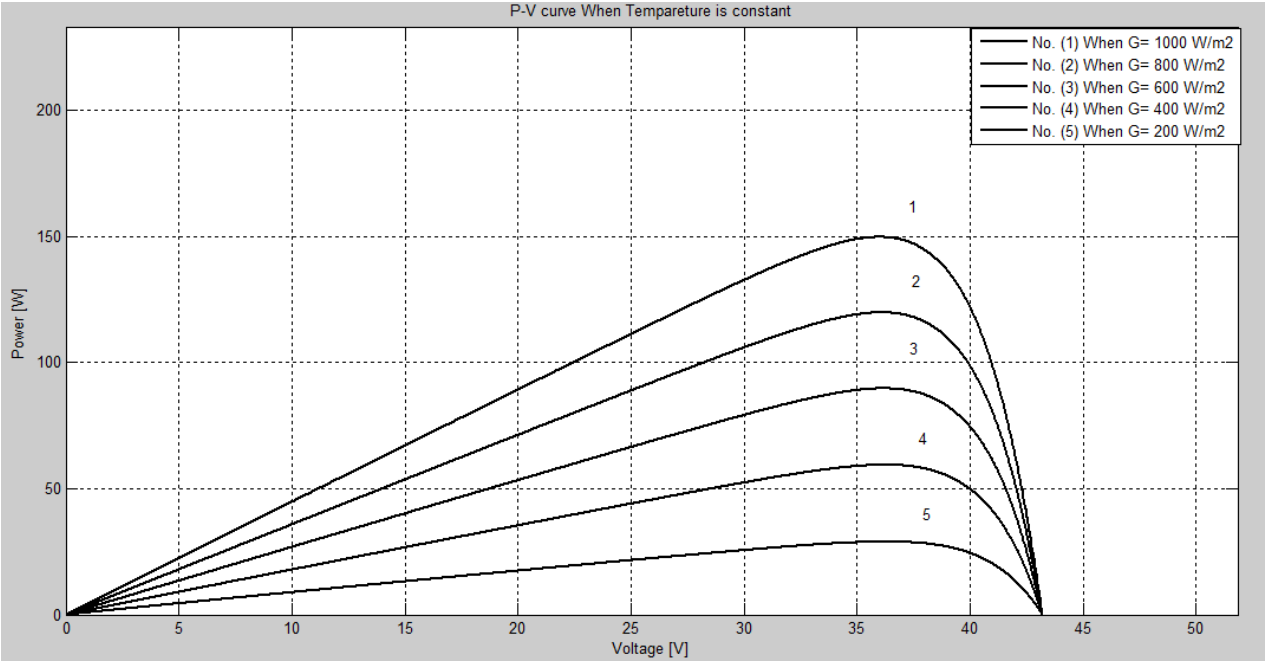

Figure 15: P-V curve when Irradiation is varying and Temperature is constant

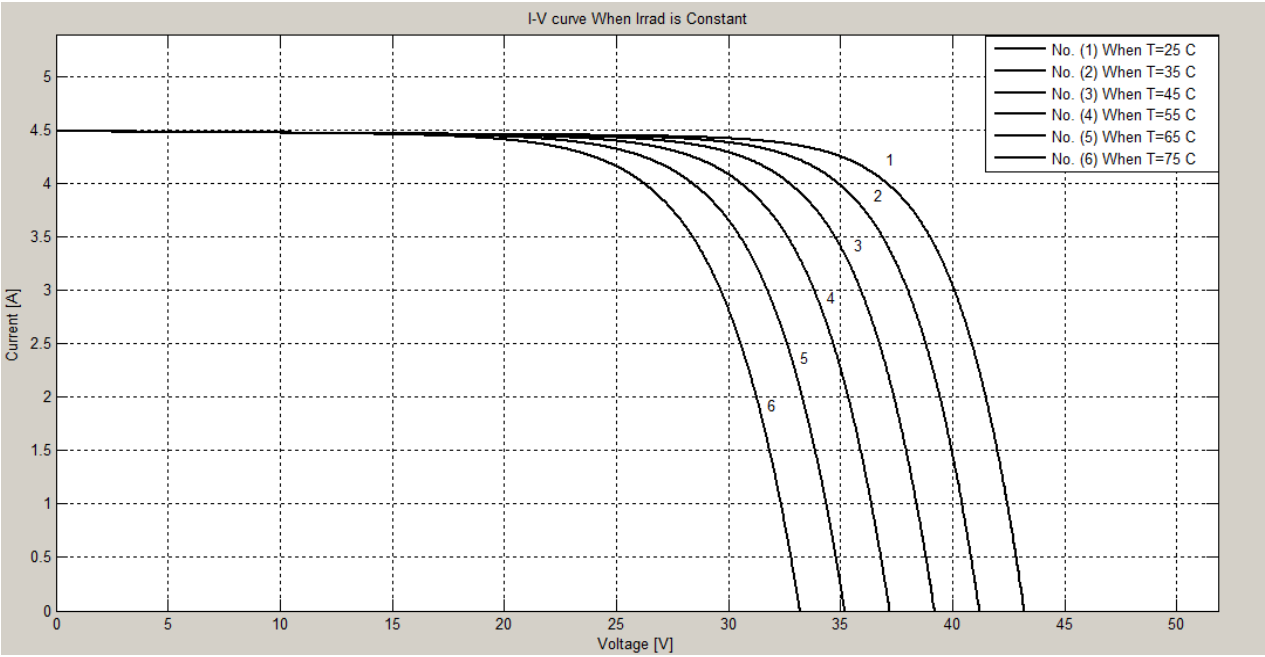

Figure 16: I-V curve when Temperature is varying and Irradiation is constant

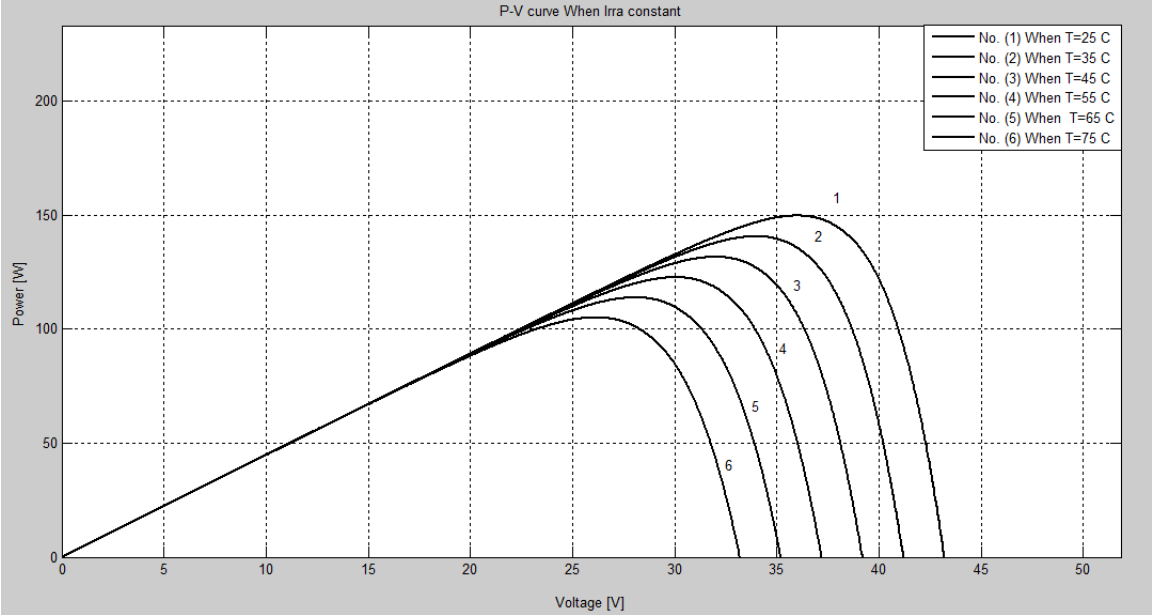

Figure 17: P-V curve when Temperature is varying and Irradiation is constant

3.2 Proposed MPPT Controller Design

The behavior PV panel generates a non-linear I-V and P-V characteristics. So it has a one point that represents the maximum value for the voltage and the current then the power, this point called maximum power point (MPP). I-V and P-V characteristics are depending on the ambient environments such as irradiation, ambient and cell temperature. So the maximum power point (MPP) is also linked to these conditions. The MPP is continuously varying during the day because it depends on the weather conditions and these conditions are different from time to time. So, the MPPT is needed to search for the MPP in the different weather conditions. It is connect to PV panel to control the operation point of PV panel and generates the possible power at that time. In the literature, researcher are suggested and developed many MPPT methods [29, 32] from the simple traditional

MPPT methods to the intelligent MPPT techniques [59]. Usually, PV panel was directly connected to the load. If the MPPT is used, there is a need to a device make an interface between the PV panel and the load and this device can be controlled by the MPPT. So, a DC-DC converter is used. DC-DC converter can use in the PV system for two purposes. First one, it gives the ability to get the maximum power from PV panel by controlling the switch device. Second purpose, the DC-DC converter can regulate the output voltage and can control it depending on the system requirements. DC-DC converter can step-up or step-down the input voltage. If the DC-DC converter works as step-down, it is called a buck converter and if it is working as step-up converter, it is called a boost converter. The system requirement is determined which type of DC-DC converter must be used. In PV system, the input voltage side for the DC-DC converter is connected to the voltage which is coming from the PV panel, this input is not constant and depends on the ambient weather conditions. The output side from the DC-DC converter provides a constant voltage and connected to the load. As we say, the MPPT can control the DC-DC converter by controlling the duty ratio of the switch device. In addition, it determines the suitable value for the duty ratio which can help to suck the maximum power from the PV panel. Without this controlling form the MPPT and the DC-DC converter, PV panel cannot be able to operate at full efficiency.

In this section, an intelligent maximum power point tracking (MPPT) based on the Adaptive Neuro-Fuzzy Inference System (ANFIS) is proposed and developed.

3.2.1 Fuzzy Logic System

Since its proposal by L. Zadeh [60] in 1965, fuzzy logic has been an active research topic. Zadeh defined fuzzy sets as "a class of objects with a continuum of grades of membership. Such a set is characterized by a membership (characteristic) function, which assigns to each object a grade of membership ranging between zero and one" [60].

In general, a fuzzy system is a static nonlinear mapping between sets of inputs and outputs. The inputs and outputs are real numbers, whereas the processes in between consists of fuzzy sets [61]. Fuzzy Logic Control (FLC) is mostly effective when the controlled process is based on human heuristic experience. As a result, it is commonly used to control nonlinear processes where there is no simple mathematical model relating between the process inputs and outputs. A FLC system mainly consists of four main blocks namely, fuzzification, rule base algorithm, fuzzification interface, and defuzzification. The following section will explain the design of each block based on the work of K. Passino and S. Yurkovich [61].

The FLC process can be summarized as follows. FLC maps between a set of inputs $u_i \epsilon U_i$; Where i=1,2,….., n (n: number of inputs) and outputs yi ϵ Yi ; where I =1,2,…, m (m; number of output). U_i and Yi are called ‘universe of discourse’ for u_i and yi respectively.

As shown in Figure 18, the fuzzification block converts the real number "crisp" inputs to fuzzy sets, and then the inference mechanism uses the fuzzy rules of the rule-base to produce the implied fuzzy sets or the fuzzy conclusions.

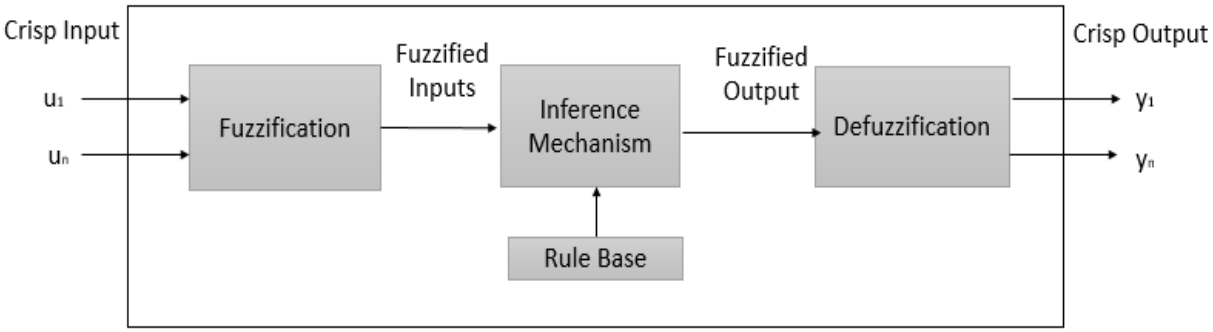

Figure 18: FLC block diagram

Finally, the defuzzification block converts these fuzzy conclusions into the crisp real number outputs. The design of a fuzzy control system goes through three main steps: choosing the fuzzy controller inputs and outputs, processing the controller inputs and outputs, and designing each of the four blocks of the fuzzy controller. While choosing the controller inputs, the designer should make sure that the FLC has enough information available to produce good decisions and efficiently control the process. In general, the choice of the inputs and the outputs will place specific limitations on the FLC design process. In some cases, the designer will be limited to a set of inputs depending on the sensors availability, in such a case observers and estimators can be used to find the needed inaccessible inputs. Choosing the FLC outputs is usually easier than choosing its inputs as the control process itself usually determines them.

They are some terminologies must be known in the fuzzy logic control design.

Linguistic Variables, Linguistic Values and Rules:

After choosing the FLC inputs and outputs, a linguistic description has to be given to each one of them. For our fuzzy system, we will describe the fuzzy input u_i by the

linguistic variable $\tilde{u}_i$, and likewise the fuzzy output y_i will be described by the linguistic variable $\check{y}_i$. Then a description has to be given to each $\tilde{u}_i$ and $\check{y}_i$.

The next step is to give a linguistic value to each linguistic variable. Let $\hat{A}^j_i$ denote the j^{th} linguistic value of the linguistic variable $\tilde{u}_i$ defined over the universe of discourse U_i . If we assume that there exist many linguistic values defined over U_i then the linguistic variable $\tilde{u}_i$ takes on the elements from the set of linguistic values denoted by

$$\hat{A}_i = \hat{A}_i^j \qquad j: 1,2, \dots \dots n_i \qquad (14)$$

Similarly, let $\check{G}^j_i$ denote the j^{th} linguistic value of the linguistic variable $\check{y}_i$ defined over the universe of discourse Y_i . If we assume that there exist many linguistic values defined over Y_i then the linguistic variable $\check{y}_i$ takes on the elements from the set of linguistic values denoted by

$$\check{G}_i = \check{G}_i^P \qquad j: 1,2, \dots \dots m_i \qquad (15)$$

Linguistic values are generally descriptive adjectives such as "big", "medium", and “small”.

For an FLC system, a set of rule has to be defined in order to map the inputs to the outputs. These rules usually have the following form

If (premise) Then (consequent)

The inputs of the fuzzy system are associated with the premise, and the outputs are associated with the consequent. The standard form to represent these rules for a multi-input single-output (MISO) process is:

$$If\ \tilde{u}_1\ is\ \hat{A}_1^j\ and\ \tilde{u}_2\ is\ \hat{A}_2^k\ and\ \ldots\ \tilde{u}_n\ is\ \hat{A}_n^h\ Then\ \hat{y}_q\ is\ \check{G}_q^p \qquad (16)$$

In order to control the system, the designer has to specify an entire set of linguistic rules of this form.

Fuzzy Sets, Fuzzy Logic, and the Rule-Base:

In order to quantify the meaning of linguistic variables, linguistic values, and linguistic rule, fuzzy sets has to be used. Fuzzy sets are set of membership function defined as follow. Let Ui denote a universe of discourse and $\hat{A}_i^j \in \hat{A}_i$ denote a specific linguistic value for the linguistic variable $\tilde{u}_i$. The function $\mu(\tilde{u}_i)$ associated with $\hat{A}_i^j$ that maps U_i to [0, 1] is called a membership function (MF). This membership function describes the "certainty" that an element of U_i , denoted u_i with a linguistic description $\tilde{u}_i$ and may be classified linguistically as $\hat{A}_i^j$. Membership functions are specified and tuned according to the experience or intuition of the designer. These MF's can be triangular, trapezoidal, or Gaussian, each shape will provide a different meaning for the linguistic values that they quantify. The illustration and the mathematical characterization of the triangular membership function are given in Figure 19.

$$\mu^L(u) = \begin{cases} 1 & if\ u \le c^L \\ \max\left(0, 1 + \dfrac{c^L - u}{w^L}\right) & otherwise \end{cases} \qquad (17)$$

$$\mu^C(u) = \begin{cases} \max\left(0, 1 + \frac{u-c}{0.5\,w^C}\right) & if\ u \le c^C \\ \max\left(0, 1 + \frac{c-u}{0.5\,w^C}\right) & otherwise \end{cases} \qquad (18)$$

$$\mu^R(u) = \begin{cases} \max\left(0, 1 + \dfrac{u - c^R}{w^R}\right) & if\ u \leq c^R \\ 1 & otherwise \end{cases} \qquad (19)$$

Where c^L is the left saturation point, w^L is the width of the non-unity and nonzero part of μ^L. c^R is the right saturation point, $w^R$is the width of the non-unity and non-zero part of μ^R. C is the center of the triangle, w^C is the triangle base-width.

Given a linguistic variable $\tilde{u}_i$ with a linguistic value $\hat{A}_i^j$ defined on the universe of discourse U_i and membership function $\mu(u_i)$ that maps U_i to [0,1]. A "fuzzy set" denoted with $\hat{A}_i^j$ is defined as: $\hat{A}_i^j = \left((u_i, \mu_{A_i^j}(u_i)) : u_i \in U_i \right.$

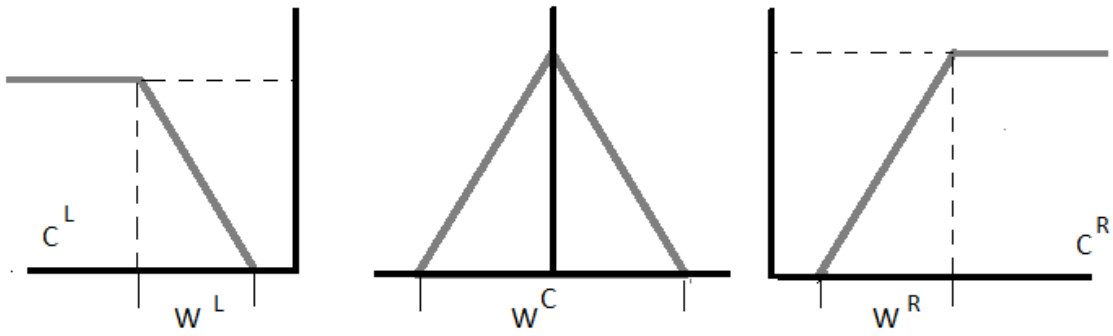

Figure 19: Triangular MF illustrations a) Left, b) Center, c) Right

As a result, a fuzzy set is simply a crisp set of pairings of elements of the universe of discourse coupled with their associated membership values.

Fuzzification:

Fuzzification is the process through which the fuzzy system converts its numerical crisp inputs $u_i \in c$ into fuzzy sets. Let U^*_i denote the set of all possible fuzzy sets that can be defined on Ui. Given ui ϵ Ui , fuzzification transforms u_i to a fuzzy set denoted $\hat{A}_i^{fuzz}$ defined on the universe of discourse Ui. This transformation is produced by the fuzzification operator F defined by

$$F : U_i \rightarrow U_i^* \qquad (20)$$

Where $$F(u_i) = \hat{A}_i^{fuzz} \qquad (21)$$

The Inference Mechanism:

Two basic tasks are performed by the Inference Mechanism namely, matching and inference step. Matching determines the degree to which each rule applies to the situation characterized by the FLC inputs u_i , whereas the inference step uses the FLC input u_i together with the information in the rule-base to draw the fuzzy conclusions.

The first step in matching is to combine inputs with rule premises through finding fuzzy sets. The second step involves finding which rules are ON. To perform inference, we must first quantify each of the rules with fuzzy logic. To do this, we first quantify the meaning of the premises of the rules that are composed of several terms, each of which involves a fuzzy controller input.

Through fuzzification, we quantified the meaning of the linguistic input terms via the membership functions. In order to quantify the "and" operation we form membership values μ (u_1, u_2 ……. u_n) for the i^{th} rule's premise $\mu_{premise}$ that represent the certainty

that each rule premise holds for the given inputs. Considering the general FLC rule given in Figure 18 for a two inputs, single output process

$$If \quad \tilde{u}_1 \ is \ \hat{A}_1^j \quad and \quad \tilde{u}_2 \ is \ \hat{A}_2^k \quad Then \quad \hat{y}_q \ is \ \check{G}_q^p \qquad (22)$$

μ_{premise} can be calculated as follow:

Minimum: Define $\mu_{premise} = \min\left\{\mu_{\hat{A}_1^j}(u_1), \mu_{\hat{A}_1^k}(u_2)\right\}$ that is using the minimum of the membership values.

Product: Define $\mu_{premise} = \mu_{\hat{A}_1^j}(u_1) * \mu_{\hat{A}_1^k}(u_2)$ that is using the product of the membership values.

Both ways of quantifying the "and" operation in the premise indicate that you can be no more certain about the conjunction of two statements than you are about the individual terms that make them up $\left(0 \leq \mu_{premise} \leq 1\right)$. If we consider all possible $\tilde{u}_1$ and $\tilde{u}_2$ values, we will obtain a multidimensional membership function $\mu_{\text{premise}}(\tilde{u}_1, \tilde{u}_2)$ that is a function of $\tilde{u}_1$ and $\tilde{u}_2$ for each rule. The value of this function represents how certain we are that the rule in (22) is applicable for specifying the output to the plant. As $\tilde{u}_1$ and $\tilde{u}_2$ change, the value of μ_{premise} changes and we become less or more certain of the applicability of this rule.

In general, we will have a different premise membership function for each of the rules in the rule-base, and each of these will be a function of $\tilde{u}_1$ and $\tilde{u}_2$ so that given specific values of $\tilde{u}_1$ and $\tilde{u}_2$ we obtain a quantification of the certainty that each rule in the rule-base applies to the current situation.

The second step of matching is to determine which rules are ON to find out which rules are relevant to the current situation. We say that a rule is "ON at time t" if its premise membership function $\mu_{\text{premise}}(\tilde{u}_1, \tilde{u}_2) > 0$. In the next step, the inference mechanism will seek to combine the recommendations of all the rules to come up with a single conclusion.

Inference Step:

The inference step determines which conclusions should be reached when the rules that are on are applied to decide what the output should be. To do this, we will first consider the recommendations of each rule independently. Then later we will combine all the recommendations from all the rules to determine the output. The minimum operation will be used to consider the conclusion reached by each rule; in general, we will never have more than four rules on at one time. Each ON rule will result in a membership function for the conclusion, which we denote by $\mu_{(\text{rule No.})}$ that is given by:

$$\mu_{(rule\ No.)}(y) = \min\left(\mu_{\check{G}}(y), \mu_{premise\ (rule,No)}\right) \qquad (23)$$

This membership function defines the "implied fuzzy set" for the ON rule. Notice that the membership function $\mu_{(rule\ No.)}(y)$ is a time-varying function of y that quantifies how certain the rule will apply and that the minimum operation will generally, "chop off the top" of the $\mu_{\check{G}}(y)$ membership function to produce $\mu_{(rule\ No.)}(y)$. While the input to the inference process is the set of rules that are on, its output is the set of implied fuzzy sets that represent the conclusions reached by all the rules that are on.

Types of Fuzzy Inference Systems:

They are two types of fuzzy inference system and different in the way how the output is determined. These types are the Mamdani type and the Sugeno type. The main difference between Mamdani and Sugeno is that the Sugeno output membership functions are either linear or constant.

Mamdani-type inference, as defined for the toolbox, expects the output membership functions to be fuzzy sets. After the aggregation process, there is a fuzzy set for each output variable that needs defuzzification. It is possible, and in many cases much more efficient, to use a single spike as the output membership function rather than a distributed fuzzy set. This type of output is sometimes known as a singleton output membership function, and it can be thought of as a pre-defuzzified fuzzy set. It enhances the efficiency of the defuzzification process because it greatly simplifies the computation required by the more general Mamdani method, which finds the centroid of a two dimensional function. Rather than integrating across the two-dimensional function to find the centroid, you use the weighted average of a few data points. Sugeno-type systems support this type of model. In general, Sugeno-type systems can be used to model any inference system in which the output membership functions are either linear or constant.

Defuzzification:

A number of defuzzification strategies exist, each provides a means to choose a single output (which we denote with y_q^{crisp}) based on the implied fuzzy sets.

Center of gravity (COG): A crisp output y_q^{crisp} is chosen using the center of area and area of each implied fuzzy set, and is given by

$$y_q^{crisp} = \frac{\sum_{i=1}^{R} b_i^q \int \mu_{\check{G}_q^i}(y_q)\, dy_q}{\sum_{i=1}^{R} \int \mu_{\check{G}_q^i}(y_q)\, dy_q} \qquad (24)$$

Where R is the number of rules, b_i^q is the center of area of the membership function of B_i^q associated with the implied fuzzy set B_i^q for the i[th] rule (j,k,….,l,p,q), and $\int \mu_{\check{G}_q^i}(y_q) dy_q$ denotes the area under $\mu_{\check{G}_q^i}(y_q)$. The COG can be easy to compute since it is often easy to find closed-form expressions for the integral, which is the area under a membership function.

Center-average: A crisp output y_q^{crisp} is chosen using the centers of each of the output membership functions and the maximum certainty of each of the conclusions represented with the implied fuzzy sets, and is given by

$$y_q^{crisp} = \frac{\sum_{i=1}^{R} b_i^q \, sup_{y_q}(\mu_{\check{G}_q^i}(y_q))}{\sum_{i=1}^{R} sup_{y_q}(\mu_{\check{G}_q^i}(y_q))} \qquad (25)$$

Where "sup" which is the "supremum" or the least upper bound, which can often be thought of as the maximum value.

3.2.2 Adaptive Neuro-Fuzzy Inference System (ANFIS)

ANFIS like Neural Network (NN), it consists from layers and these layers are linked together to give the suitable outputs by learning data. In ANFIS, the layers are linked together by using the Fuzzy Inference System (FIS). ANFIS differ from neural network in the number of input and output. ANFIS has a limitation to the input and output data. There is only two inputs (X & Y) and one output (F). The ANFIS system using the Sugeno inference system which consists of two parts, the antecedent part (IF part) and the consequent part (THEN part). Figure.20 demonstrates a simple ANFIS architecture. X&Y are the input for the ANFIS. These input must fuzzify by using the membership functions A1, A2 and B1, B2 [62].

In the Sugeno inference system, the rule can be written in this form:

$$If\ X\ is\ A_1\ and\ Y\ is\ B_1 \quad THEN \quad f_1 = p_1 x + q_1 y + r_1 \tag{26}$$

$$If\ X\ is\ A_2\ and\ Y\ is\ B_2 \quad THEN \quad f_2 = p_2 x + q_2 y + r_2 \tag{27}$$

The ANFIS structure has a Five Layers as shown in Figure 20 and the next part to talk about each layers in details.

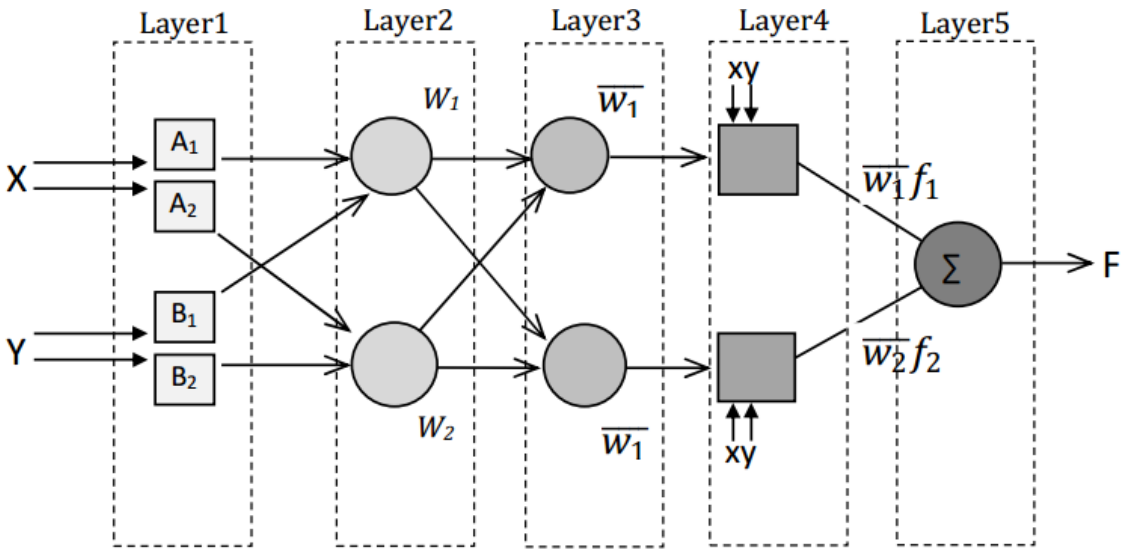

Figure 20: ANFIS architecture

Layer 1:

This layer is used to fuzzify the inputs data by using the membership functions. The number of the nodes depends on the number of membership functions used. It can be three or five or seven nodes. The nodes in this layer can be called an adaptive nodes because it can be changed. The output from these nodes can be given as:

$$O_{1,i} = \mu_{A_i}(x) \qquad for\ i = 1,2 \qquad (28)$$

$$O_{1,i} = \mu_{B_{i-2}}(x) \qquad for\ i = 3,4 \qquad (29)$$

Where, X represent the input value which is a crisp value, μ is the membership function and $O_{1,i}$ is the membership value for two inputs. The subscripted 1 and i represent the layer number and node number. The triangle shaped, the trapezoidal shaped and the gaussian shaped can be used to represent the μ (membership functions). Usually, the bell shaped is the famous one used and can be given by:

$$\mu_A(x) = \frac{1}{1 + \left|\frac{x - c_i}{a_i}\right|^{2b_i}} \qquad (30)$$

Where a_i, b_i and c_i are the boundary of the membership function and they are determined by the training process.

Layer 2:

In this layer, the output from each node in layer 1 will be the input for the node in layer 2. So, the nodes in this layer can be called a fixed nodes. Each node in layer 2 multiply all signals come from the nodes in layer 1 and the product is performing the node output. This output represent the strength of a Sugeno rule and this can be represented as:

$$O_{2,i} = w_i = \mu_{A_i}(x)\, \mu_{B_i}(y) \quad for\ i = 1,2 \qquad (31)$$

Layer 3:

In this layer, the values which are coming from layer 2 are normalized. Every output from layer 2 is divided by the sum of all output from the nodes in layer 2 and we can describe the node as a fixed node. It is given by:

$$O_{3,i} = \bar{w}_i = \frac{w_i}{w_1 + w_2} \quad for\ i = 1,2 \qquad (32)$$

Layer 4:

In this layer, the value of the output linear function parameters are determined by the learning process (p,q and r). The node here described as adaptive node and given by:

$$O_{4,i} = \bar{w}_i f_i = \bar{w}_i(p_i x + q_i y + r_i) \quad for\ i = 1,2 \qquad (33)$$

Where p_i, q_i and r_i is the consequent parameters.

Layer 5:

In this layer, there is only one node. This node sum all the values coming from the nodes in the layer 4 and gives the final output. It can be described as a fixed node and given by:

$$O_{5,i} = \sum_i \overline{w}_i f_i = \frac{\sum_i w_i f_i}{\sum_i w_i} \quad for\ i = 1,2 \qquad (34)$$

Training Process (Learning Algorithm):

ANFIS can predict the correct output if the parameters are optimized and adapted in a correct way. So the training process is important. In this process, the ANFIS use the training data sets to determine these parameters and optimized to be sure that the ANFIS can work with a high accuracy. The rule in the Sugeno inference system can be divided to two parts, the first one is the nonlinear parameters which is called the premise parameters and a linear parameters or rules parameters which is called the consequent parameters [63].

They are many learning algorithms which are proposed and developed by the researchers. In this work, a hybrid learning method is used. It is estimated the suitable ANFIS parameters by using the back propagation (BP) method and least square estimation (LSE) method [6262].

So, there is a premise parameters and consequent parameters. These parameters must determine through the learning process. LSE is applied, during that the premise

parameters are not changed and the consequent parameters are calculated. This can be called the forward pass learning method. Then, back propagation method is applied, during that the consequent parameters are not changed and the premise parameters are calculated. This can be called the backward pass algorithm.

In the learning process, there are two output data, one from the training data set and the other is the predicted output during the training process. LSE calculates the error between those output the consequence parameters are modified and adapted by this calculated error. The same thing is applied in the backward pass, the error between the two outputs is calculated and used in the back propagation gradient descent method to update the premise parameters.

3.2.3 MPPT Controller Using ANFIS

MPPT techniques can be classified in two categories as literature: basic MPPT techniques and artificial intelligent techniques. Because of the non-linear behavior of the output characteristics of the PV panel, the artificial intelligent methods are more useful in improving the efficiency of the MPPT controller comparing to the basic techniques. In fuzzy logic, it is easy to deal with the non-linear equations. It converts the linguistic terms to numerical values and numerical values to linguistic terms using membership functions. Neural network is mapping the input output nonlinear equations as multilevel neural networks, so it is good in the nonlinear system. But it works as a black box and does not have the heuristic nature. The ANFIS is coming to make a hybrid system

combined from the fuzzy logic principle and the neural network map to reduce the drawbacks and the difficulty and integrated the advantages.

In the ANFIS controller, there is a need to a training data. This training data depends on the system which is integrated to the ANFIS. In our system, ANFIS controller connected to PV panel. So, the input-output data can be obtained from the PV model which is explained in the beginning of this chapter.

The training parameters are:

N_{MAX}: $_N$umber of training data points.

T_{MIN}: Minimum Temperature.

T_{MAX}: Maximum Temperature.

G_{MIN}: Minimum Irradiation.

G_{MAX}: Maximum Irradiation.

Where, T_{MIN} and T_{MAX}: the minimum and the maximum of the PV panel temperature, G_{MIN} and G_{MAX}: the minimum and the maximum for the irradiation values in the same location where the PV is installed. Figure.22 shows the flow chart for the process to generate the training data using in the ANFIS-based MPPT.

Now, the way to generate the training data is known. These training data set generates at random operation conditions with specified range. So it contains all the possible situations that can be happen during the day. After that, the voltage which is given the maximum power at these weather conditions is stored. This voltage value can be

determined by solving the transcendental non-linear equation Eq.2 and the proficient numeric technique (Newton-Raphson method). This operation is repeated until the input training data is finished. Then, the ANFIS-based MPPT controller is ready to design.

In the ANFIS-based MPPT controller, the input is the weather conditions (in our case, irradiation and temperature) and the output from the ANFIS controller is the voltage reference (Vref). This reference voltage value converts to a pulse and this pulse controlled the switch device in the DC-DC converter. This controlled switch force the PV panel to work on specific operation points and maintained the reference value to get the maximum power at these irradiation and temperature.

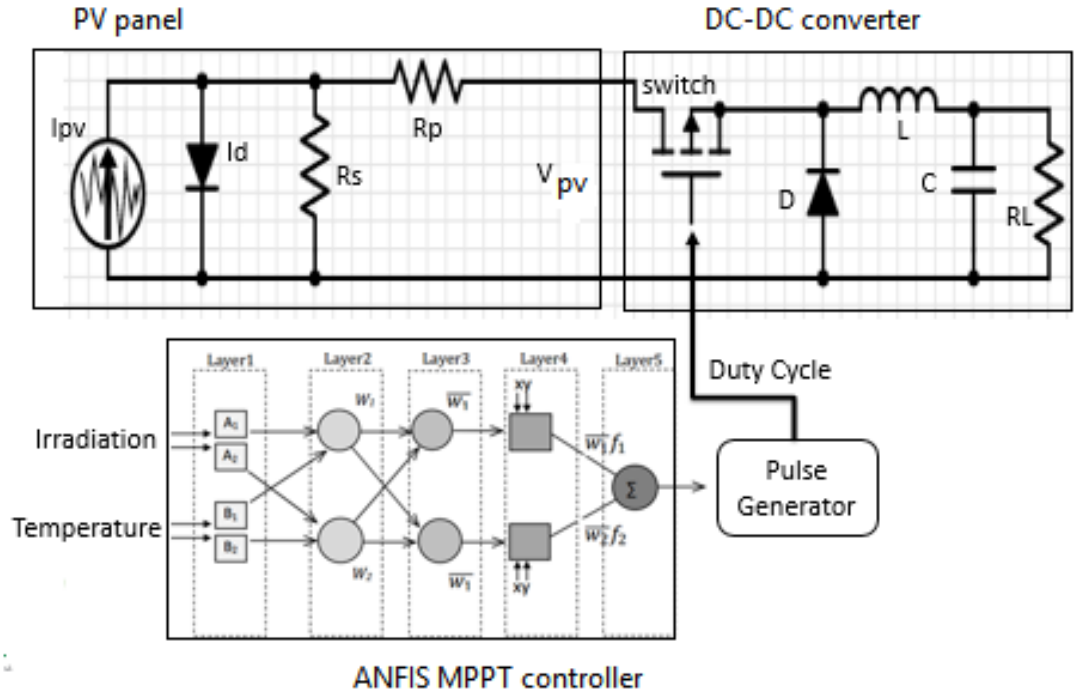

Figure 21: PV System with MPPT Controller

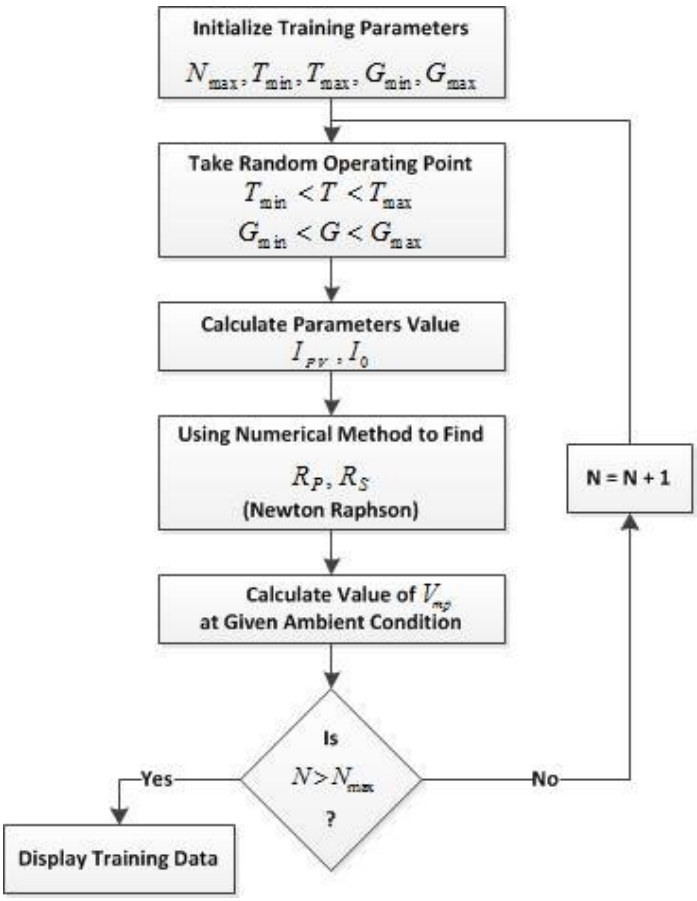

Figure 22: Proposed method flow chart to generate data set for ANFIS training

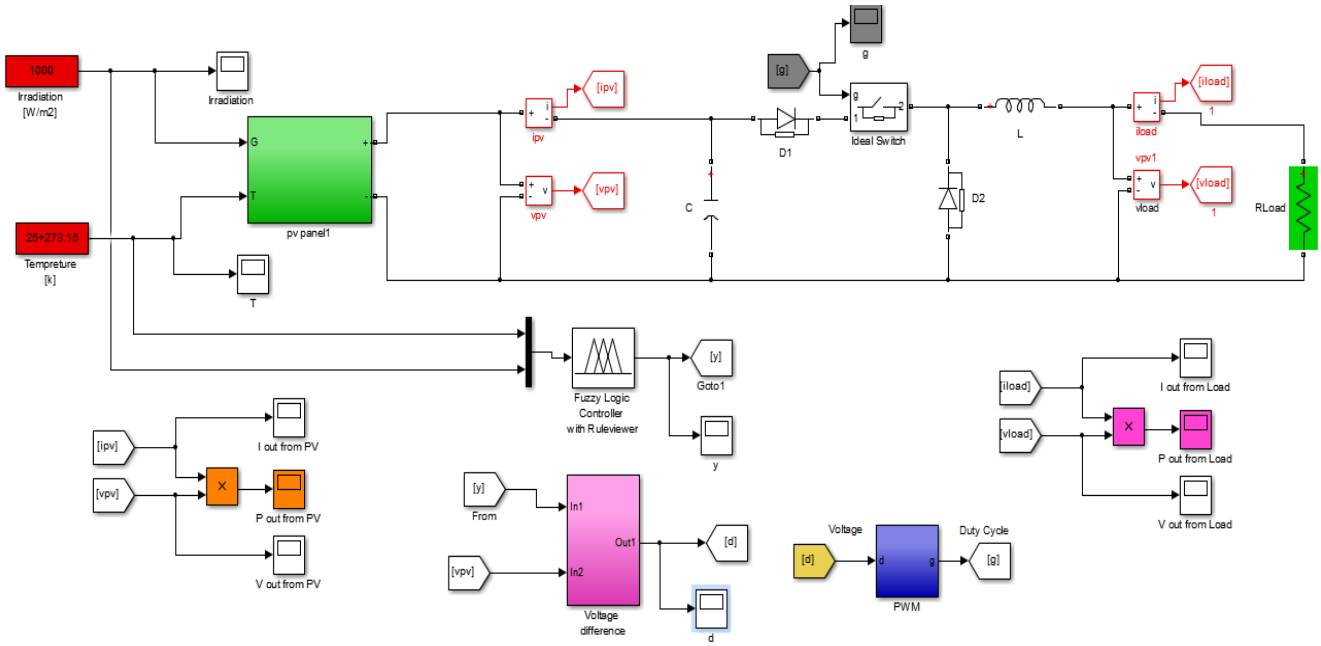

Figure 23: ANFIS controller integrated to PV system in Matlab/Simulink

3.2.4 ANFIS Testing

The proposed ANFIS-based controller is tested by connecting to the whole system Figure.23. The system consists from a PV panel, DC-DC buck converter, MPPT controller and load. The PV voltage depending on the weather conditions (irradiation & temperature in our case). Buck converter is utilized to control the voltage and step-up or step-down according to the load. MPPT is controlled the switch device in the DC-DC converter. This controlled switch force the PV panel to work on specific operation points and maintain the reference value to get the maximum power at these irradiation and temperature.

PV panel specifications and parameters are shown in Table 1. Buck converter can work in two modes, first mode is the continuous conduction mode (CCM) and the second one discontinuous conduction mode (DCM). Only one of this modes can be used, so buck converter can design as CCM or DCM. The values of inductor and the capacitor are determined the chosen mode. In our system, the buck converter is designed as CCM and the values of its parameters are: C_1= 180 μF, L= 5 mH, C_2= 90 μF and switching frequency is 5 KHz.

In the training process, the values of its parameters to generate the data are: N_{MAX} = 2000, T_{MAX} = 80ºC, T_{MIN} = 0ºC, G_{MAX} = 2000 W/m2 and G_{MIN} = 0 W/m2. In the training process, the generated data must cover all the possible situations that can be happen.

After that, ANFIS controller is ready to design. All dynamic data required is available. Matlab/Simulink is used to develop the proposed ANFIS controller. As mention before, all training data must fuzzify by using the membership functions. In our case, the bell

shaped function is used and the number of membership functions for each input is five. Then, the LSE method and Back propagation method are use in the forward pass and in the backward pass to adapt the premise and consequent parameters.

ANFIS takes the irradiation level and the temperature degree as an input. According to these values, it gives the reference voltage which the PV panel must operate at this value. Then we calculated the voltage difference between the PV voltage and the reference voltage from ANFIS. This calculated voltage compare to a saw-tooth signal to generate the suitable pulse width modulation signal and the switch device in the buck converter can be on / off related to this controlling PWM signal. Every value for the irradiation and temperature have a PWM signal different from other.

We can take two cases, the first case if we supposed the value of irradiation around 1000 w/m^2 and the temperature degree equal 25^0C.

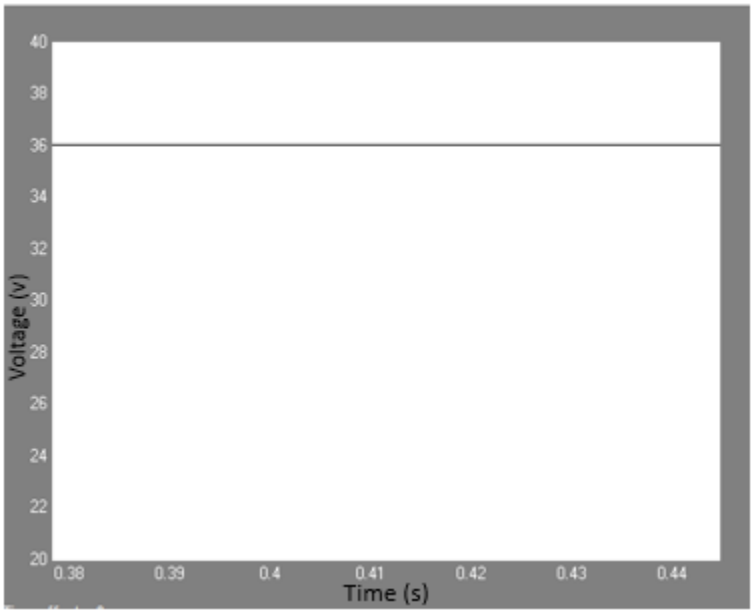

Figure 24: Reference voltage generated by ANFIS controller.

Figure 24 shows the reference voltage that PV panel must work on it. Figure 25 shows the PWM signal that generated for this specific reference value. The PV voltage must change to work on the reference value and this illustrated in Figure 26.

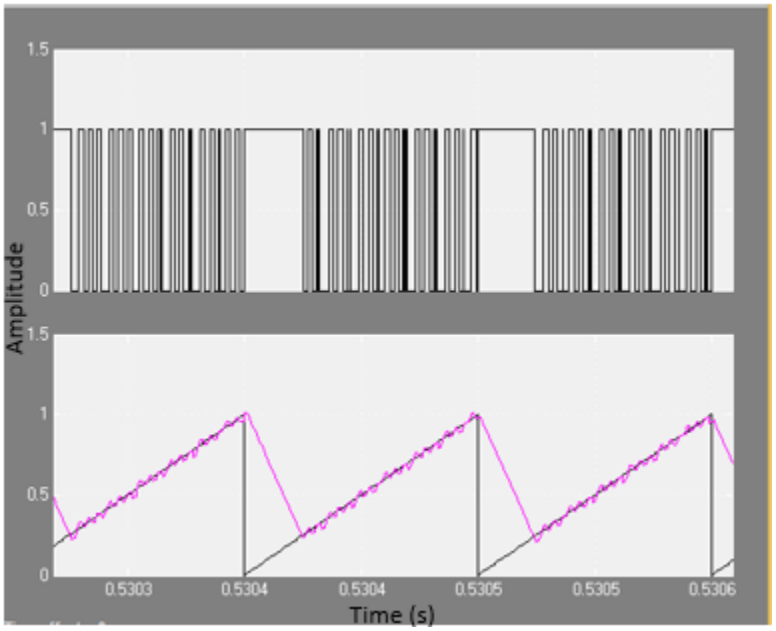

Figure 25: PWM signal.

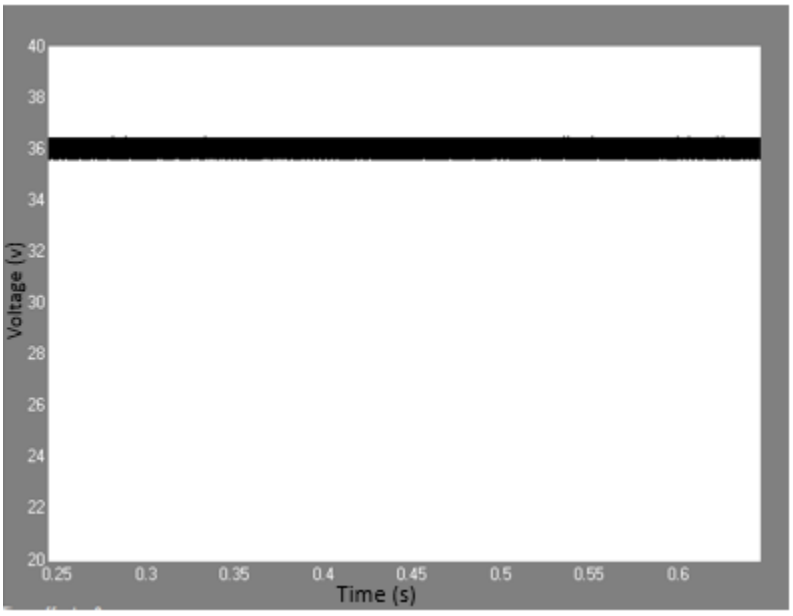

Figure 26: PV voltage after applied ANFIS-MPPT controller.

The second case if we supposed the value of irradiation around 800 w/m^2 and the temperature degree equal 45^0C. Figure 27 shows the reference voltage that PV panel must work on it.

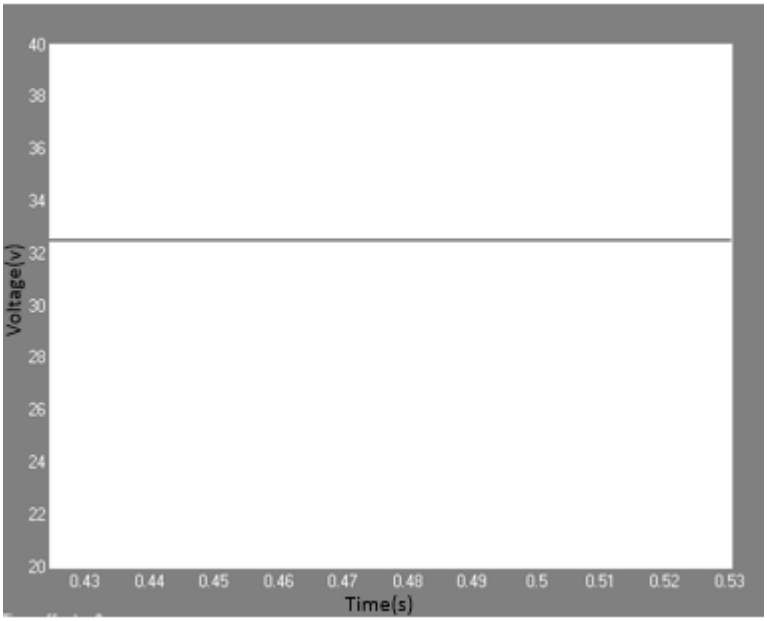

Figure 27: Reference voltage generated by ANFIS controller.

Figure 28 shows the PWM signal that generated for this specific reference value. The PV voltage must change to work on the reference value and this illustrated in Figure 29.

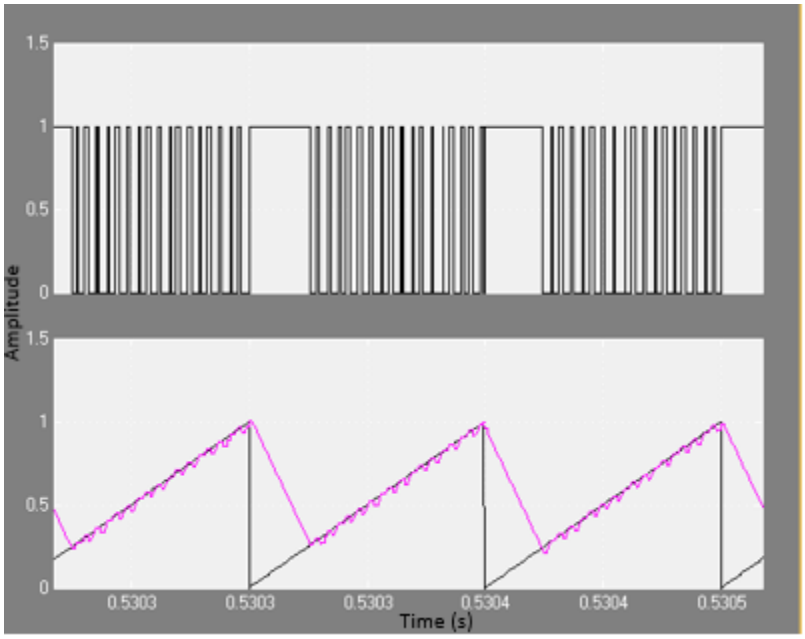

Figure 28: PWM signal.

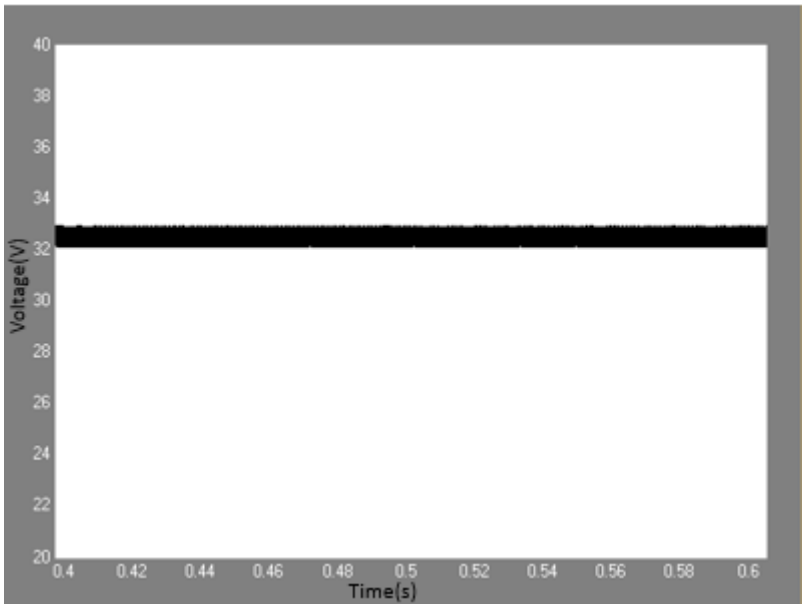

Figure 29: PV voltage after applied ANFIS-MPPT controller.

CHAPTER 4

EXPERIMENTAL SETUP

In this chapter a brief description for the components which are used to verify the proposed ANFIS-based MPPT controller. The PV panel is developed and prepared to connect direct to the DC-DC converter and load. The ANFIS-based MPPT controller is designed on dSPACE controller. All the setup is developed in the Department of Electrical Engineering, King Fahd University of Petroleum and Minerals (KFUPM) under the supervision of Dr. Chokri Ahmad.

4.1 Experimental Setup Components

4.1.1 LabVIEW environment experimental

The developed system is used to monitor and analyze a stand-alone photovoltaic system located at KFUPM campus, Dhahran, Saudi Arabia. This system is formed by a solar panel, environmental parameters and irradiation sensors, isolation amplifier, resistive load banks and compact data acquisition instrument (DAQ). The entire system is monitored and controlled by LabVIEW environment.

Figure 30 shows the block diagram of the stand-alone PV system experimental setup. The panel has a maximum power of 150 W, open circuit voltage of 43.2 V, short circuit current of 4.49 A, maximum power voltage of 36 V and maximum power current of 4.16

A. All of these characteristics are under clean standard test condition of 1000 W/m^2 at 25º C. The panel has a length of 1580 mm, width of 808 mm and the actual irradiation exposed area of 1.5 m^2. The panel are installed and exposed to whole day sun irradiation and inclined are fixed angle of 23º from horizontal surface. Two temperature sensors Type-E are used. The first one is dedicated to measure the ambient temperature and the second one to measure the panel temperature. These data are processed in an input module having model number NI 9211 and transferred to PC by using the National instrument device Compact DAQ chassis and controllers model number NI 9178. The continuous irradiation measurement is conducting using the Eppley Radiometer (Pyranometer) device having model number 36353F3 and this voltage are connected to the national instrument input module having model number NI 9239. The voltage of the Pyranometer are multiplied by a factor ($8.22 * 10^{-6}$ $V/W/m^2$) to get the actual value of the irradiation in W/m^2. Panel voltage and current are measured through LEYBOLD four channel highly linear, noise-immune isolating amplifiers model number (735 261). The conditioned currents and voltages are channeled to LabVIEW environment through National instrument module input NI 9263 and transfer to PC through the same Compact DAQ chassis and controllers model number NI 9178.

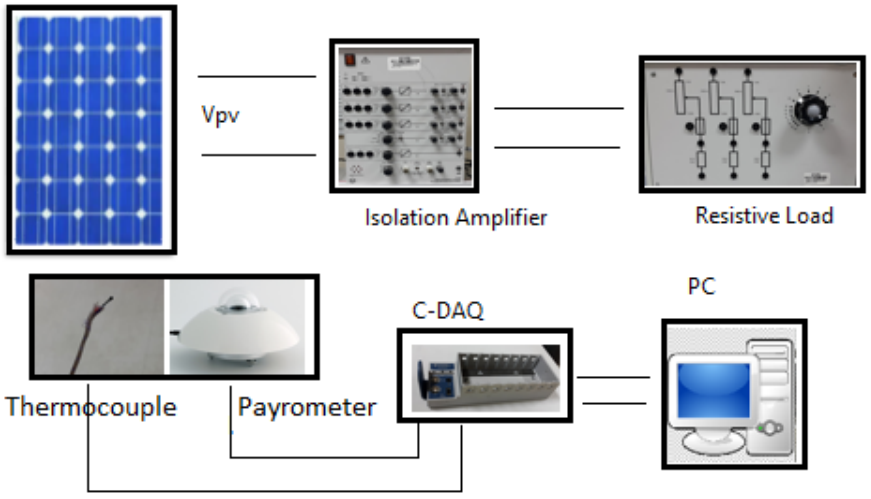

Figure 30: Block Diagram of LabVIEW System Development

Figure 31: NI Chassis c-DAQ 9178

Figure 32: NI 9263 Analog Output Module

Figure 33: NI 9239 Analog Input Module

Figure 34: NI 9211 Thermocouple Input.

4.1.2 dSPACE Controller

The dSPACE controller offers an inclusive solution for electronic control unit (ECU) software development. It can be a useful tool for the purposes depending on the function prototyping, target implementation, and ECU testing. The dSPACE can design and

implement the real time control systems. In this study, a controller board dSPACE DS1103 R&D is used. It is a standard board that can be plugged into a PCI (Peripheral Component Interconnect) slot of a PC. This board can handle the applications which need a digital controllers and real time simulations because it can follow the high-speed multivariable changes. It is a complete real-time control system based on a 603 PowerPC floating-point processor running at 250MHz. For advanced I/O purposes, the board includes a slave-DSP subsystem based on the TMS320F240 DSP microcontroller. The dSPACE DS1103 Controller Card is shown in Figure 35.

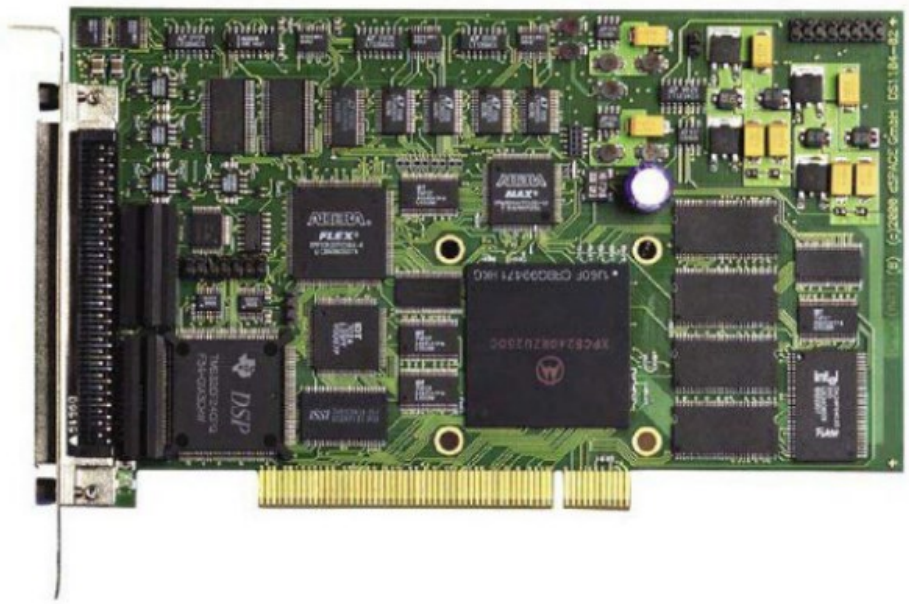

Figure 35: dSPACE controller card.

To connect an external signal from the I/O connector (100-pin I/O connector) on the board to the D-sub miniature connectors an adapter cable is used. So, during the Sub-D connectors, a one can make a high-density connection between the board and the devices of your application. To get a good interface to the input and output signals of the DS1103

Controller Board and access to control them, a specific interface connector panels (CP1103) are used. Therefore, the connection between the DS1103 controller board and the devices that connected to it is easier. A BNC (Bayonet Neill–Concelman) connectors and Sub-D connectors are used to connect or disconnect or interchanged the devices to the DS1103 controller board. This simplifies system construction, testing and troubleshooting. Besides to the CP1103, They are an array of LEDs illustrated the states of the digital signals which is called a Combi Panel Connector/LED (CLP1103).

From the above discussion, the easiest way to deal with the I/O signals of the board is to use the special interface connector and connector panels which help in the RCP (Rapid control prototyping). Thus, the dSPACE DS1103 Controller Board is the best device for RCP applications. Characteristic of using the dSPACE in the applications work on the Matlab/Simulink platform. A control desk which is a graphical user interface can be another advantage to use the dSPACE controller. In this graphical interface, the user can monitor, observe, display and plot any system signal running through the dSPACE controller. The dSPACE needs an interface to help in working which is called the Real Time Interface (RTI). This interface can be joining between the MATLAB/SIMULINK and dSPACE real-time systems. The run process for the Simulink model by using the RTI is simple and the model can easily execute on dSPACE real-time hardware. The RTI generates a C code for the model and then running in the real time. When the Simulink model is ready to use and the input and the output of the system are determined, the real time interface generates the C code from the model. The file generated from the RTI has an extension .sdf while the Simulink mode file has the .mdl as an extension. This .sdf generated file are using in ControlDesk – software which can give us the ability to

monitor and manage the real time and Simulink experiments. The dSPACE connecter panel (PCI) controller board is shown in Figure 36.

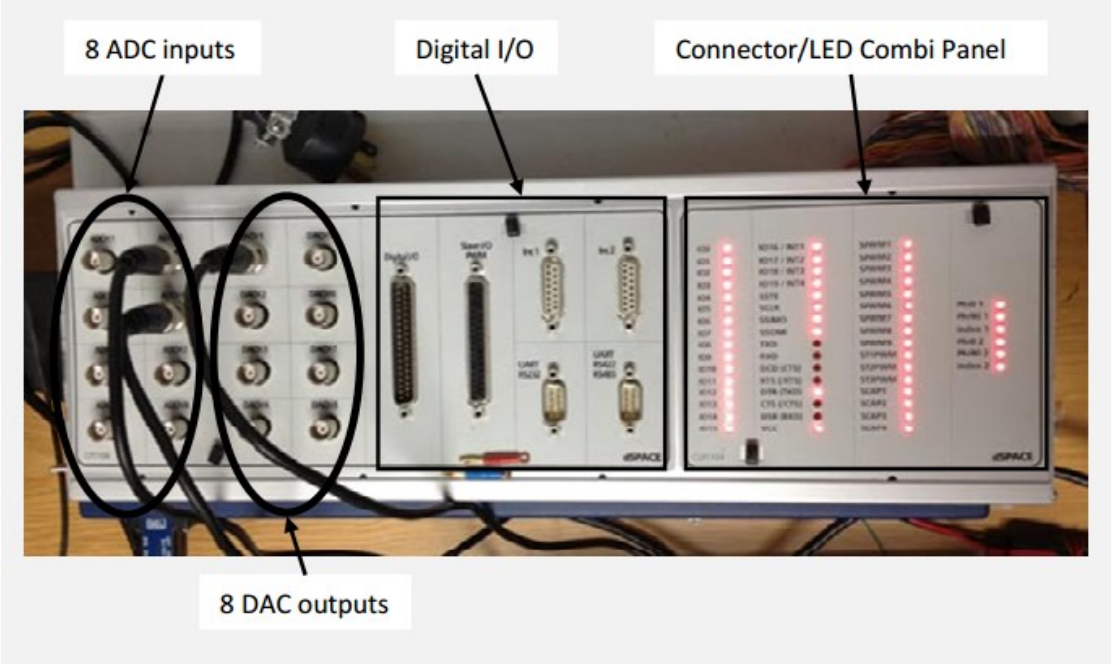

Figure 36: dSPACE panel connector board.

4.1.3 Design Buck Converter

The weather conditions are continuously changing with time, which keeps varying the MPP. So the need to a maximum power point tracking controller (MPPT) is necessarily. Instead of connected the PV panel direct to the load a DC-DC converter (buck converter) can operate as an interface between the PV panel and the load to apply the principle of the MPPT.

The main purpose from using the buck converter is achieving and controlling the maximum power point for the PV panel. The buck converter has an input and output, the input side is connected to the voltage which is coming from the PV panel (VPV), this

input is not constant and depends on the irradiation and temperature conditions. The output side from the buck converter provides a constant voltage and connected to the load. MPPT can control the buck converter by changing the duty ratio of the switch device. In addition, it determines the suitable value for the duty ratio which can help to suck the maximum power from the PV panel under the changing ambient conditions. Without this controlling form the MPPT and the buck converter, PV panel cannot be able to operate at full efficiency.

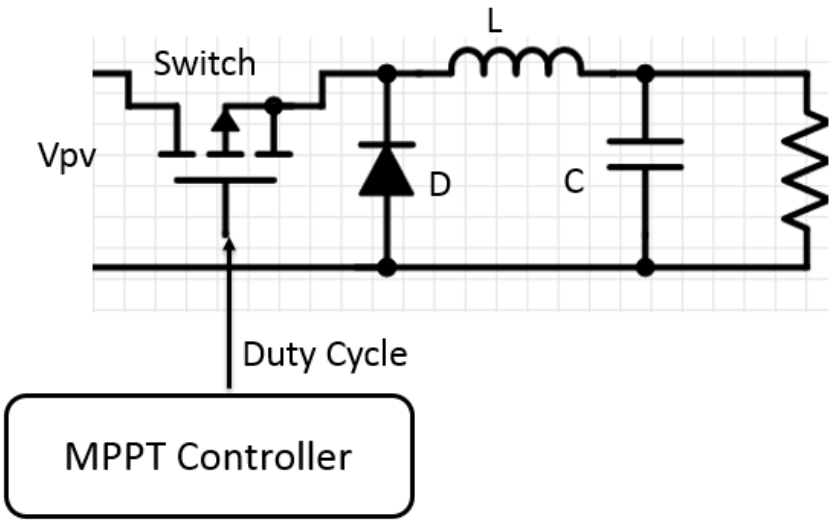

Figure 37: Buck Converter with MPPT Controller

The buck converter consists from a DC input voltage (in our case V_{PV}), Switch device (controlled by the MPPT controller), Diode (D), Inductor (L), Capacitor (C) and Resistance (R). From the Figure 37, when the switch (S) is on, the diode is in the reverse bias and the inductor is charging. After the inductor charged, the current pass and go to the resistance. If the switch (S) is off, the charge on the inductor is reduced and the diode works in the forward bias. The voltage appeared on the resistance was depending on the

time at which the switch is on or off. So, there is a factor called Duty Ratio (D) defined as a ratio when the switch is on divided by the sum of the on and off times.

$$D = \frac{T_{ON}}{T_{ON} + T_{OFF}} \qquad (35)$$

Where T=1/f is the period of the switching frequency.

The average output dc voltage on the resistance can give in this relationship

$$V_{out} = D * V_{IN} \qquad (36)$$

From this relation, the output voltage always smaller than the input voltage. The buck converter can operate in two modes according to the inductor current. The first one is the Continuous conduction mode (CCM) which is the inductor current is greater than zero and the Discontinuous conduction mode (DCM). In our application, the buck converter designed in the CCM because it is giving a high efficiency and good utilization. The value of the inductor determines the operation mode for the buck converter and it is given by

$$L_b = \frac{(1 - D) * R}{2f} \qquad (37)$$

So, the value of the inductor used in the buck converter should be greater than the boundary value (L_b) to work in the CCM. The value of the capacitor can effect on the output ripple voltage. Capacitor depends on the value of the inductor which is used in the circuit and it is given by

$$C_{min} = \frac{(1 - D)}{8 * L * f^2} \qquad (38)$$

The value of capacitor should be greater the C_{min} value. Equation (37) & (38) are the key design equations in the buck converter.

In our practical work, the PV panel is the input source or the buck converter (V_{OC} = 43 V and I_{SC} = 5 A). A MOSFET switch device is used (BUZ 312 transistor). Heat sink is connected to the switch to dissipate the heat generated by the source. The values of the inductor and the capacitor are calculated (L= 100mH, C= 180 μF). Finally, there was problem of the low current capability of the inductor. There is an inverse relation in the value of the inductance and the current capability (inductance increased, the current capability decreased). So, to overcome this problem, the inductor was connected in series and parallel combination to get the appropriate value and also handling the current.

4.2 Building MPPT in dSPACE

The proposed ANFIS--based MPPT controller designed in chapter 3 is implemented in real domain using dSPACE DS1103 shown in Figure 38. Inputs to the proposed controller are irradiation and temperature and these are represented by DS1103ADC_C3 and DS1103ADC_C4 blocks in real time SIMULINK model, respectively. These blocks are obtained from a dSPACE library in SIMULINK and convert the analog signal to digital signal. Here ADC in the name of the blocks depicts the analog to digital conversion. Similarly the output of the proposed controller is V_{REF} and represented by DA1103DAC_C5 and converts the digital signal to analog (DAC). Basically these blocks are used to integrate the dSPACE controller with external analog signals and devices. In our case these blocks are linked to the signals come from LabVIEW. DS1103ADC_C1,

DS1103ADC_C3 and DS1104ADC_C4 blocks are accepted the analog signals of Panel Voltage (Vpv), irradiation (G) and temperature (T) as input. In the same way, DA1104BIT_OUT_G2 is sending the control signal back to DC-DC converter. The gain blocks in Figure 38 are used to get the actual values of inputs. The value of Vref is converted to pulses in Matlab, then it generates from the output digital port DA1104BIT_OUT_G2. After designing the controller in the Simulink next step is to set time-step of a model to 100µsec to synchronous with the time-step of dSPACE. In every time-step, the designed MPPT controller (DS1103) monitors the input quantities (irradiation and temperature) and after making the decision, based on the designed algorithm, generates the controlled output signal (*D*). Real time implementation of a controller should run continuously for infinite time therefore set the stop time to infinite. Then the designed controller is converted into real time code and becomes ready to work in a real time domain.

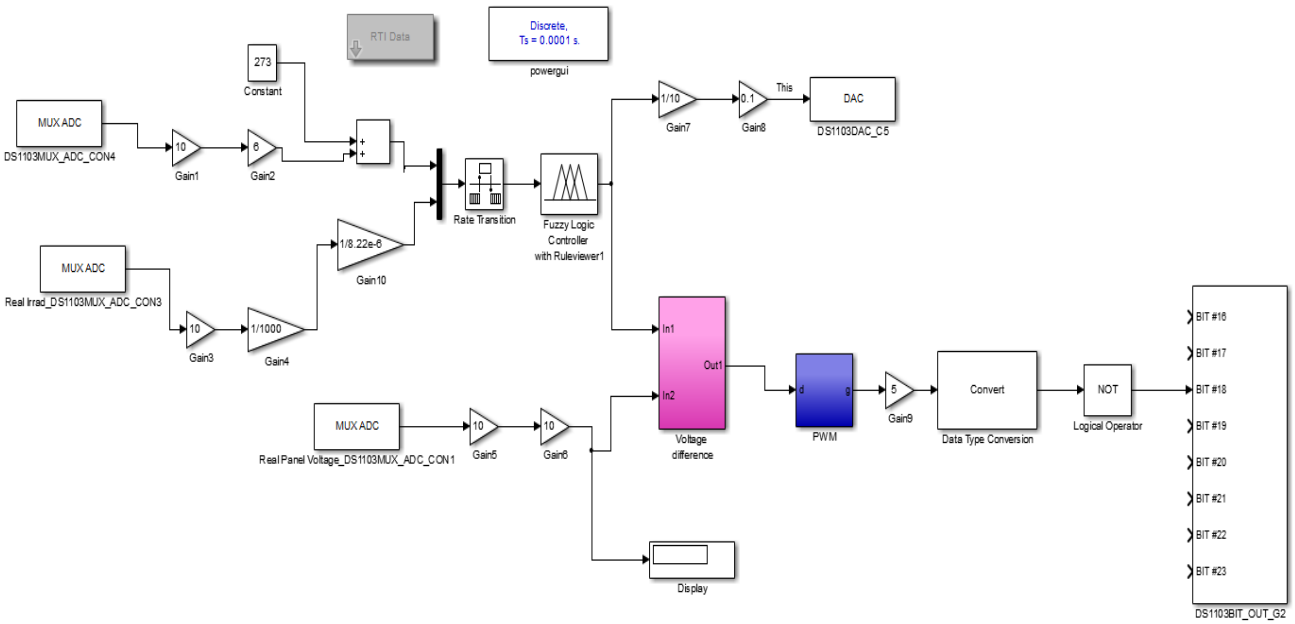

Figure 38: ANFIS-based MPPT controller in Simulink to build in dSPACE.

4.3 Integrated all the system and LabVIEW Development

LabVIEW software manages communication between CPU and the I/O modules. Measurement & automation explorer (MAX) software tool is used for the configuration of data acquisition hardware device and the software. This tool creates tasks, channels, scales, interfaces and virtual instruments. The serial instrument or device includes software utilities and hardware drivers for communication, and also includes the documentation on the stop bits, parity bits, baud rates, and packet size that the instrument used. In LabVIEW programming, computer processors can execute the code when the graphical icons are joined and wired together, and then directly compiled to machine code. A block diagram functions in the data flow path that actually dictates when and in what order the program will execute. All inputs data must be available at a node for execution, and then it carries out data to its output and supplies to the next node in the path. We also used Express VIs (Virtual Instrument) that simplifies common programming tasks and algorithm creation. DAQ Assistant Express VI is used on the block diagram and configures it to execute the function. The DAQ Assistance Express VI prompts you to select the channels you want to send and receive data to I/O module (DAQ), and configure parameters like terminal configuration, scales, sample rate, triggering, and synchronization, see Figure 39. After completing the configuration, the LabVIEW development environment writes the necessary code (represented by the Express VI) for you which actually is the task of reading real outer signals into inner files for analysis. In the front panel we configure and customize the control parameters to communicate with serial port and in the block diagram window we connect the blocks for serial connection.

Figure 40 shows LabVIEW data processing path coming from the data acquisition system through the Express DAQ Assistant. The VI allows to setup different channels for parameters with scaling factor and corresponding calibration of each channel. The instantaneous values of all variables like voltages, currents, temperature and irradiation could then be processed, analyzed, used for online control, online display and storage.

I and V data are measured and P is calculated. The data points are collected in an array and then converted to dynamic format in order to build the corresponding X and Y axis.

The temperature and irradiation are measured as a voltage signals. So, it is converted to the actual values by doing different simple mathematical operations. Calibration process is needed especially to the temperature values. The calibration are doing by VelociCale Plus device (model #: 8386A). After that, these temperature and irradiation values are transmitted to the dSPACE analog input through output module NI 9263. Finally all measured data are stored in a measurement file and in Excel format. The dSPACE runs ANFIS-based on MPPT and generate the suitable duty ratio that controls the switch device in the buck converter. This forces the PV panel to work at specific operation point and extract the maximum power at that weather conditions.

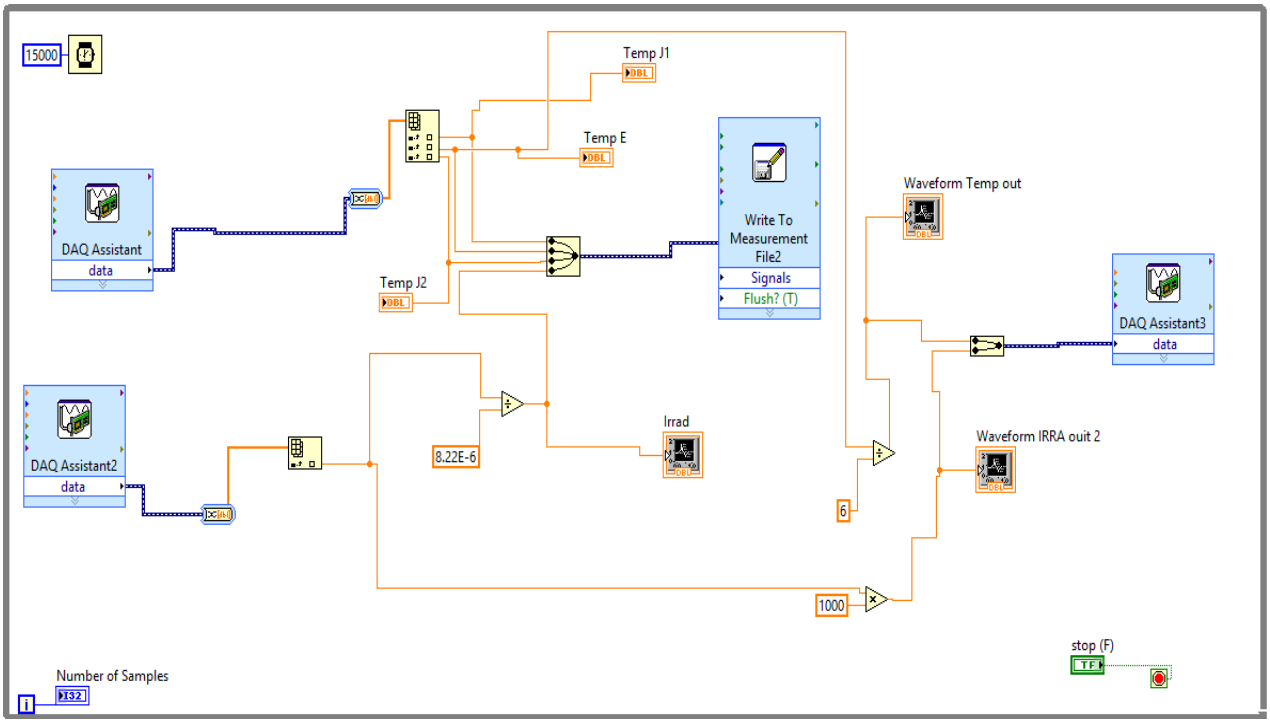

Figure 39: DAQ Assistant data processing

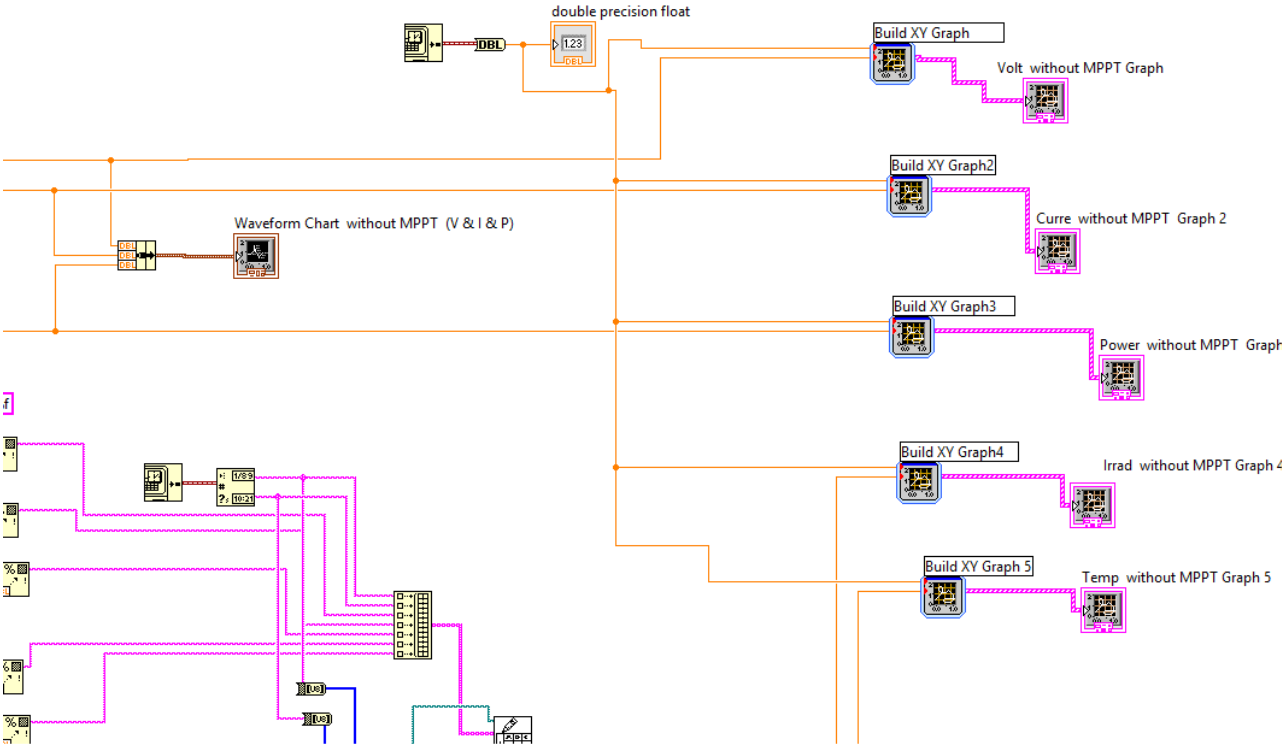

Figure 40: Developed module for I-V and P-V curves

CHAPTER 5

RESULTS AND DISCUSSION

In this chapter, simulation and experimental results for the proposed ANFIS-based MPPT are illustrated. Four different tests are discussed to verify the effectiveness of the proposed controller. These tests are step-up change in the irradiation, step-down change in irradiation, step-up change in temperature and step-down change in temperature. Then, experiment results are illustrated to verify our proposed technique.

5.1 Step-up Change in Irradiation

This is the first test under step-up changing in the irradiation level. In this test, the value of the temperature is constant and equal 25^{o}C. Figure 41 shows the irradiation level is constant with a value 500 W/m^2 during the period from 0s up to 0.25s and then is rapidly increasing to 1000 W/m^2. The value of power is changed according to the irradiation level. When the value of irradiation is high, the PV panel generates more power. Figure 42 shows the P-V curves for the two values of irradiation. When the irradiation level is 500 W/m^2 (graph labeled as B) and the temperature is 25^{o}C, the maximum power can PV panel generates is around 69 W. If the irradiation level are increased to 1000 W/m^2 (graph labeled as A), the operation point for the PV panel is changed and the panel gives a maximum power around 150 W.

PV panel is integrated to the ANFIS-based MPPT, buck converter and the load. As a result, it must follow these changed in the irradiation level and force PV panel to work at

specific operation point to generate maximum power as shown in Figure 43. It can be seen from the graph that the ANFIS controller follows the changing in the irradiation level and PV panel generates the MPP at each irradiation levels.

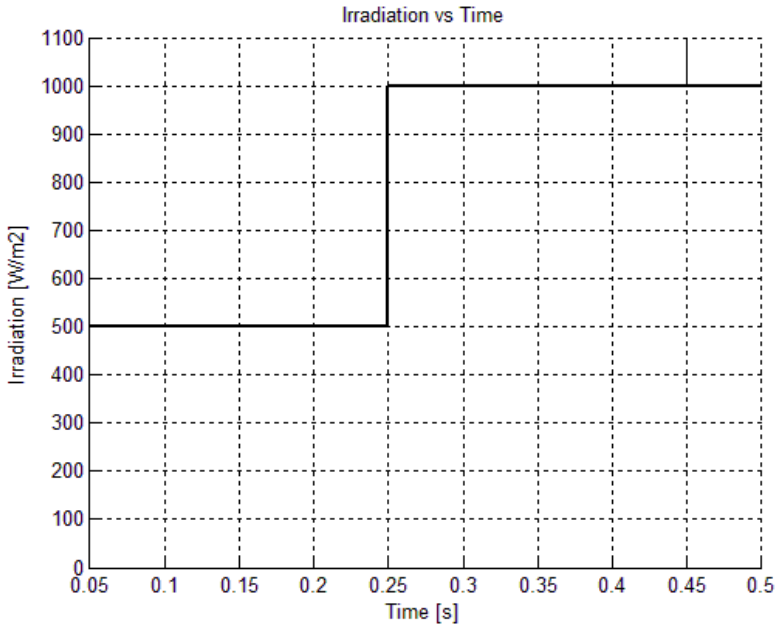

Figure 41: Setup-up irradiation pattern

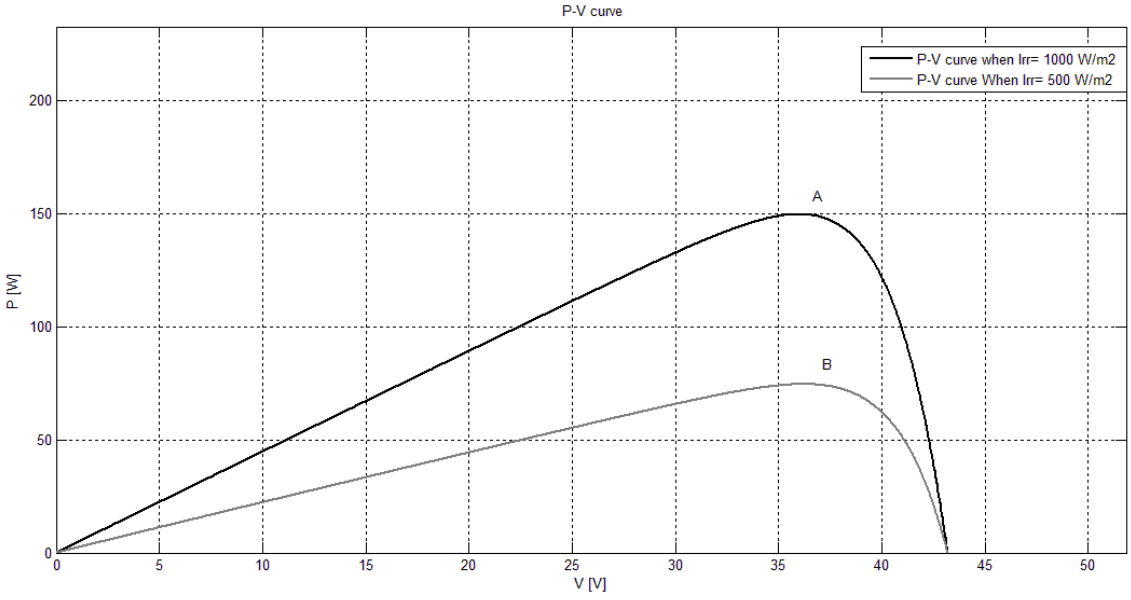

Figure 42: PV curve under normal and low irradiation conditions.

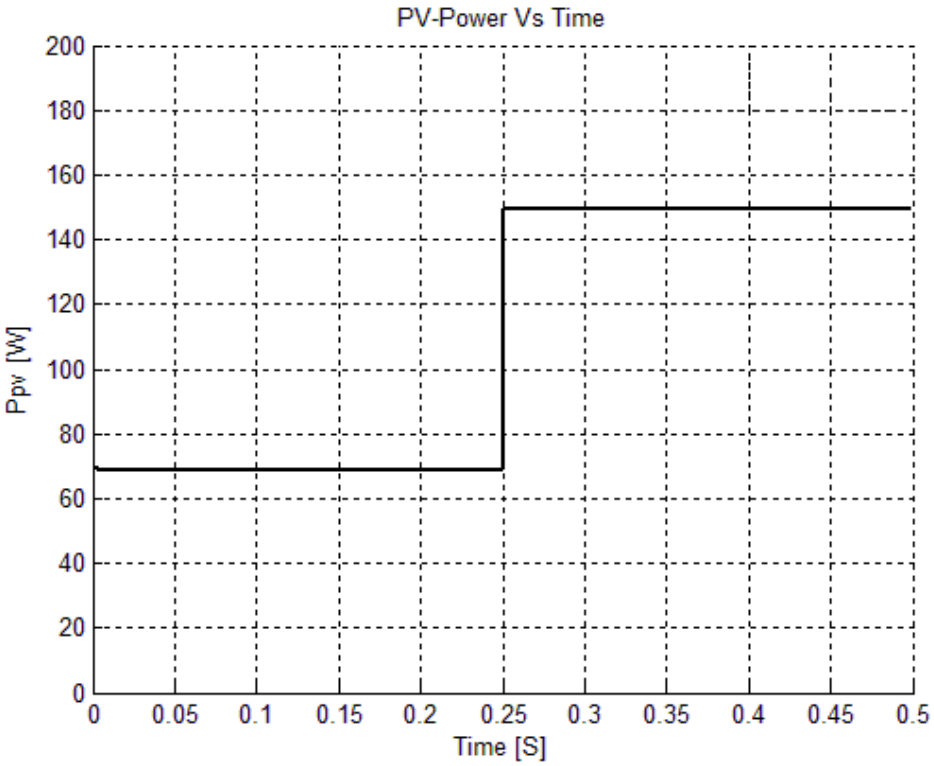

Figure 43: Characteristics of PV power output under step-up irradiation change

The simulation results for the reference voltage comes from the ANFIS controller which is generated the correct pulse (Duty Cycle) to drive the switch device in the buck converter , PV array voltage (V_{PV}) and current (I_{PV}) are shown in Figure 44, Figure 45, Figure 46, respectively, and verify the effectiveness of the proposed MPPT under the rapidly changing irradiation condition.

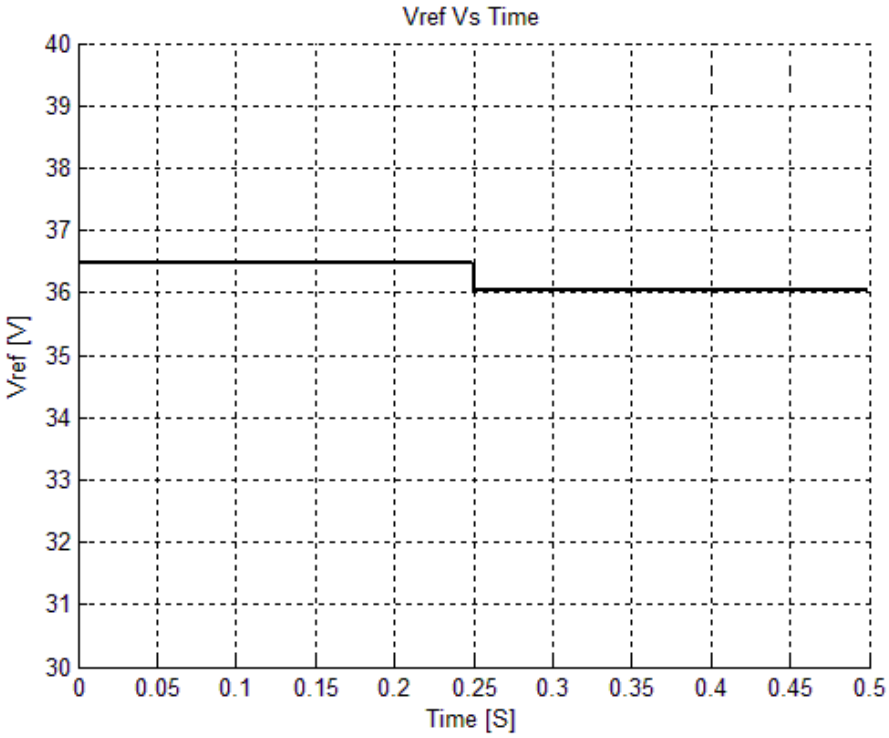

Figure 44: Plot of reference voltage under step-up change in irradiation

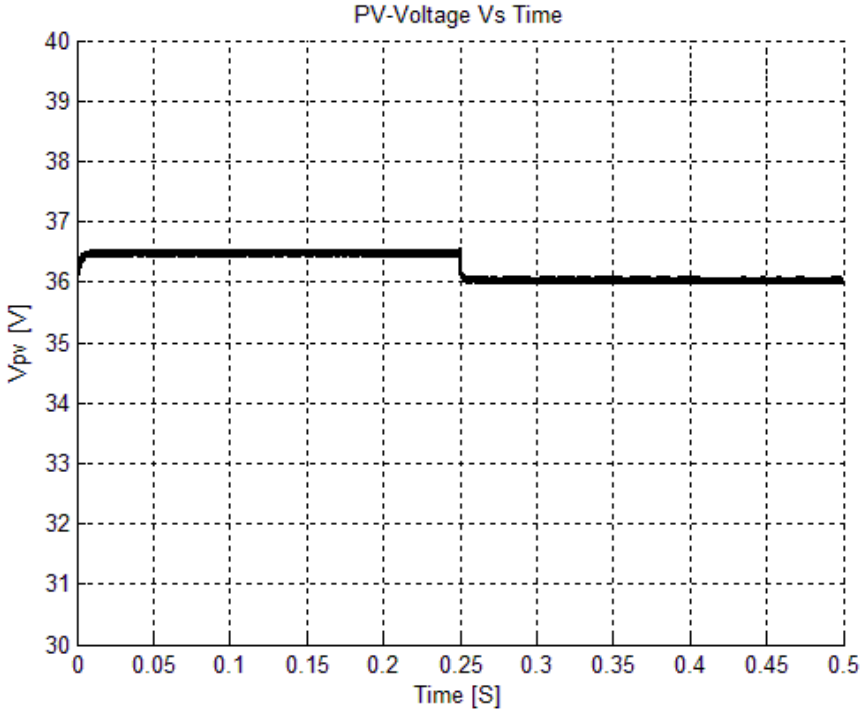

Figure 45: Characteristics of PV voltage under step-up irradiation change.

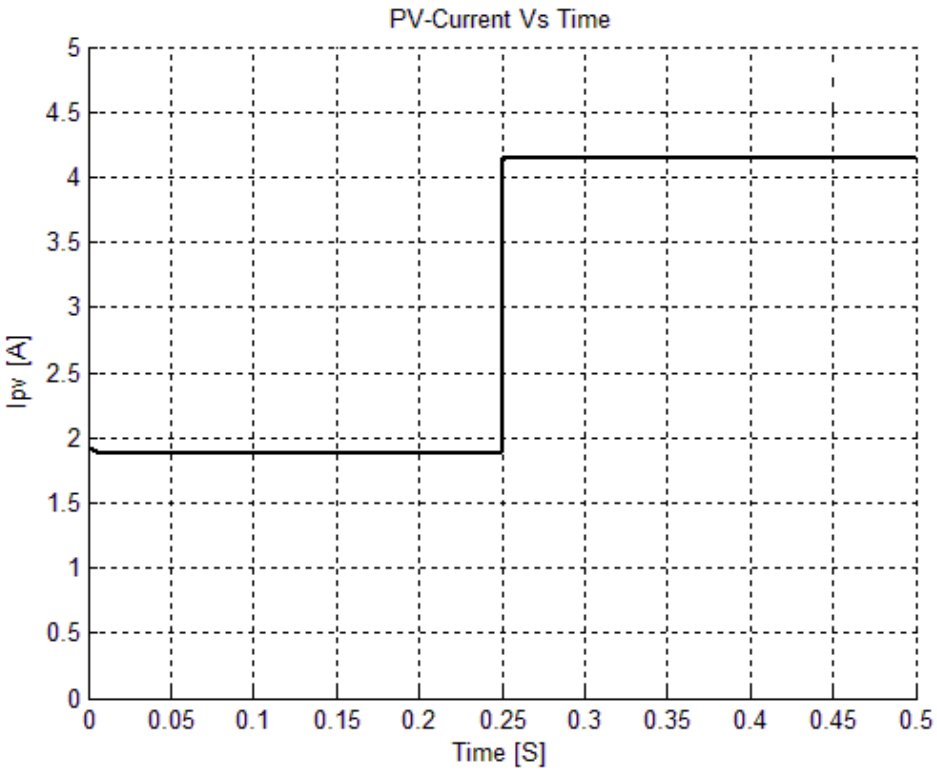

Figure 46: Characteristics of PV current under step-up irradiation change.

5.2 Step-down Change in Irradiation

This is the second test under step-down changing in the irradiation level. In this test, the value of the temperature is constant and equal 25ºC. Figure 47 shows the irradiation level is constant with a value 1000 W/m^2 (graph labeled as A) during the period from 0s up to 0.25s and then is rapidly increasing to 500 W/m^2 (graph labeled as B). The value of power is changed according to the irradiation level. When the value of irradiation is high, the PV panel generates more power. Figure 48 shows the P-V curves for the two values of irradiation. PV panel is integrated to the ANFIS-based MPPT, buck converter and the load. As a result, it must follow these changed in the irradiation level and force PV panel

to work at specific operation point to generate maximum power as shown in Figure 49. It can be seen from the graph that the ANFIS controller follows the changing in the irradiation level and PV panel generates the MPP at each irradiation levels.

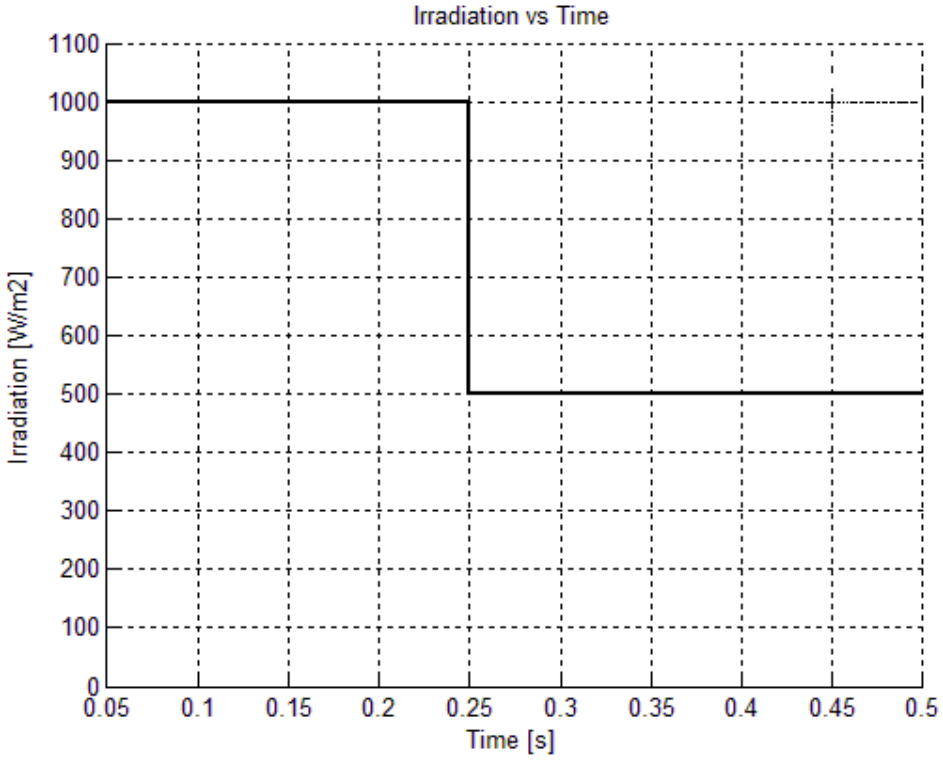

Figure 47: Setup-down irradiation pattern

The simulation results for the reference voltage comes from the ANFIS controller which is generated the correct pulse (Duty Cycle) to drive the switch device in the buck converter , PV array voltage (V_{PV}) and current (I_{PV}) are shown in Figure 50, Figure 51, Figure 52, respectively, and verify the effectiveness of the proposed MPPT under the rapidly changing irradiation condition.

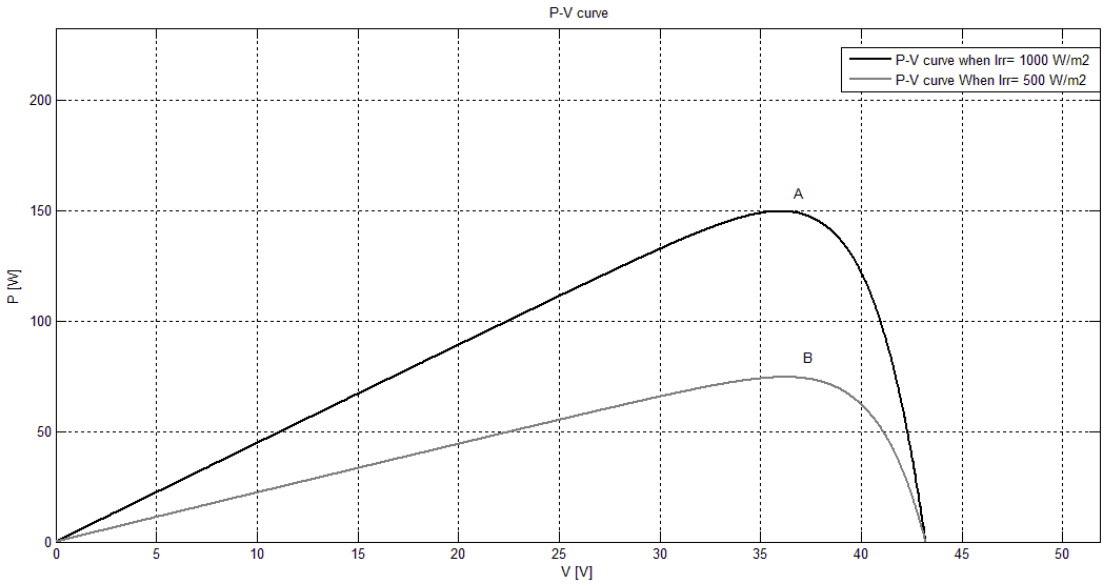

Figure 48: PV curve under normal and low irradiation conditions.

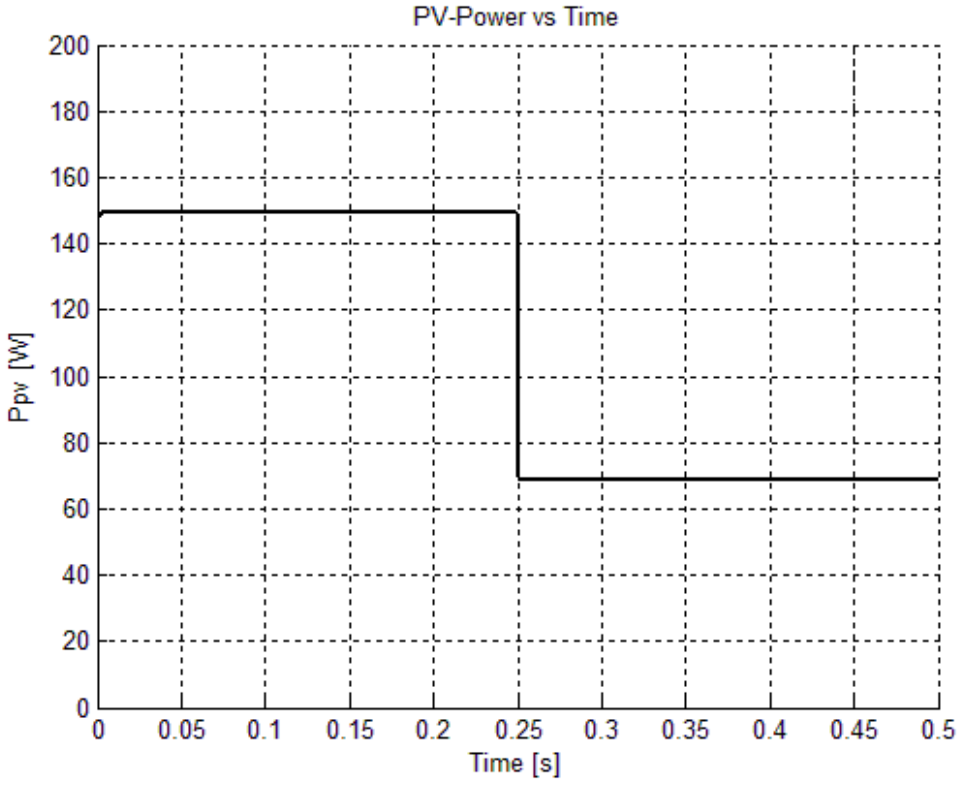

Figure 49: Characteristics of PV power output under step-down irradiation change.

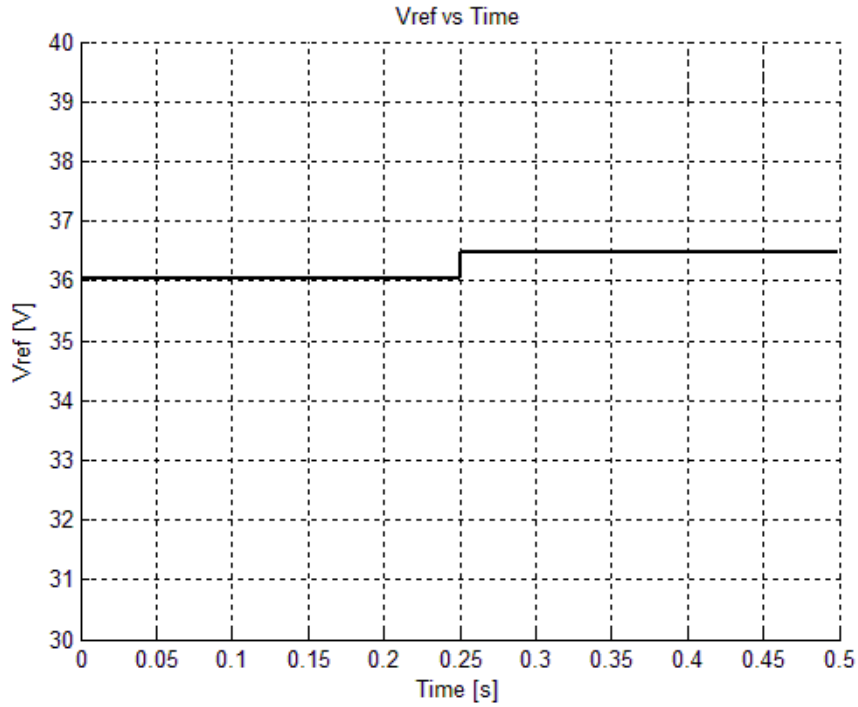

Figure 50: Plot of reference voltage under step-down irradiation change.

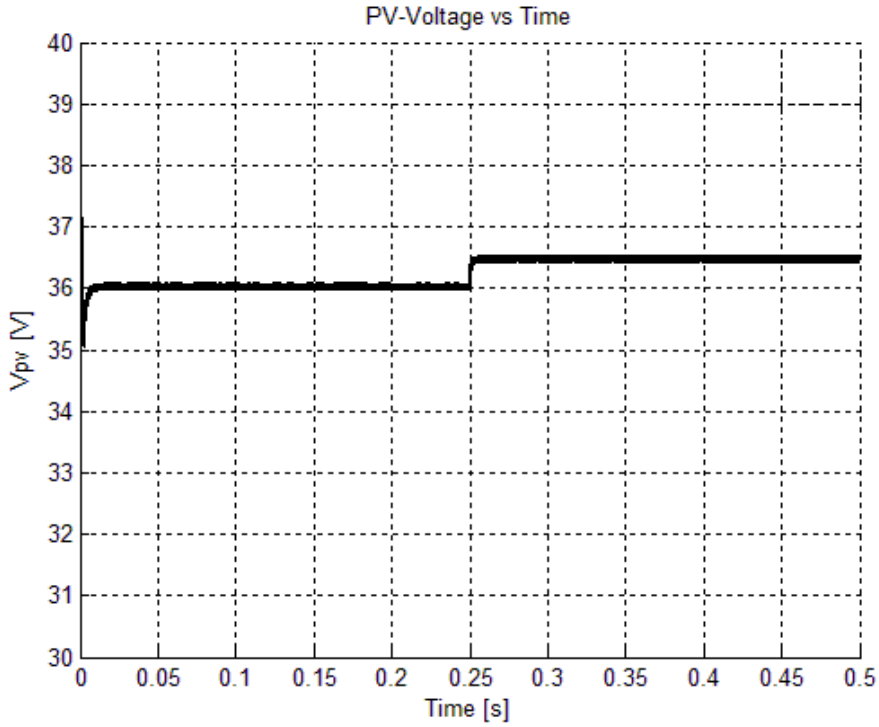

Figure 51: Characteristics of PV voltage under step-up irradiation change.

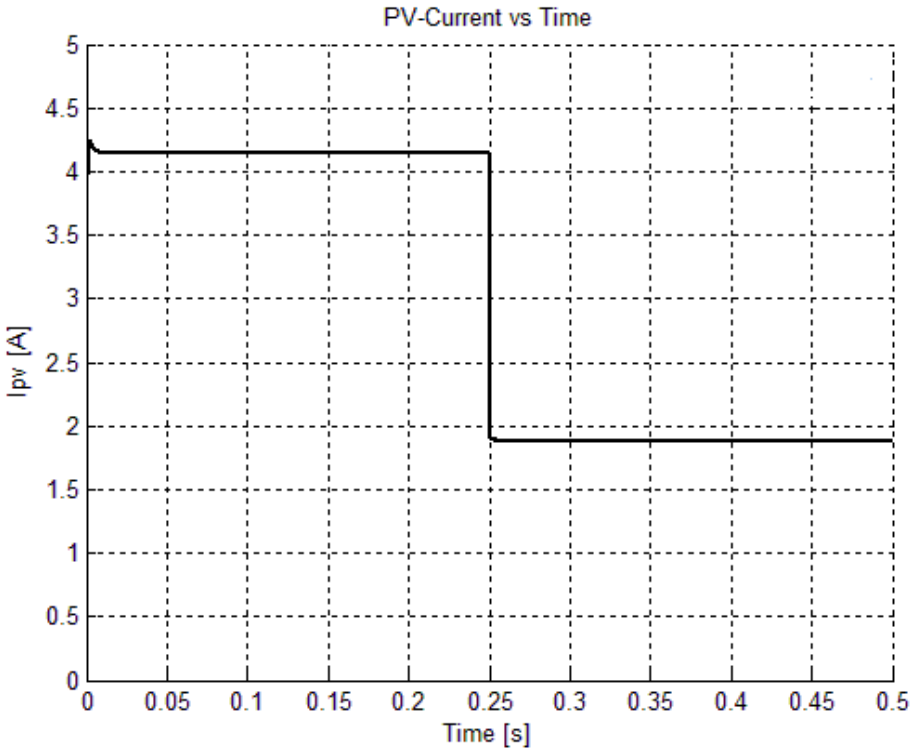

Figure 52: Characteristics of PV current under step-up irradiation change.

5.3 Step-up Change in Temperature

This is the third test under step-up changing in the temperature degree. In this test, the value of the irradiation is constant and equal 1000 W/m^2. Figure 53 shows the temperature degree is constant with a value 15^{o}C (graph labeled as A) during the period from 0s up to 0.25s and then is rapidly increasing to 25^{o}C (graph labeled as B). The value of power is changed according to the temperature degree. When the value of temperature is low, the PV panel generates more power. Figure 54 shows the P-V curves for the two values of temperature. When the temperature degree is 15^{o}C and the irradiation is 1000 W/m^2, the maximum power can PV panel generates is around 69 W. If the temperature

degree is increased to 25°C, the operation point for the PV panel is changed and the panel gives a maximum power around 150 W.

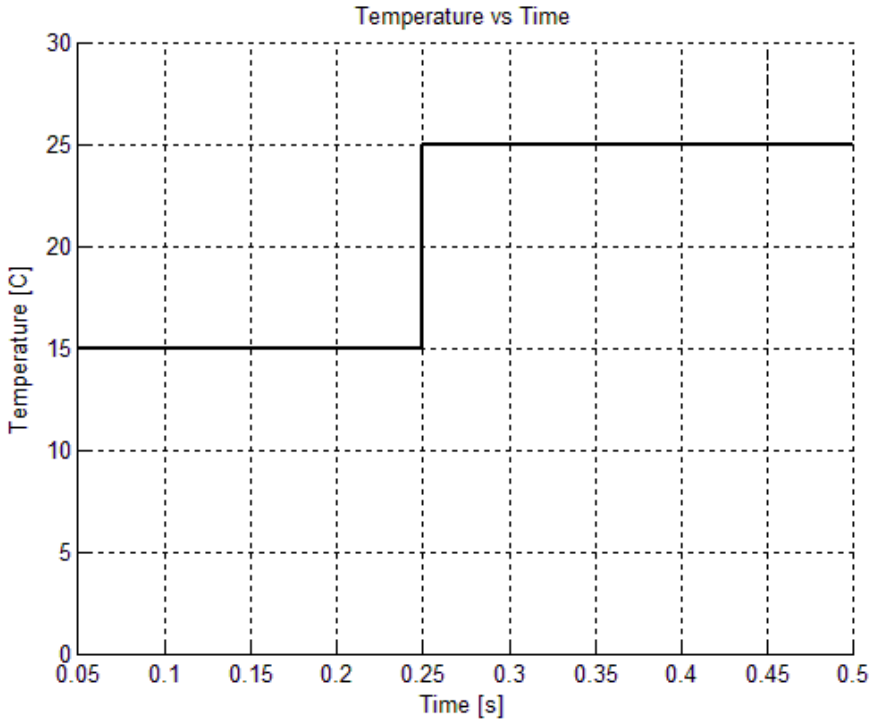

Figure 53: Step-up temperature pattern

PV panel is integrated to the ANFIS-based MPPT, buck converter and the load. As a result, it must follow these changed in the temperature degree and force PV panel to work at specific operation point to generate maximum power as shown in Figure 55. It can be seen from the graph that the ANFIS controller follows the changing in the temperature degree and PV panel generates the MPP at each temperature degree.

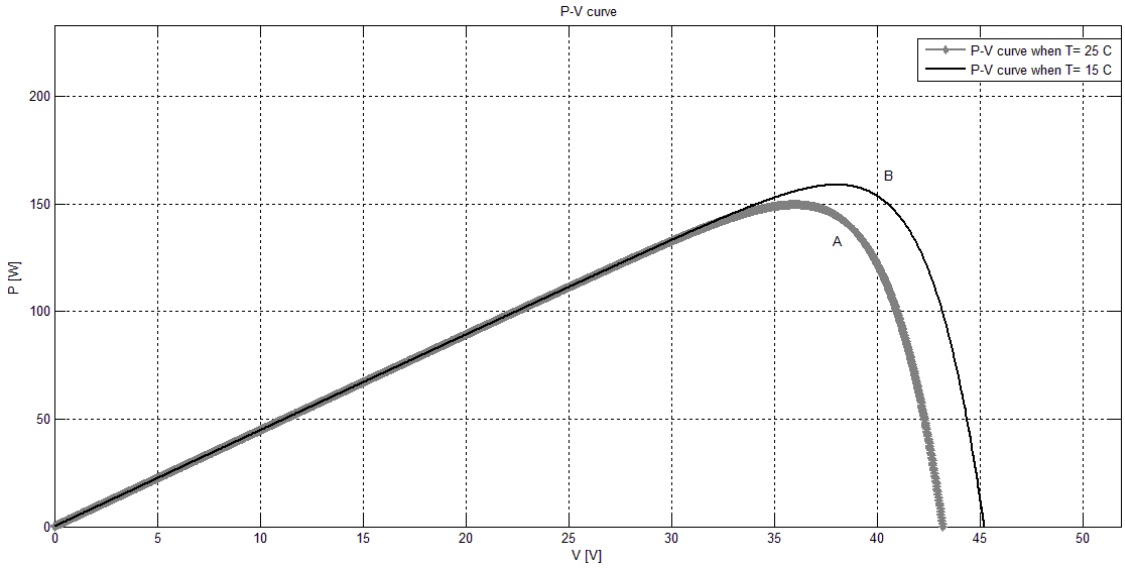

Figure 54: PV curve under normal and low temperature conditions.

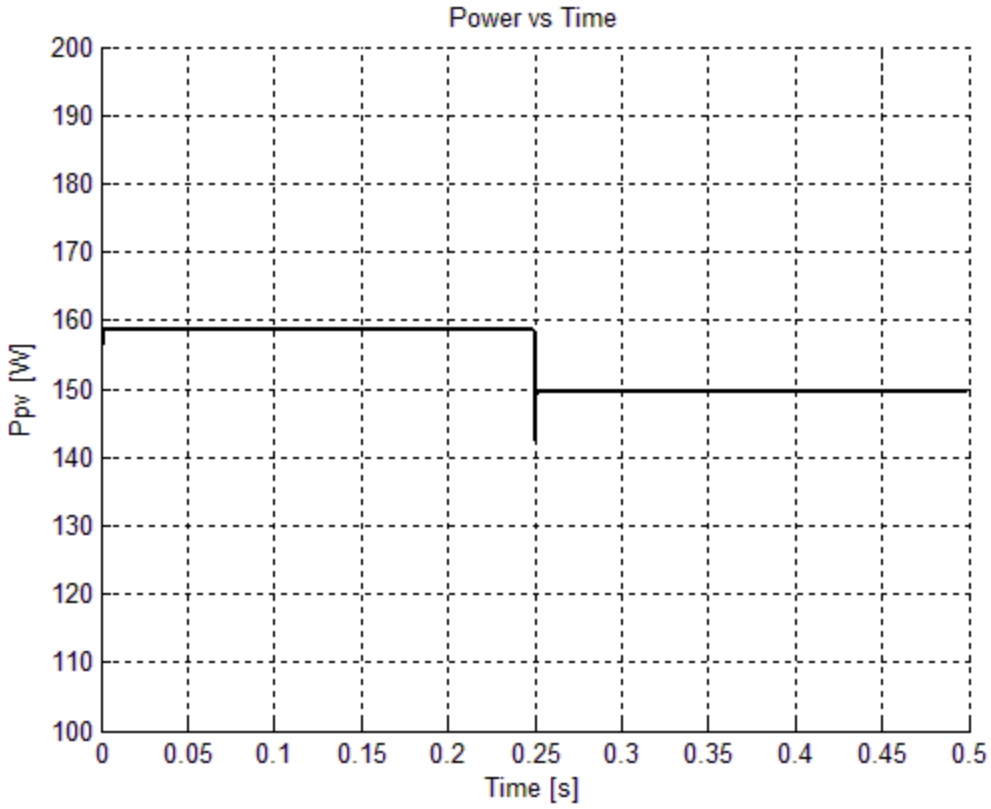

Figure 55: Characteristics of PV power output under step-up temperature change.

The simulation results for the reference voltage comes from the ANFIS controller which is generated the correct pulse (Duty Cycle) to drive the switch device in the buck converter , PV array voltage (V_{PV}) and current (I_{PV}) are shown in Figure 56, Figure 57, Figure 58, respectively, and verify the effectiveness of the proposed MPPT under the rapidly changing temperature degrees.

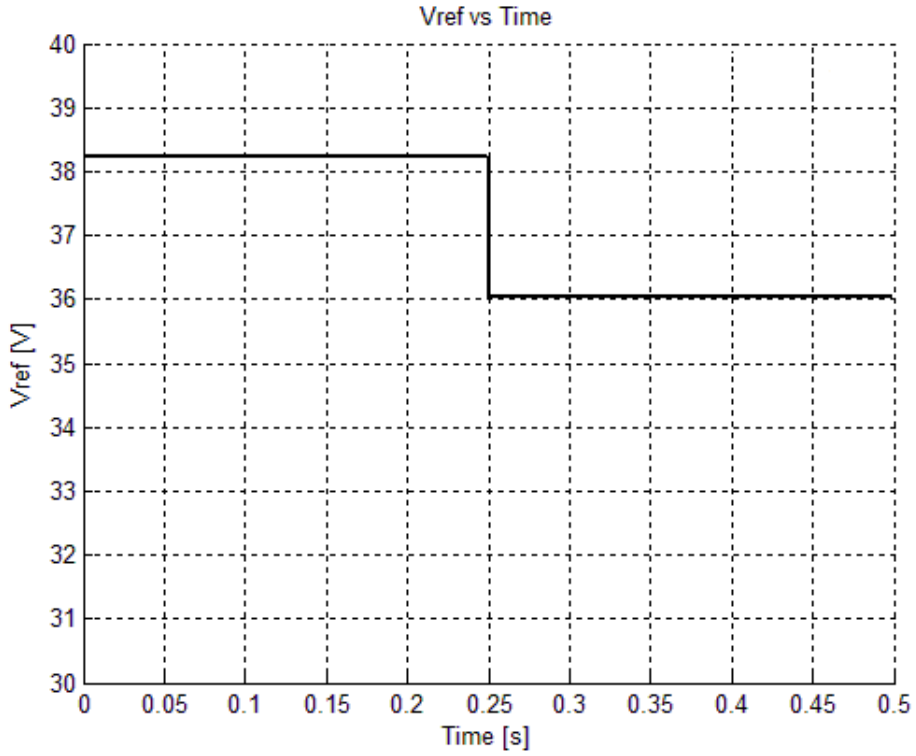

Figure 56: Plot of reference voltage under step-up temperature change.

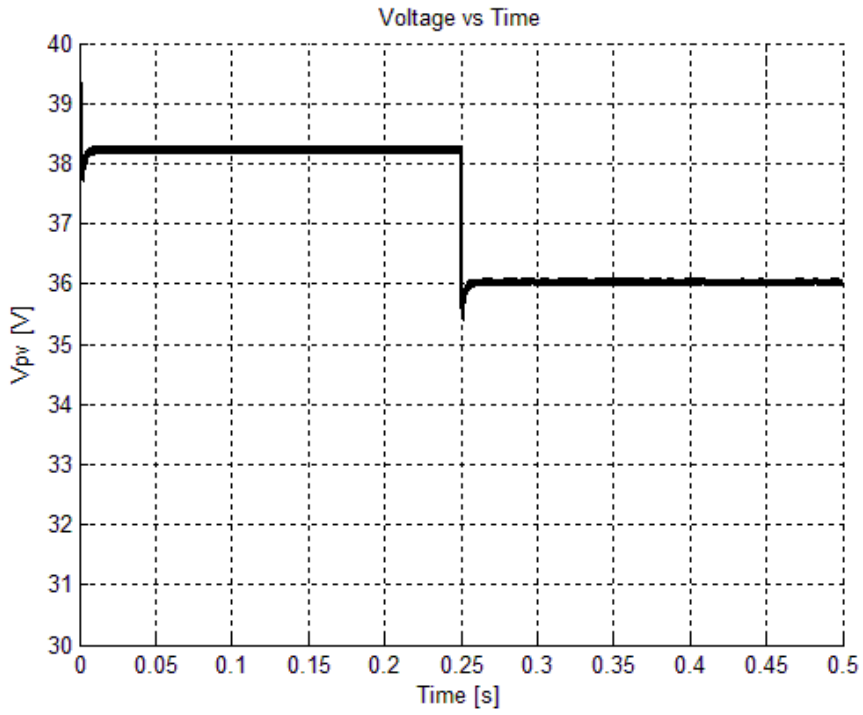

Figure 57: Characteristics of PV voltage under step-up temperature change.

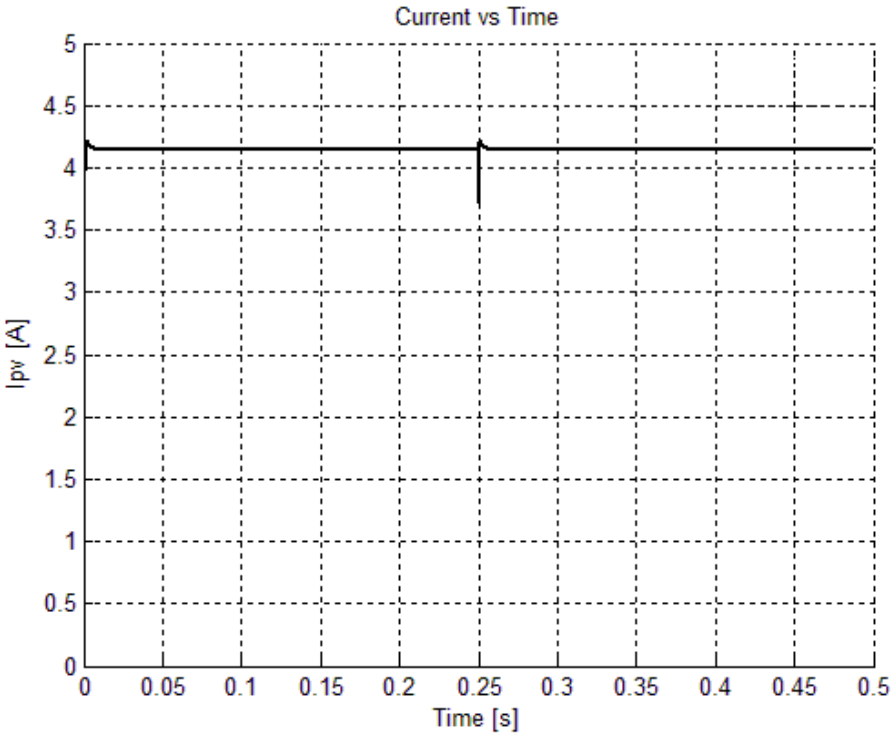

Figure 58: Characteristics of PV voltage under step-up temperature change.

5.4 Step-down Change in Temperature

This is the final test under step-down changing in the temperature degree. In this test, the value of the irradiation is constant and equal 1000 W/m^2. Figure 59 shows the temperature degree is constant with a value 25^{o}C (graph labeled as B) during the period from 0s up to 0.25s and then is rapidly decreasing to 15^{o}C (graph labeled as A). The value of power is changed according to the temperature degree. When the value of temperature is low, the PV panel generates more power. Figure 60 shows the P-V curves for the two values of temperature. When the temperature degree is 25^{o}C and the irradiation is 1000 W/m^2, the maximum power can PV panel generates is around 69 W. If the temperature degree is decreased to 15^{o}C, the operation point for the PV panel is changed and the panel gives a maximum power around 150 W.

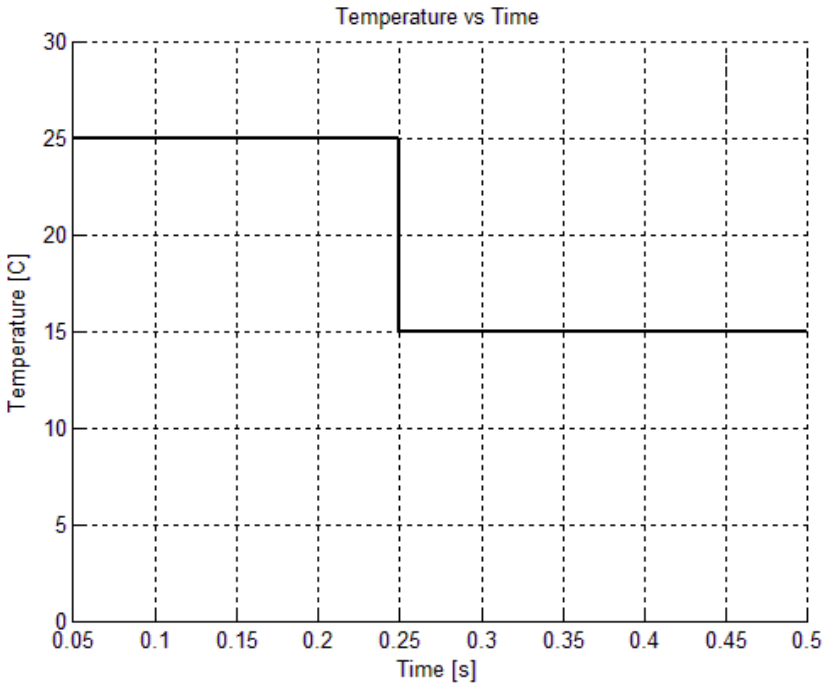

Figure 59: Step-down temperature pattern.

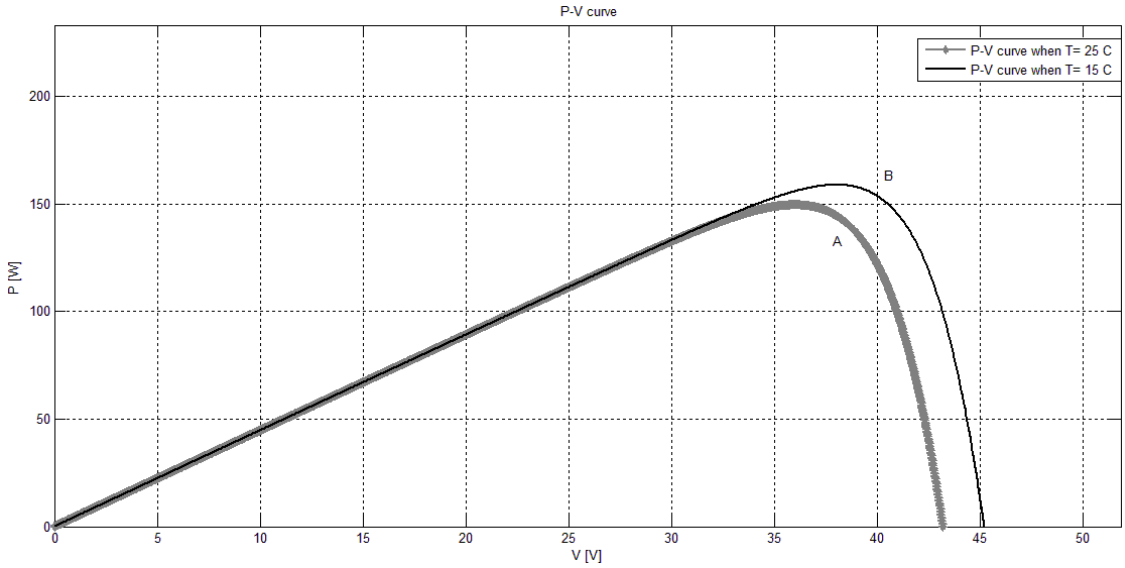

Figure 60: PV curve under normal and low temperature conditions.

PV panel is integrated to the ANFIS-based MPPT, buck converter and the load. As a result, it must follow these changed in the temperature degree and force PV panel to work at specific operation point to generate maximum power as shown in Figure 61. It can be seen from the graph that the ANFIS controller follows the changing in the temperature degree and PV panel generates the MPP at each temperature degree.

The simulation results for the reference voltage comes from the ANFIS controller which is generated the correct pulse (Duty Cycle) to drive the switch device in the buck converter , PV array voltage (V_{PV}) and current (I_{PV}) are shown in Figure 62, Figure 63, Figure 64, respectively, and verify the effectiveness of the proposed MPPT under the rapidly changing temperature degrees.

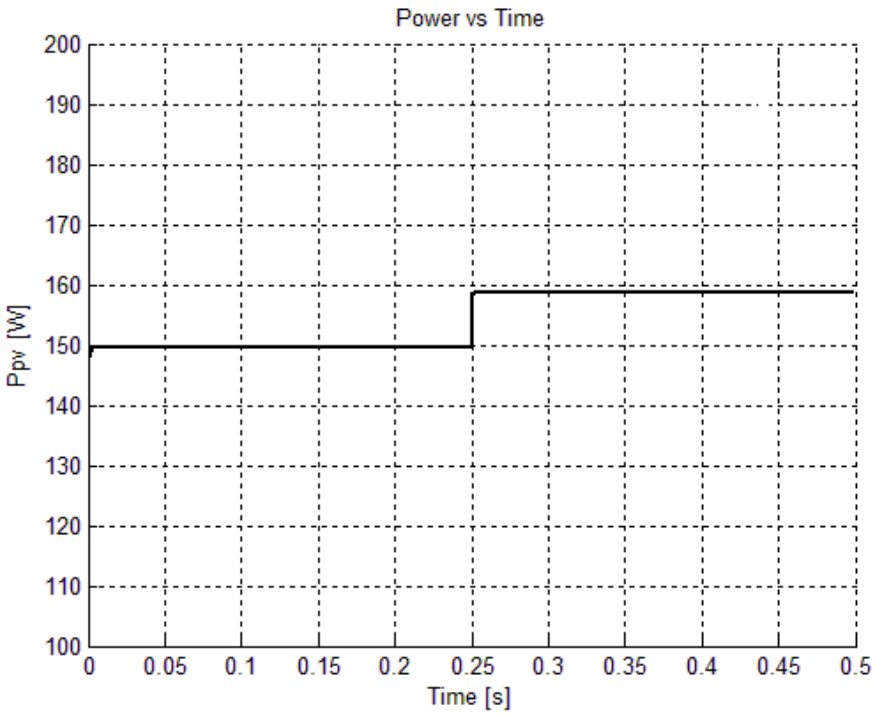

Figure 61: Characteristics of PV power output under step-down temperature change.

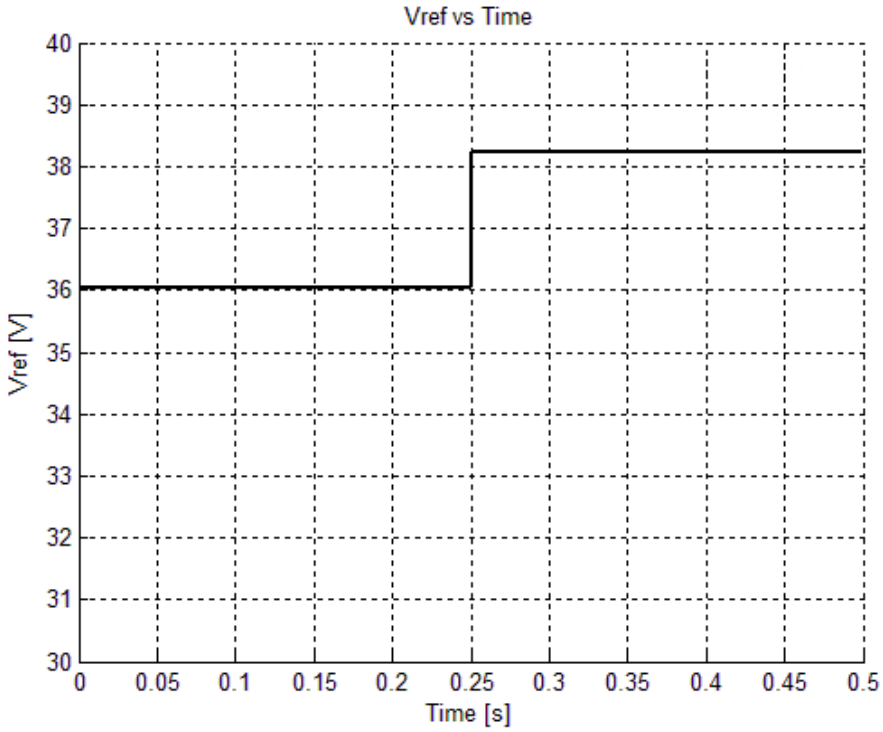

Figure 62: Plot of reference voltage under step-down temperature change.

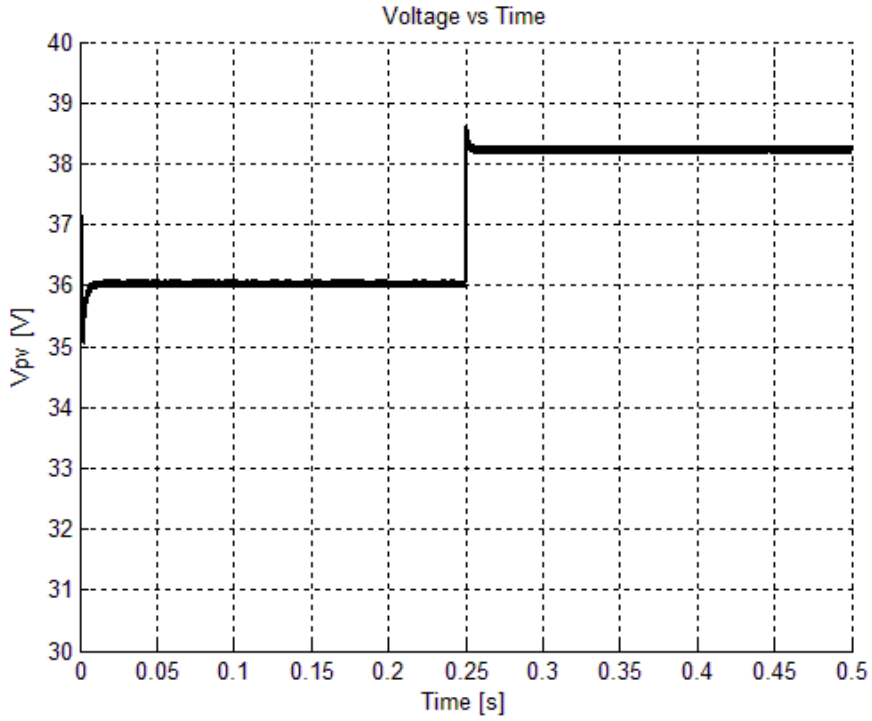

Figure 63: Characteristics of PV voltage under step-down temperature change

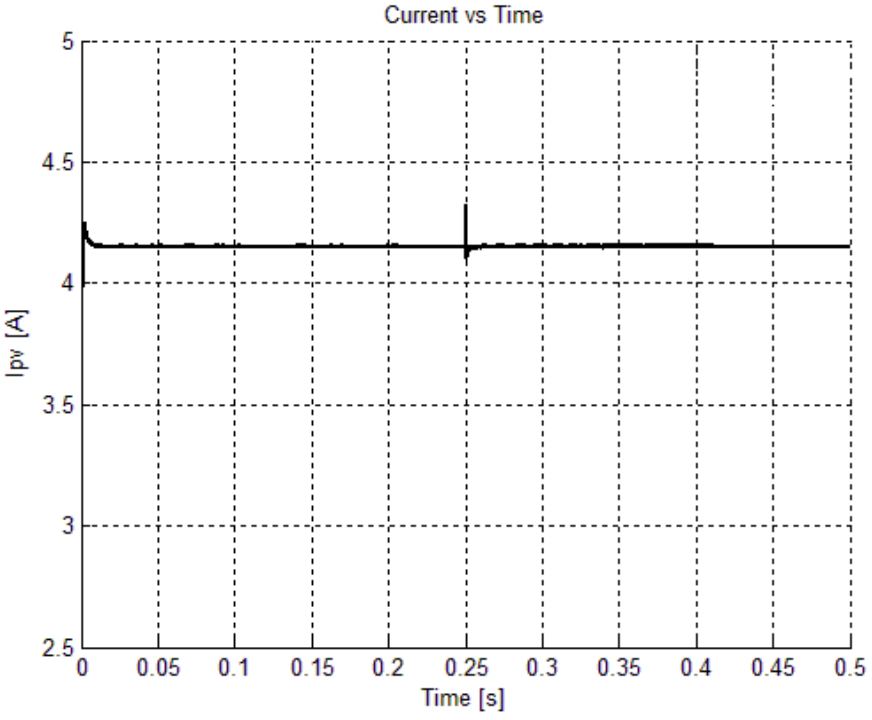

Figure 64: Characteristics of PV current under step-down temperature change.

5.5 Experimental Result

In this section, the experimental results are discussed. This experiment conducted on May 12, 2016. The weather conditions (Irradiation, Panel Temperature and Ambient Temperature) are measured from 7:00 am to 5:45 pm. Figure 65 shows the behavior of the irradiation during this time. Figure 666 and 67 display the ambient and panel temperature during the same period.

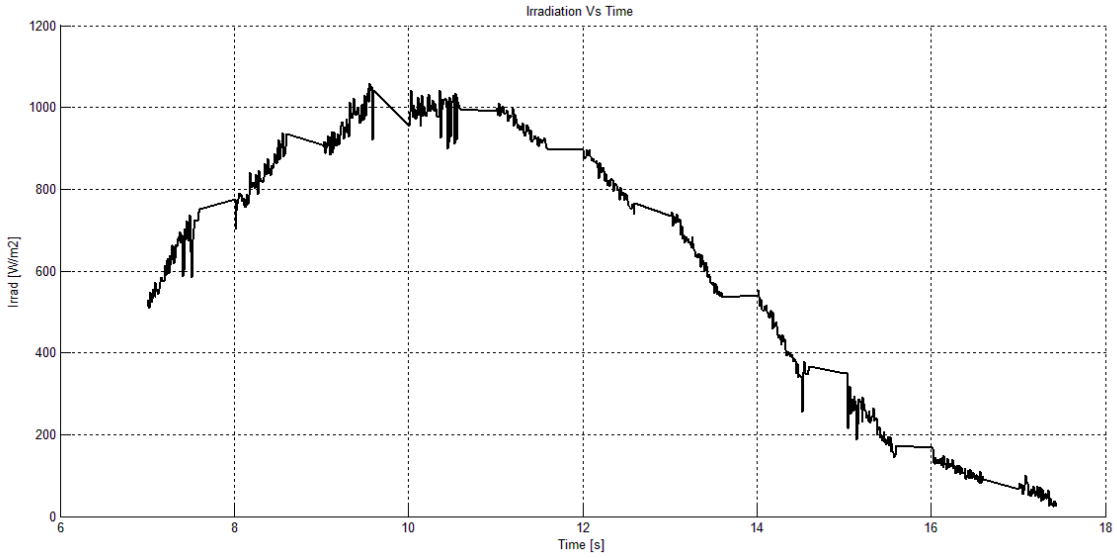

Figure 65: Irradiation change.

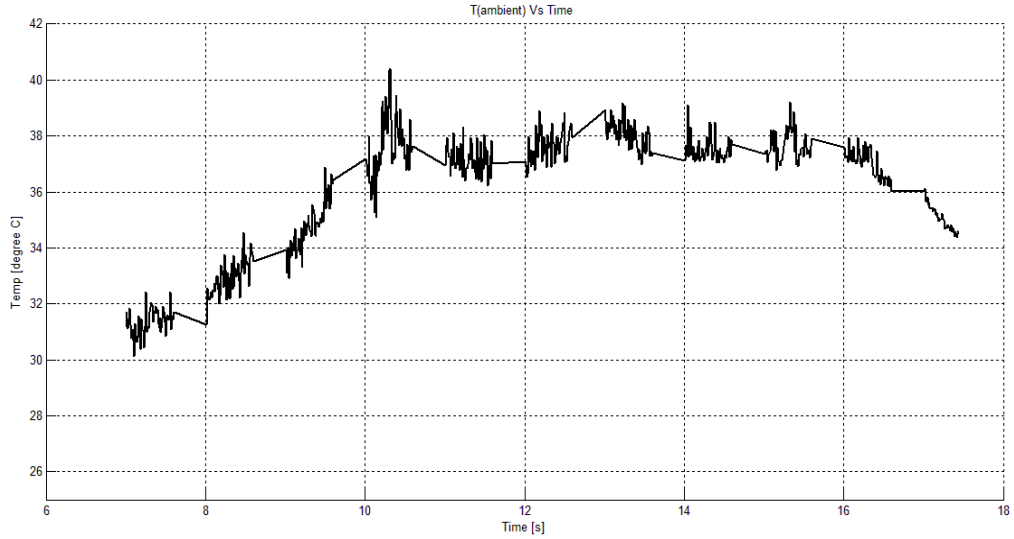

Figure 66: Ambient Temperature change in degree C.

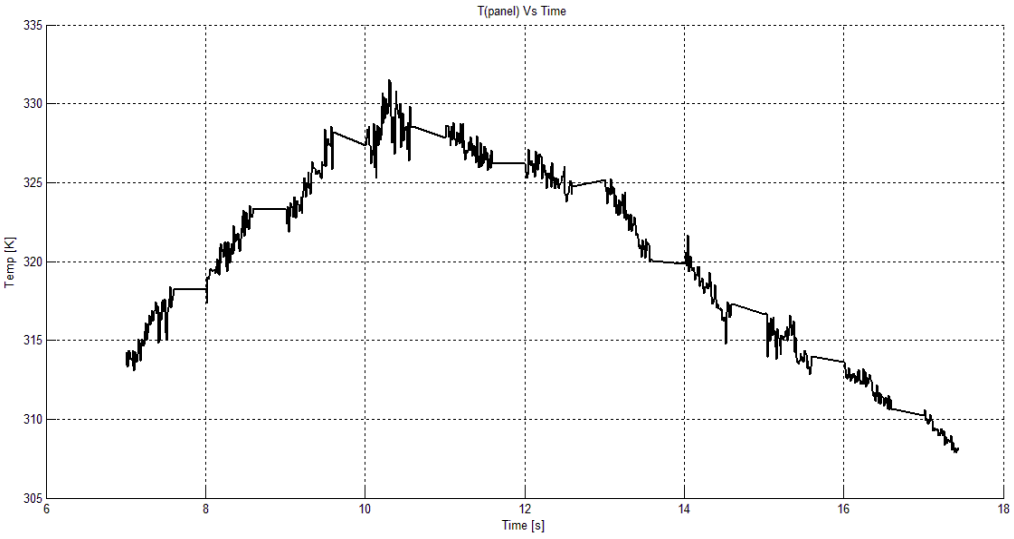

Figure 67: Panel Temperature change in degree K.

This irradiation levels and panel temperature values are applied to the system with and without MPPT controller to test the proposed technique in simulation. Figure 68 shows

the power on the load side with MPPT controller and without it. We can see the difference between the power values when the proposed controller is applied.

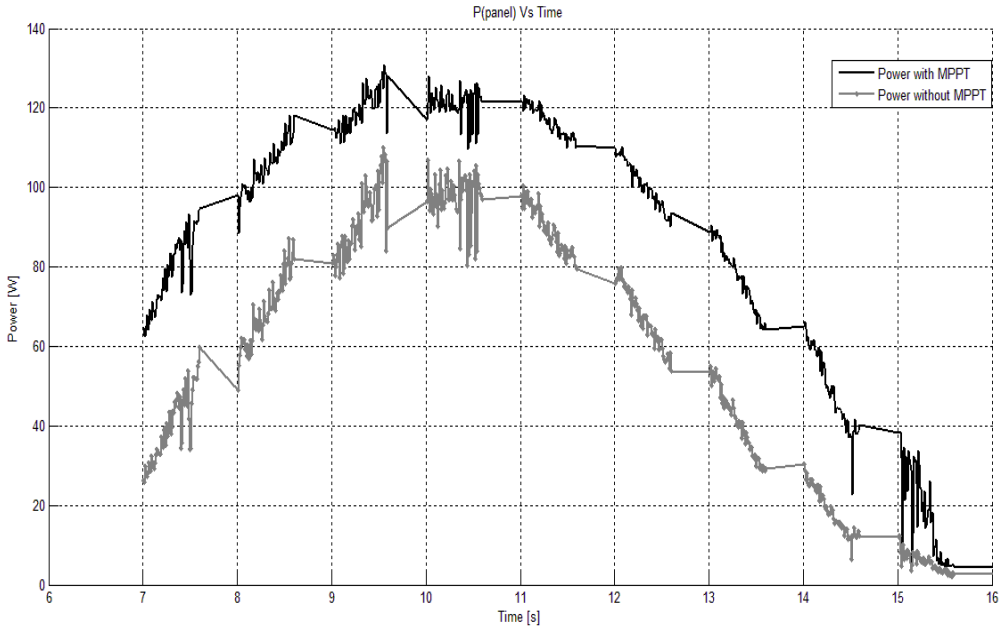

Figure 68: Power with and without MPPT.

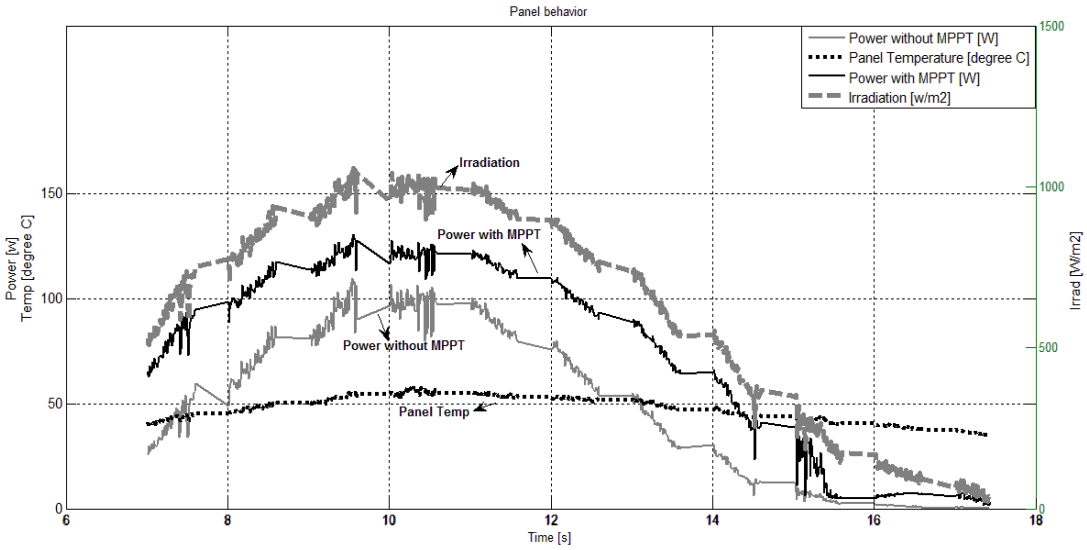

Figure 69: Panel Behavior during one day.

From the figures above, the performance of the PV system is stable when the proposed MPPT controller is applied. PV panel is integrated to the ANFIS-based MPPT controller, buck converter and the load. MPPT controller follows the changed in the irradiation and temperature level. MPPT controller forces PV panel to work at specific operation point to generate the maximum power.

Both temperature and the presence of cloud in the sky causes a rapid change in the value of irradiation and in the PV output. So, the power generated from the PV panel changes continuously. As we can see from the graphs, ANFIS-MPPT controller has the capability to follow these fast changes and extract the maximum power at any operation point in a stable manner.

Energy generated from the PV panel with MPPT controller and without are very much different. The amount of energy generated when the PV panel is integrated to ANFIS-MPPT controller is around 47736 Joules, while the energy generated from the PV panel without using MPPT controller is around 31234 Joules. This mean, PV panel gives more power with MPPT controller. The efficiency of PV panel with MPPT controller is 34% higher than when the PV panel works without MPPT controller. The ANFIS-MPPT has shown high degree of sensitivity and stability in its performance.

CHAPTER 6

CONCLUSION:

This thesis has analyzed mathematical PV panel modeling method and algorithm development in MATLAB/SIMULINK. This model has used the five electric circuit parameters. Then, ANFIS-based MPPT controller was proposed and developed. ANFIS controller was tested to verify the performance when it is integrated to PV panel.

LabVIEW system experimental set-up was built for a standalone PV system connected with DC-DC converter and load. A dSPACE controller was used to run the ANFIS-based MPPT in the experimental part. The whole integrated system was tested for real time measurements.

- A novel ANFIS-based MPPT controller was proposed and tested.
- ANFIS controller was tested under four tests. These tests can evaluate the ANFIS controller efficiency. Results showed that the proposed ANFIS controller can follow the rapidly changes in the weather conditions and it has a good dynamic behavior and steady state performance.
- Experimental setup is done to verify the effectiveness of the proposed ANFIS controller. Whole system is integrated together standalone PV panel, DC-DC converter, dSPACE controller, and load.
- Finally, comparison between the experimental and MATLAB/Simulink results.

Future Recommendation

There is a need for further PV model development based on experimental data. The developed PV panel model can be modified by introducing Rp and Rs model for the clean PV panel.

Dusty, heat and other environment conditions are one of the major issues causes the degradation of efficiencies of PV panel.

Partial shading condition is one of the major issues and causes multiple peaks in the PV curve and made it difficult to track the global MPP. The proposed ANFIS-based MPPT controller is designed for uniform irradiation condition and it can be improved to work in the partial shading conditions.

The developed PV system model and proposed MPPT controller can be interfaced with the power grid through inverter and effects of changing environmental conditions on power grid can be studied.

References

1. Conti, J., et al., *International energy outlook 2011.* Washington: Independent Statistics and Analysis of US Energy Information Administration, 2011. **12**.

2. Deilmann, C. and K.-J. Bathe, *A holistic method to design an optimized energy scenario and quantitatively evaluate promising technologies for implementation.* International Journal of Green Energy, 2009. **6**(1): p. 1-21.

3. Jefferson, J., *Global climate change and the challenges for renewable energy.* Renewable energy, 1998. **15**(1): p. 1-7.

4. Masson, G., M. Latour, and D. Biancardi, *Global market outlook for photovoltaics until 2016.* European Photovoltaic Industry Association, 2012: p. 6.

5. Agarwal, V. and A. Vishwakarma. *A comparative study of PWM schemes for grid connected PV cell*. in *Power Electronics and Drive Systems, 2007. PEDS'07. 7th International Conference on*. 2007. IEEE.

6. Bhatnagar, P. and R. Nema, *Maximum power point tracking control techniques: State-of-the-art in photovoltaic applications.* Renewable and Sustainable Energy Reviews, 2013. **23**: p. 224-241.

7. Li, J. and H. Wang. *Maximum power point tracking of photovoltaic generation based on the fuzzy control method*. in *Sustainable Power Generation and Supply, 2009. SUPERGEN'09. International Conference on*. 2009. IEEE.

8. Kim, Y., et al., *A strong regioregularity effect in self-organizing conjugated polymer films and high-efficiency polythiophene: fullerene solar cells.* Nature Materials, 2006. **5**(3): p. 197-203.

9. Marion, B., et al. *PVWATTS version 2–enhanced spatial resolution for calculating grid-connected PV performance*. in *Proceedings of the 2001 NCPV Program Review Meeting, Lakewood, CO*. 2001.

10. Hishikawa, Y., Y. Imura, and T. Oshiro. *Irradiance-dependence and translation of the IV characteristics of crystalline silicon solar cells*. in *Photovoltaic Specialists Conference, 2000. Conference Record of the Twenty-Eighth IEEE*. 2000. IEEE.

11. Marion, B., S. Rummel, and A. Anderberg, *Current–voltage curve translation by bilinear interpolation.* Progress in Photovoltaics: Research and Applications, 2004. **12**(8): p. 593-607.

12. King, D.L., J.A. Kratochvil, and W.E. Boyson, *Photovoltaic array performance model*. 2004: United States. Department of Energy.

13. Kou, Q., S. Klein, and W. Beckman, *A method for estimating the long-term performance of direct-coupled PV pumping systems.* Solar Energy, 1998. **64**(1): p. 33-40.

14. Celik, A.N. and N. Acikgoz, *Modelling and experimental verification of the operating current of mono-crystalline photovoltaic modules using four-and five-parameter models.* Applied energy, 2007. **84**(1): p. 1-15.

15. Ishaque, K., Z. Salam, and H. Taheri, *Modeling and simulation of photovoltaic (PV) system during partial shading based on a two-diode model.* Simulation Modelling Practice and Theory, 2011. **19**(7): p. 1613-1626.

16. Patel, H. and V. Agarwal, *MATLAB-based modeling to study the effects of partial shading on PV array characteristics.* Energy Conversion, IEEE Transactions on, 2008. **23**(1): p. 302-310.

17. Zagrouba, M., et al., *Identification of PV solar cells and modules parameters using the genetic algorithms: application to maximum power extraction.* Solar energy, 2010. **84**(5): p. 860-866.

18. Kim, W. and W. Choi, *A novel parameter extraction method for the one-diode solar cell model.* Solar Energy, 2010. **84**(6): p. 1008-1019.

19. Villalva, M.G. and J.R. Gazoli, *Comprehensive approach to modeling and simulation of photovoltaic arrays.* Power Electronics, IEEE Transactions on, 2009. **24**(5): p. 1198-1208.

20. Chatterjee, A., A. Keyhani, and D. Kapoor, *Identification of photovoltaic source models.* Energy Conversion, IEEE Transactions on, 2011. **26**(3): p. 883-889.

21. Boyd, M.T., et al., *Evaluation and validation of equivalent circuit photovoltaic solar cell performance models.* Journal of Solar Energy Engineering, 2011. **133**(2): p. 021005.

22. De Soto, W., S. Klein, and W. Beckman, *Improvement and validation of a model for photovoltaic array performance.* Solar energy, 2006. **80**(1): p. 78-88.

23. Elshatter, T.F., et al. *Fuzzy modeling of photovoltaic panel equivalent circuit*. in *Photovoltaic Specialists Conference, 2000. Conference Record of the Twenty-Eighth IEEE*. 2000. IEEE.

24. Almonacid, F., et al., *Characterisation of Si-crystalline PV modules by artificial neural networks.* Renewable Energy, 2009. **34**(4): p. 941-949.

25. Aranda, E.D., et al., *Measuring the IV curve of PV generators.* Industrial Electronics Magazine, IEEE, 2009. **3**(3): p. 4-14.

26. Coelho, R.F., F.M. Concer, and D.C. Martins. *Analytical and experimental analysis of DC-DC converters in photovoltaic maximum power point tracking applications*. in *IECON 2010-36th Annual Conference on IEEE Industrial Electronics Society*. 2010. IEEE.

27. Xiao, W., et al., *Regulation of photovoltaic voltage.* Industrial Electronics, IEEE Transactions on, 2007. **54**(3): p. 1365-1374.

28. Subudhi, B. and R. Pradhan, *A comparative study on maximum power point tracking techniques for photovoltaic power systems.* Sustainable Energy, IEEE Transactions on, 2013. **4**(1): p. 89-98.

29. Ishaque, K. and Z. Salam, *A review of maximum power point tracking techniques of PV system for uniform insolation and partial shading condition.* Renewable and Sustainable Energy Reviews, 2013. **19**: p. 475-488.

30. Hua, C.-C. and J.-R. Lin. *Fully digital control of distributed photovoltaic power systems*. in *Industrial Electronics, 2001. Proceedings. ISIE 2001. IEEE International Symposium on*. 2001. IEEE.

31. Kasa, N., T. Lida, and H. Iwamoto. *Maximum power point tracking with capacitor identifier for photovoltaic power system*. in *Electric Power Applications, IEE Proceedings-*. 2000. IET.

32. Esram, T. and P.L. Chapman, *Comparison of photovoltaic array maximum power point tracking techniques.* IEEE Transactions on Energy Conversion EC, 2007. **22**(2): p. 439.

33. Houssamo, I., F. Locment, and M. Sechilariu, *Maximum power tracking for photovoltaic power system: Development and experimental comparison of two algorithms.* Renewable Energy, 2010. **35**(10): p. 2381-2387.

34. Ahn, C.W., et al., *Adaptive Maximum Power Point Tracking Algorithm for Photovoltaic Power Systems.* IEICE Transactions on Communications, 2010. **93**(5): p. 1334-1337.

35. Zhang, C., et al. *A modified MPPT method with variable perturbation step for photovoltaic system*. in *Power Electronics and Motion Control Conference, 2009. IPEMC'09. IEEE 6th International*. 2009. IEEE.

36. Li, J. and H. Wang. *A novel stand-alone PV generation system based on variable step size INC MPPT and SVPWM control*. in *Power Electronics and Motion Control Conference, 2009. IPEMC'09. IEEE 6th International*. 2009. IEEE.

37. Masoum, M.A., H. Dehbonei, and E.F. Fuchs, *Theoretical and experimental analyses of photovoltaic systems with voltageand current-based maximum power-point tracking.* Energy conversion, IEEE transactions on, 2002. **17**(4): p. 514-522.

38. Abido, M. and N. Al-Ali, *Multi-objective optimal power flow using differential evolution.* Arabian Journal for Science and Engineering, 2012. **37**(4): p. 991-1005.

39. Mohamed, A. and H. Shareef, *Hopfield neural network optimized fuzzy logic controller for maximum power point tracking in a photovoltaic system.* International Journal of Photoenergy, 2011. **2012**.

40. Alajmi, B.N., et al., *Fuzzy-logic-control approach of a modified hill-climbing method for maximum power point in microgrid standalone photovoltaic system.* Power Electronics, IEEE Transactions on, 2011. **26**(4): p. 1022-1030.

41. Ishaque, K., et al., *An improved Particle Swarm Optimization (PSO)–based MPPT for PV with reduced steady-state oscillation.* Power Electronics, IEEE Transactions on, 2012. **27**(8): p. 3627-3638.

42. Taheri, H., Z. Salam, and K. Ishaque. *A novel maximum power point tracking control of photovoltaic system under partial and rapidly fluctuating shadow conditions using differential evolution*. in *Industrial Electronics & Applications (ISIEA), 2010 IEEE Symposium on*. 2010. IEEE.

43. Kaliamoorthy, M. and V. Rajasekaran. *A novel MPPT scheme for solar powered boost inverter using evolutionary programming*. in *Recent Advancements in Electrical, Electronics and Control Engineering (ICONRAEeCE), 2011 International Conference on*. 2011. IEEE.

44. Ramaprabha, R., et al. *Maximum power point tracking using GA-optimized artificial neural network for Solar PV system*. in *electrical energy systems (ICEES), 2011 1st international conference on*. 2011. IEEE.

45. Ngan, M.S. and C.W. Tan, *Multiple peaks tracking algorithm using particle swarm optimization incorporated with artificial neural network.* World Academy of Science, Engineering and Technology, 2011. **58**: p. 379-385.

46. Younis, M.A., et al., *An Improved Maximum Power Point Tracking Controller for PV Systems Using Artificial Neural Network.* Przegląd Elektrotechniczny, 2012. **88**: p. 116-121.

47. Otieno, C., G.N. Nyakoe, and C.W. Wekesa. *A neural fuzzy based maximum power point tracker for a photovoltaic system*. in *AFRICON, 2009. AFRICON'09.* 2009. IEEE.

48. Won, C.-Y., et al. *A new maximum power point tracker of photovoltaic arrays using fuzzy controller*. in *Power Electronics Specialists Conference, PESC'94 Record., 25th Annual IEEE*. 1994. IEEE.

49. Nejila, V. and A.I. Selvakumar. *Fuzzy-logic based hill-climbing method for maximum power point tracking in PV systems*. in *Power, Energy and Control (ICPEC), 2013 International Conference on*. 2013. IEEE.

50. Arulmurugan, R. and N. Suthanthira Vanitha. *Intelligent fuzzy MPPT controller using analysis of DC to DC novel buck converter for photovoltaic energy system applications*. in *Pattern Recognition, Informatics and Medical Engineering (PRIME), 2013 International Conference on*. 2013. IEEE.

51. Simoes, M.G. and N. Franceschetti. *Fuzzy optimisation based control of a solar array system*. in *Electric Power Applications, IEE Proceedings-*. 1999. IET.

52. Masoum, M. and M. Sarvi. *Design, simulation and construction of a new fuzzy-based maximum power point tracker for photovoltaic applications*. in *Proceedings of the Australasian University Power System Engineering Conference (AUPEC'02)*. 2002.

53. Kottas, T.L., Y.S. Boutalis, and A.D. Karlis, *New maximum power point tracker for PV arrays using fuzzy controller in close cooperation with fuzzy cognitive networks.* Energy Conversion, IEEE Transactions on, 2006. **21**(3): p. 793-803.

54. Duffie, J.A., *William A. Beckman Solar Engineering of Thermal Processes*. 2006, JOHN WILEY & SONS, INC. NY.

55. Nelson, J., *The physics of solar cells*. Vol. 1. 2003: World Scientific.

56. Benghanem, M., A.H. Arab, and K. Mukadam, *Data acquisition system for photovoltaic water pumps.* Renewable energy, 1999. **17**(3): p. 385-396.

57. Blaesser, G., *PV system measurements and monitoring the European experience.* Solar energy materials and solar cells, 1997. **47**(1): p. 167-176.

58. Kim, I.-S., M.-B. Kim, and M.-J. Youn, *New maximum power point tracker using sliding-mode observer for estimation of solar array current in the grid-connected photovoltaic system.* Industrial Electronics, IEEE Transactions on, 2006. **53**(4): p. 1027-1035.

59. Mellit, A. and S.A. Kalogirou, *Artificial intelligence techniques for photovoltaic applications: A review.* Progress in energy and combustion science, 2008. **34**(5): p. 574-632.

60. Zadeh, L.A., *Fuzzy sets.* Information and control, 1965. **8**(3): p. 338-353.

61. Passino, K.M., *Stephen Yurkovich. Fuzzy Control*. 1998, Boston (USA): Addison Wesley Longman.

62. Jang, J.-S.R., *ANFIS: adaptive-network-based fuzzy inference system.* Systems, Man and Cybernetics, IEEE Transactions on, 1993. **23**(3): p. 665-685.

63. Jang, J.-S.R. and C.-T. Sun, *Neuro-fuzzy modeling and control.* Proceedings of the IEEE, 1995. **83**(3): p. 378-406.

VITAE

Name:	Fadi Mohammad Fareed Abu Samra
Date of birth:	5 November, 1988
Nationality:	Palestine
Permanent Address:	Jenin, Palestine
Email Address:	g201203340@kfupm.edu.sa
	fsamra88@gmail.com

Educational Qualification:	M.Sc. (Electrical Engineering- Power)
	December, 2015
	King Fahd University of Petroleum and Mineral,
	Dhahran, Saudi Arabia.
	B.Sc. (Electrical Engineering)
	June, 2010
	Palestine Technical University
	Tulkarm, Palestine.
Certificates and Courses:	Training Course in P.L.C. Industrial application.
	Electrical installations design “residential, Industrial”.
	Training Course in wired & wireless network.